INTERACTIONS OF N-ALKYL-2-PYRROLIDINONE SURFACTANTS WITH DMPC BILAYERS

by

YASEMİN KOPKALLI

A dissertation submitted to the Graduate Faculty in Chemistry
in partial fulfillment of the requirements for the degree of

Doctor of Philosophy

The City University of New York

2006

ProQuest Information and Learning Company
300 North Zeeb Road
P.O. Box 1346
Ann Arbor, MI 48106-1346

This manuscript has been read and accepted for the Graduate Faculty in Chemistry in satisfaction of the dissertation requirement for the degree of Doctor of Philosophy.

Chair of Examining Committee	Lesley Davenport, Professor
Executive Officer	Gerald Koeppl, Professor
Supervisory Committee	Milton J. Rosen, Professor Emeritus
	Ruth E. Stark, Professor
	Brian Williams, Professor

THE CITY UNIVERSITY OF NEW YORK

ABSTRACT

INTERACTIONS OF N-ALKYL-2-PYRROLIDINONE SURFACTANTS WITH DMPC BILAYERS

by

Yasemin Kopkallı

Adviser: Professor Lesley Davenport

There is great interest in identifying and characterizing new surfactants with predictable solubilization and reconstitution characteristics for use in membrane research. Among them, Triton X-100 and octyl glucoside (OG) are the best-studied surfactants. However, no physical data is available characterizing the interactions of two non-ionic pyrrolidinone surfactants, N-(2-ethylhexyl)-2-pyrrolidinone (C2,6P) and N-octyl-2-pyrrolidinone (C8P), with lipid bilayers. In the present study, their physical effects on dimyristoylphosphatidylcholine small unilamellar vesicles (DMPC SUVs) above the lipid phase transition temperature are described using surface tension, fluorescence spectroscopy, and isothermal titration calorimetry (ITC) methodologies.

Surface tension methods show significant deviations from ideal behavior (attractive interactions) for these surfactant/lipid mixtures. In addition, fluorescence intensity studies of DPH and TMA-DPH labeled SUVs suggest that C8P interacts more favorably with

both the acyl chain and head group regions of the bilayer over the corresponding branched chain C2,6P analogue. This is further supported by fluoresecence emission anisotropy measurements (EA). Both surfactants affect the membrane lipid order within the acyl chain region, and the corresponding phospholipid 'melt' transition temperature (T_m) values, which decrease linearly with increasing surfactant concentrations. Using the van't Hoff model, the lipid bilayer-water partition coefficients for these surfactants have been estimated from the depression of the lipid phase transition temperature. Values for the lipid partition coefficient for C8P [$(1.22\pm0.08)\times 10^4$] *versus* C2,6P [$(4.09\pm0.78)\times 10^3$] further supports a more favorable bilayer association for C8P.

ITC data reveals an endothermic association for both C8P and C2,6P together with a somewhat higher binding affinity [$(6.78\pm0.92)\times10^{-4}$M] for C8P compared with C2,6P [$(8.46\pm0.83)\times10^{-4}$ M], as predicted from fluorescence studies.

We propose that C8P interacts and affects the lipid packing of bilayer membranes to a greater extent than C2,6P. Interactions of C2,6P appears to be more localized within the head group region of the bilayer. We conclude that C8P has great potential for biological applications, particularly membrane solubilization and membrane formation from micellar mixtures. In contrast, C2,6P may have potential for solubilization of extrinsic surface associated membrane proteins.

To my father-in-law, Veli Kopkallı, who showed me the value of education and taught me to never give up, no matter what the cost.

ACKNOWLEDGEMENTS

I would like to thank Professor Lesley Davenport, my mentor, and Professor Milton J. Rosen, Professor Ruth E. Stark, and Professor Brian Williams, for serving on my thesis committee. I am very grateful to them for having reviewed this project at various stages and for providing valuable input given their individual areas of expertise.

This dissertation would not have been possible without the tireless efforts of my advisor, Professor Lesley Davenport. She has taught me to work as an independent researcher and has been a steady source of wise encouragement and support throughout my doctoral studies.

Very special thanks go to Professor Milton J. Rosen, director of the Surfactant Research Institute for providing N-alkyl-2-pyrrolidinone surfactants, opening his laboratory for surface tension measurements and more importantly for introducing me to the fascinating world of surfactants.

A debt of gratitude goes to Professor Richard Magliozzo and to people in his laboratory for sharing isothermal titration calorimetry instrument with me in their laboratory.

I am grateful to labmates and fellow graduate students Caleen Ramsook and Natalya Voloshchuk for always being there, their kindness and friendship.

I want to thank my entire family, especially my mother and father Gülser and Ekrem Tura, for everything they have done for me. They have been by my side, with their unconditional love and support, throughout my entire life.

Finally, and most importantly, I want to thank my husband and best friend, Halûk Kopkallı for drawing some figures in this thesis. His support, encouragement, and companionship turned my journey through graduate school into a pleasure. Let it go on record that he promised to read my entire thesis once it is submitted.

LIST OF ABBREVIATIONS

A_{min}	minimum area/molecule at the interface
a_0	optimal lipid headgroup area
C_1^0	molar concentration of surfactant *1* in the solution phase
C_2^0	molar concentration of surfactant *2* in the solution phase
C_{12}	molar concentrations of surfactant mixtures in the solution phase
C_1^M	critical micelle concentration of surfactant *1* in the mixed micelle
C_2^M	critical micelle concentration of surfactant *2* in the mixed micelle
C_{12}^M	critical micelle concentration of surfactant mixture in the mixed micelle
C2,6P	N-(2-ethylhexyl)-2-pyrrolidinone
C8P	N-octyl-2-pyrrolidinone
C10P	*N*-decyl-2-pyrrolidinone
C12P	*N*-dodecyl-2-pyrrolidinone
C_{12}PC	n-dodecyl phosphocholine
C_{16}PC	n-hexadecyl phosphocholine
C12SNa	sodium dodecanesulfonate
C_{20}	efficiency of surface tension reduction by a surfactant.
C_L^0	surfactant concentration in the ligand delivery syringe
$C_{i,L}$	surfactant concentration in the sample cell, after n_i injections
C_M^0	DMPC SUVs concentration in the sample cell
$C_{i,M}$	DMPC SUVs concentration in the sample cell, after n_i injections
cmc	critical micelle concentration
cmt	critical micelle temperature
cp	cloud point
DHPC	1, 2-diheptanoyl-sn-glycero-3-phosphocholine
DMPC	L-α-dimyristoylphosphatidylcholine
DPH	1,6-diphenyl-1,3,5-hexatriene
DPS	dimethyl-dodecylamniopropane sulfonate
EA	fluorescence emission anisotropy
F	fluorescence emission intensity
F_0	fluorescence intensities in the absence of surfactant
GUV	giant unilamellar vesicle
h_i	heat of reaction
HLB	hydrophile-lipophile balance number
i	number of titration
ITC	isothermal titration calorimetry
K	binding constant (K_a)
K_a	association constant; $1/K_d$
K_d	dissociation constant; $1/K_a$
K_p	partition coefficient
k_q	biomolecular quenching constant

K_{SV}	Stern-Volmer quenching constant
[L]	free ligand concentration
$[L]_t$	total ligand concentration
l_c	critical chain length
LAS	linear alkylbenzenesulfonate
LUV	large unilamellar vesicles
$[M]_t$	total macromolecule concentration
MLV	large multilamellar vesicles
MVV	multivesicular vesicles
n	surfactant to lipid molar ratio
N	aggregation number
OG	octyl glucoside
pC_{20}	efficiency of interfacial tension reduction
PC	phosphatidylcholines
PE	phosphatidylethanolamines
POPC	1-palmitoyl-2-oleoyl-*sn*-glycero-3-phosphocholine
POPG	1-palmitoyl-2-oleoyl-sn-glycero-3-phosphoglycerol
Q	cumulative heat of binding
<r>	steady-state fluorescence emission anisotropy
r_0	limiting anisotropy
R	gas constant
R^2	correlation coefficient
Re^{sat}	molar ratio at saturation point
Re^{sol}	molar ratio at solubilization point
SDS	sodium dodecyl sulfate
S/L	surfactant to DMPC SUVs molar ratio
SUVs	small unilamellar vesicles
T	temperature
T_m	gel to liquid-crystalline phase transition
TMA-DPH	trimethylammonium 1,6-diphenyl-1,3,5-hexatriene
UV	ultraviolet
V_{cell}	sample cell volume
V_{inj}	volume of injection
V_0	volume of the cell
X_1	mole fraction of surfactant *1* in the total mixed monolayer
X_1^M	mole fraction of surfactant *1* in the total mixed micelles
α	mole fraction
β^M	molecular interaction parameters for mixed micelle formation
β^σ	molecular interaction parameters for mixed monolayer formation
Γ	surface excess concentration
γ	surface tension
δhi	corrected heat of titrations
ΔG	free energy of binding
ΔG_{ad}^0	standard free energy of adsorption

ΔH	enthalpy of binding
ΔS	entropy of binding
$-\Delta T$	depression of the phase transition temperature
ε	molar extinction coefficient
λ_{max}	wavelength with maximum emission intensity
v	hydrocarbon volume
Π_{max}	effectiveness of interfacial tension reduction
τ	lifetime
Φ	quantum yield

TABLE OF CONTENTS

LIST OF TABLES

Table **Page**

LIST OF FIGURES

Figure **Page**

Figure **Page**

CHAPTER 1: INTRODUCTION

1.1. Aim of the Research

The aim of this research is to assess the effects of two non-ionic N-Alkyl-2-pyrrolidinone surfactants, N-(2-ethylhexyl)-2-pyrrolidinone (C2,6P) and N-octyl-2-pyrrolidinone (C8P) on the physical structure of lipid bilayers (Figure 1). While the physical properties of these surfactants are well studied [1-6], their biological impact on bilayer and integral membrane protein solubilization, or membrane permeability has not been investigated. In the following, the physical interactions of two pyrrolidinone surfactants (C2,6P and C8P) with dimyristoylphosphatidylcholine (DMPC) vesicles has been investigated using surface tension, fluorescence spectroscopy, and isothermal titration calorimetry (ITC).

The non-ionic surfactants most commonly used in biological research are Triton X-100 and octyl glucoside. In this research we have studied two highly-purified two isomeric surfactants: N-(2-ethylhexyl)-2-pyrrolidinone (C2,6P) and N-octyl-2-pyrrolidinone (C8P). The C8 series of pyrrolidinones were selected because of their acyl chain length similarity to commonly used octyl glucoside (eight carbon acyl chain). Triton X-100 is a complex mixture of compounds varying greatly in their surface and colloid properties. Because of the impossibility of drawing valid chemical structure/performance relationships from such a complex mixture, much of the research is flawed. The only nonionic surfactant currently used in biological /biochemical research that does not exist as a complex mixture of compounds is octyl glucoside. Octyl glucoside has a great capacity for interaction with lipid membrane

components via hydrogen bonding. In contrast, N-alkyl-2-pyrrolidones act only as hydrogen bond acceptors. Use of C8P (saturated chain) and C2,6P (branched chain) surfactants in biological /biochemical research can provide important insights into the effect of such difference in hydrogen bonding capacity on biological structures and processes.

In addition, C2,6P and C8P have recently been found to be the first agents to specifically inhibit gamete fusion in *Chlamydomonas rheinhardii*, suggesting possible unique biological properties for these surfactants [7].

1.2. Significance

Surfactants play a vital role in biochemical and pharmacological applications. Due to their amphipathic character, they have the unique ability to form micelles which can serve as efficient carriers or vectors for biologically important molecules, including DNA, drugs and proteins [8]. In addition, surfactants are particularly valuable in studies of the denaturation, solubilization, stabilization, or reconstitution of a variety of soluble and membrane-associated proteins [9-10]. Surfactants solubilize membranes by intercalating with the phospholipid molecules until the mole fraction of surfactant is so high that the bilayer structure is disrupted, leading to the formation of lipid-surfactant or protein-surfactant mixed micelles. In this fashion intrinsic membrane proteins may be purified without conformational disruption arising from exposure to the aqueous environment. Hence, there is a great interest in finding surfactants with predictable solubilization and reconstitution characteristics for use in membrane research and pharmacological applications. The choice of a

particular surfactant molecule for such applications is based on non-evasive chemical and physical properties, including surfactant solubility and critical micelle concentration.

1.3. Rationale

In this study, surface tension, fluorescence spectroscopy, and isothermal titration calorimetry studies have been employed to provide a detailed and critical examination of the interactions of two pyrrolidinone surfactants, C2,6P (branched chain) (Figure 1A) and C8P (straight chain) (Figure 1B) with lipid bilayers.

Significant research has focused on understanding the physicochemical properties of mixed-micelle formation by two or more surfactants using surface tension methods [11-26]. Phospholipids which are known amphiphiles owing to the zwitterionic nature of their polar head group also form micelles. In the present study, surface tension was measured using the Wilhelmy plate method to explore the mixed-monolayer and mixed-micelle formation of N-alkyl-2-pyrrolidinones with DMPC monomers and to study their interfacial and bulk micellar behavior at the air/aqueous solution interface.

Mixed-micelle formation has considerable importance compared with single-surfactant micelle formation for various reasons. Generally, a mixture of two or more surfactants has better surface activity than that of their constituents. In the mixed-micelle process, three kinds of interactions exist between the monomers of two unlike surfactants, i.e., favorable interactions, nonfavorable interactions, or ideal mixing (no interaction).

Fluorescence spectroscopy provides a sensitive tool for the examination of the resultant effects of surfactants on the physical properties of lipid membranes and bilayers [27-55]. To achieve our aim fluorescence bilayer probes were introduced into small unilamellar vesicles (SUVs) composed of dimyristoylphosphatidylcholine (DMPC) (Figure 2A) (diameter 250-300Å). Bilayers were labeled with either diphenylhexatriene (DPH) (Figure 2B), which partitions into the hydrophobic bilayer matrix, or trimethylammonium diphenylhexatriene (TMA-DPH) (Figure 2C). Because of its charge, TMA-DPH resides exclusively in the more polar head group region of the bilayer [56-71]. The rotational motions of these two fluorescent fatty acyl chain analogs are sensitive to packing perturbations occurring within specific regions of the bilayer, arising from the addition of surfactant molecules. Both the chemical and physical properties of the DMPC bilayer system have previously been well documented using a variety of biophysical methods and hence serves as an excellent model for the proposed studies [56-73].

A number of studies have utilized isothermal titration calorimetry (ITC) to analyze surfactant partitioning into lipid bilayers and surfactant-induced solubilization of lipid vesicles [74-92]. The insertion of a surfactant into the bilayer membrane is generally accompanied by absorption or release of heat, which can be measured quickly with reliability using modern titration calorimeters. In a single experiment, ITC measures the association constant Ka (=1/Kd), stoichiometry (n), free energy (ΔG), enthalpy (ΔH) and entropy (ΔS) of binding. Since changes in the heat of the system occur during many physicochemical processes, ITC has a broad

application ranging from chemical and biochemical binding studies to more complex processes involving enthalpy changes, such as enzyme kinetics [93-97].

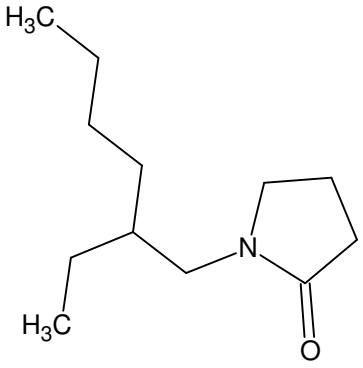

(A) C2,6P

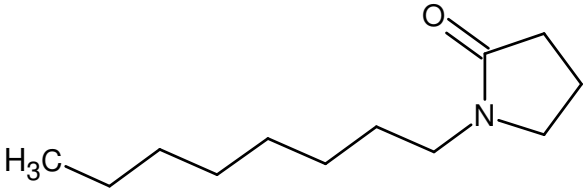

(B) C8P

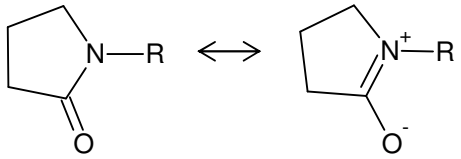

Nonionic structure Zwitterionic structure

(C)

Figure 1: Structures of the N- alkyl-2- pyrrolidinones used in this study: (A) N-(2-ethylhexyl)-2-pyrrolidinone (C2,6P); (B) N-octyl-2-pyrrolidinone (C8P); and (C) Resonance hybrid of the nonionic and zwitterionic pyrrolidinone structures.

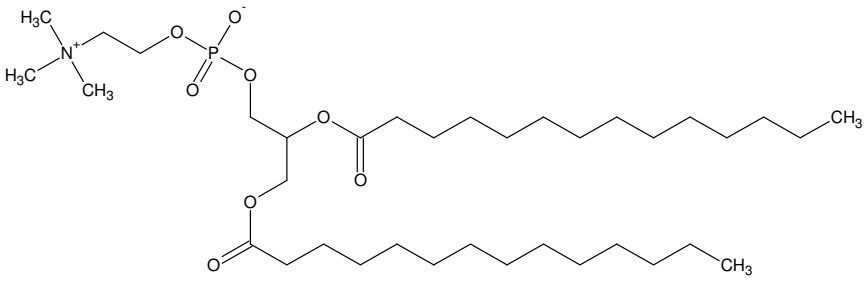

(A) DMPC

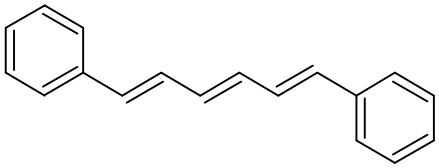

(B) DPH

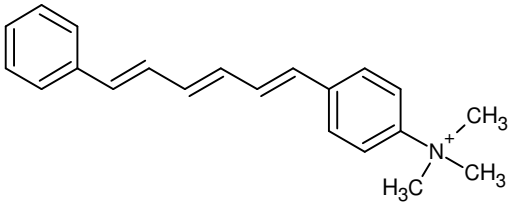

(C) TMA-DPH

Figure 2: Structures of: (A) dimyristoylphosphatidylcholine (DMPC); (B) 1,6-diphenyl-1,3,5-hexatriene (DPH); and (C) trimethylammonium 1,6-diphenyl-1,3,5-hexatriene (TMA-DPH).

1.4. Surfactants

Surfactants have great versatility. They have applications in many areas, including chemistry (for kinetic studies), biology (as membrane mimics), and medical applications via liposomes (as drug delivery agents) [8, 98].

Surfactants are defined as compounds that contain both a hydrophilic and hydrophobic moiety. The resulting amphiphilic character of the molecule gives rise to the phenomenon of surface activity. However, unlike biological amphiphiles such as phospholipids or cholesterol that are integral components of cell membranes, surfactants form micelles and are significantly soluble in water. As such, surfactants are often referred to in the literature as surface-active agents, soaps, or detergents. However, N-alkyl-2-pyrrolidinones used in this study (C2,6P and C8P) have limited solubility in water at room temperature.

The hydrophobic moieties of surfactants are commonly one or more water-insoluble hydrophobic tails, which are long-chain hydrocarbon residues, halogenated or oxygenated hydrocarbons or polysiloxane chains. In contrast, the water-soluble hydrophilic moieties of surfactants are much more varied. Based on their physicochemical properties, surfactants are generally classified as [99(a)]:

1. Anionic: Here the surface-active portion of the molecule bears a negative charge. They are commercially available as the salt form of an alkali metal (Na^+ or K^+). Common examples include: carboxylic acid salts; sulfonic acid salts; sulfuric acid ester salts; phosphoric and polyphosphoric acid esters; and fluorinated anionics.
2. Cationic: The surface-active moiety bears a positive charge. They are usually available as the halide salt form. Examples include: long-chain amines and their salts;

acylated diamines and polyamines and their salts; polyoxyethylenated long-chain amines; alkyl trimethylammonium bromides; and alkyl ammonium chloride.

3. Nonionic: Here the surface-active portion bears no apparent ionic charge. Their hydrophilic properties usually arise from hydroxyl groups. Examples include: alkylphenyl polyoxyethylene ethers; alkyl polyoxyethylene ethers; alkyl pyranosides; alkylpolyglycosides; and n-alkylpyrrolidinones, as described in the current study. N-alkylpyrrolidones, like polyvinyl pyrrolidone, act as complexing agents, particularly for phenols and other organic compounds that are capable of forming hydrogen bonds with the pyrrolidone ring.

4. Zwitterionic: Here both formal positive and negative charges may be present in the surface-active portion. Examples include: β-n-alkylaminopropionic acids; n-alkyl-β-iminodipropionic acids; imidazoline carboxylates; n-alkylbetaines; and sulfobetaines.

Several parameters are used to describe surfactant behavior. The most important with regard to biological solubilization are: 1) the critical micelle concentration (cmc); 2) the aggregation number (N); 3) the critical micelle temperature (cmt); and primarily for nonionics: 4) the cloud point (cp); and 5) the hydrophile-lipophile balance number (HLB).

In aqueous solution surfactant molecules can exist in the form of monomers and micelles. The critical micellar concentration (cmc) is a convenient, but inexact parameter in the description of micellar formation usually definable within a narrow concentration range. At low surfactant concentrations, below the cmc, only monomers exist, whereas at high concentrations (above the cmc) both monomers and

micelles can exist in equilibrium. For practical purposes the cmc thus represents the highest monomeric surfactant concentration (and thereby the highest surfactant chemical potential) obtainable. The cmc is usually definable within a narrow concentration range where micelles begin to form (Figure 3). The cmc is often determined by measuring the change in a particular physical property (such as, chemical potential, surface tension, conductivity, fluorescence, light scattering or interfacial tension) as a function of varying surfactant concentration [99(b)-100]. Figure 3 also shows the C_{20} parameter, which is defined as the concentration of surfactant in the bulk phase that produces a 20 dyn/cm reduction in the surface tension of the solvent [99(b)].

Micelles are fairly monodisperse compact aggregates where the apolar groups of the surfactant molecules are sequestered into the center and the polar groups form the "shell" of the micelle and are in contact with the aqueous environment. In contrast, so-called inverted or reverse-micelles can form in nonaqueous solvents. In these aggregates, the polar head groups are sequestered into the center of the micelle and the hydrophobic tails form the" shell" that are in contact with organic non-polar solvent (Figure 4) [100-101].

The aggregation number (N) is the number of monomeric surfactant molecules contained in a single micelle. It is calculated by dividing the micellar molecular weight by the molecular weight of the surfactant monomer. Several methods are available to determine the N value for a micelle and include light scattering, diffusion, viscosity, sedimentation velocity, ultra filtration, nuclear magnetic resonance (NMR) and fluorescence [102-106]. The aggregation process depends on

the surfactant type and the conditions of the system in which the surfactant is dissolved.

The cmt is the temperature at which a surfactant/solvent system passes from a hydrated crystalline state to an isotropic micellar solution. Some surfactants exhibit a consolute temperature or cloud point. At the cloud point, a surfactant solution passes from an isotropic micellar system to a two-phase system. One phase is depleted of surfactant and the other is rich in giant micelles. In general, the recorded cloud point is the temperature at which a warmed and cloudy 1% (w/v) surfactant solution clears upon cooling [107].

The hydrophile-lipophile balance (HLB) is a measure of hydrophilic character of the surfactant. It is simply calculated using one of several empirical equations. For the nonionic surfactants, HLB can be calculated using the following equation 1:

$$HLB = 20 \bullet \left(\frac{MH}{MH + ML} \right) \qquad (1)$$

Where *MH* is the formula weight of the hydrophilic portion of the molecule and *ML* is the formula weight of the lipophilic (hydrophobic) portion of the molecule. The most hydrophobic molecules have a low *HLB* value (1-10) and increasing *HLB* value corresponds to increasing hydrophilic character [9, 99(c)-100, 107-108].

Several generalizations can be made about the aggregation number (N) and the cmc value. First, the aggregation number (N) for micelles in aqueous media increases rapidly with increase in the length of the hydrophobic group of the surfactant molecule. An increase in the cmc is also observed with branching of the hydrophobic

tail. Addition of a double bond to the end of the hydrophobic tail decreases the hydrophobicity of the surfactant and thus increases the cmc value. Second, the factors that increase N tends to lower the cmc. Third, at and above the cmc concentration, micelles are roughly spherical and relatively dispersed. Fourth, in the presence of a polar organic solvent, the cmc of the surfactant increases. Fifth, in general, nonionic surfactants have lower cmc values than ionic surfactants with similar hydrophobic group. This is due to an increase in the hydrophobicity of nonionic surfactants as compared to ionic surfactants. Finally, the addition of salt lowers the cmc of ionic micelles and hence increases N. This is because ions decrease the repulsive forces among the charged head groups of the micelle, and with a consequent reduction in energy required for micelle formation. The structure of the micelle is dictated by equilibrium between the repulsive forces among hydrophilic “head” groups and attractive forces among hydrophobic “tails”.

A high cmc value is desirable whenever dialysis across a membrane is necessary, and in other situations where rapid removal or displacement of surfactant is required. On the other hand, a low cmc is desirable if one needs to measure the binding of surfactant to protein, so as to minimize the ratio of free to bound surfactant. With excess surfactant most or the entire lipid around the membrane protein is exchanged for the surfactant resulting in the formation of soluble protein-surfactant complexes and mixed lipid surfactant micelles. Often the concentration of surfactant required to obtain a desired effect depends on its cmc value, the micelle size, temperature and the nature of the membrane and surfactant [9, 108].

The physical properties of commonly employed non-ionic surfactants for membrane research are summarized in Table 1 [109-110].

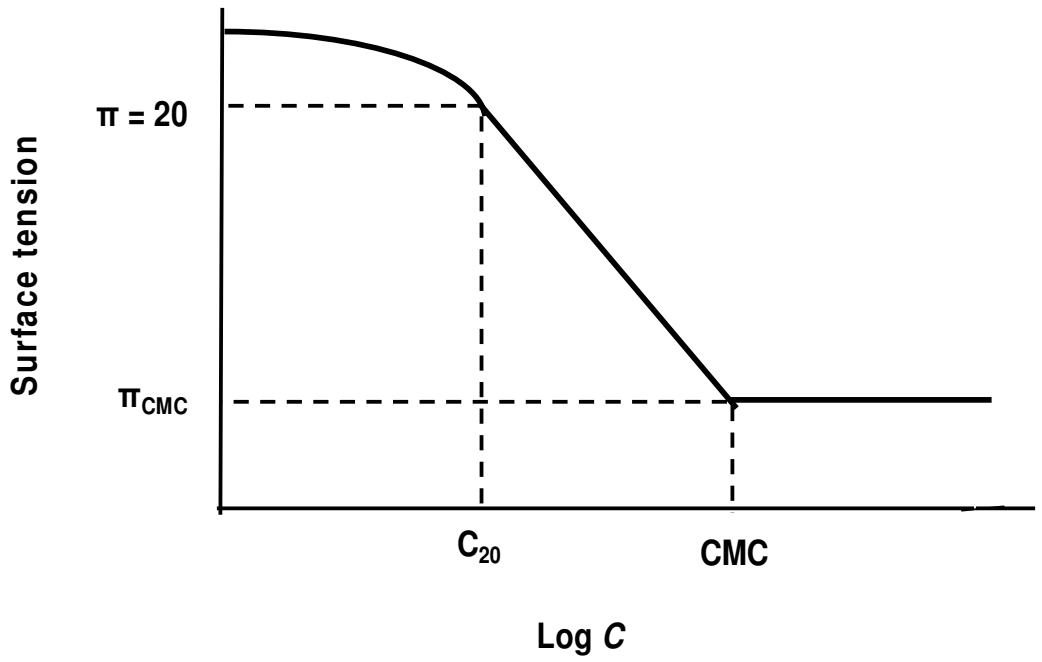

Figure 3: Surface tension versus Log *C* plot illustrating efficiency, -log C_{20} (pC_{20}), effectiveness of surface tension reduction, π_{CMC} and critical micelle concentration, CMC.

Adapted from Ref. 99, p.212. Rosen, M.J. *Surfactants and Interfacial Phenomena*, 3rd. Edition, John Wiley & Sons, Inc. 2004.

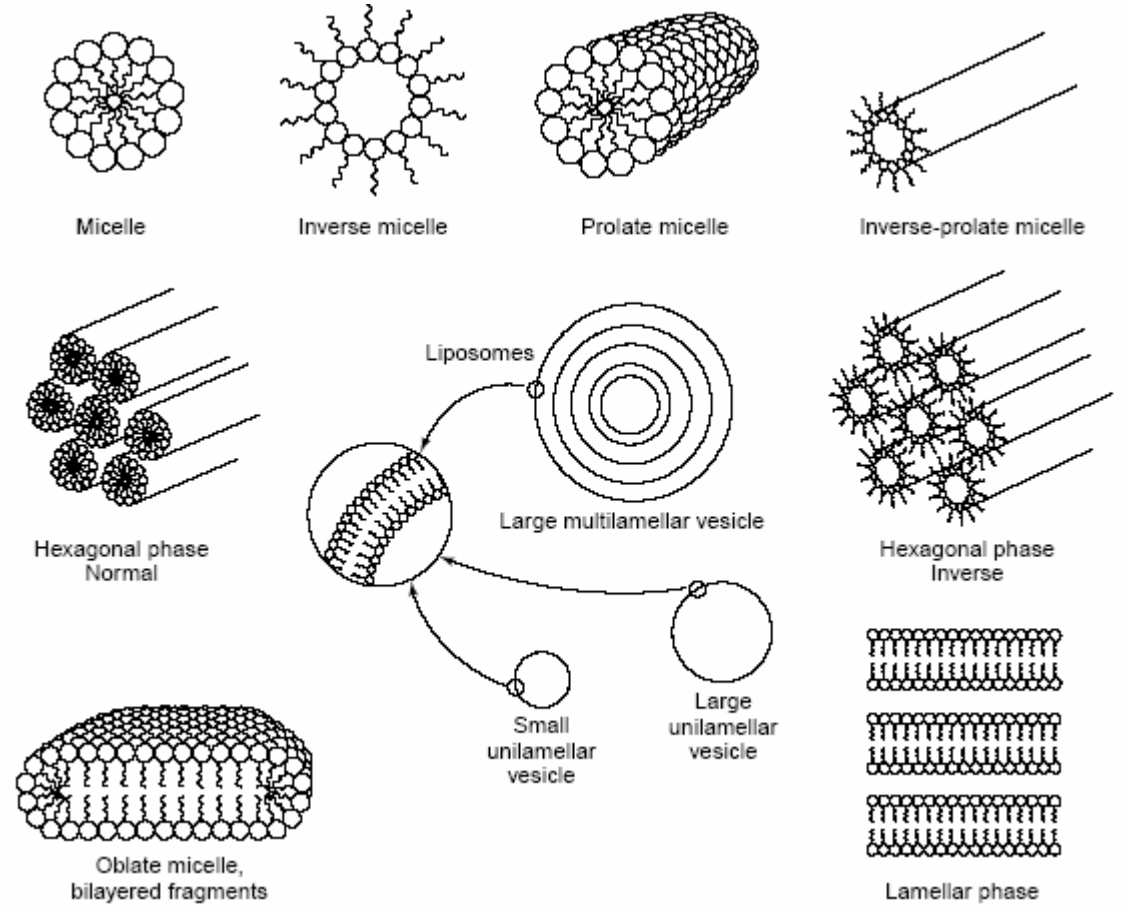

Figure 4: Micelle structures and self aggregation of polar lipid molecules.

Taken from Ref. 101. Lasic, D. D. Tibtech. *Novel Applications of Liposomes*. 1998, 16, 307-321.

Table 1
Physical properties of some common non-ionic surfactants
(From Ref.109-110)

Surfactant	***Molecular weight of monomer***	***Commercial name***	***cmc (mM)***	***N***	***HLB***	***cp (^0C)***
tert-$C_8\phi E_{7-8}$	536	Triton X-114 (TX114)	0.17	-	12.4	22
tert-$C_8\phi E_{9.6}$	628	Triton X-100 (TX100), Nonidet P-40 (NP40)	0.30	140	13.5	65
tert-$C_8\phi E_{9.6}$, reduced	634	Triton X-100, reduced (RTX100)	0.25	100-155	-	-
$C_{12}E_8$	539	Atlas G2127, POE(8) dodecyl ether	0.087	120	13.7	75
$C_{12}E_9$	583	POE(9) dodecyl ether	0.1	-	14.2	-
C_{12} sorbitan E_{20}	1228	Tween 20, polysorbate20	0.049	-	16.7	76
$C_{16}E_{10}$	683	POE(10) hexadecyl ether, Brij 56	0.19	-	13.4	68
$C_{18:1}$ sorbitan E_{20}	1310	Tween 80, polysorbate 80	0.01	-	15.0	65
Cyclohexyl-n-ethyl- β-D-Maltoside	452.5		120			
Cyclohexyl-n-hexyl- β-D-Maltoside	508.6		0.56			
Cyclohexyl-n-methyl- β-D-Maltoside	438.5		340			
n-Decanoylsucrose	496.6		2.5			
Decanoyl-N-methyl Glucamide	349	MEGA-10	7	-	-	-
Digitonin	1229			60		
n-Dodecyl- β-D-glucopyranoside	381	0.19	200			

Helenius, A., and Simons, K. Solubilization of membranes by detergents. *Biochim. Biophys. Acta*. 1975, 415, 29-79 [109].
Tanford, C., and Reynolds, J. A. Characterization of membrane proteins in detergent solution. *Biochim. Biophys. Acta*. 1976, 457, 133-170 [110].

Table 1
Physical properties of some common non-ionic surfactants
(From Ref.109-110)

Surfactant	***Molecular weight of monomer***	***Commercial name***	***cmc (mM)***	***N***	***HLB***	***cp (^{0}C)***
n-Dodecyl- β-D-maltoside	512		0.15	98		
N,N-Bis-3-D-glucon amido propyl-cholamide	850	BigCHAP	2.9	10	-	
n-Heptyl- β-D-glucopyranoside	278.3		79			-
n-Heptyl- β-D-thioglucoside	294		30			
Nonanoyl-*N*-methyl glucamide	335	MEGA 9	25	-	-	-
Octanoyl-N-methylglucamide	321	MEGA 8	58			
n-Octanol- β-D-glucosylamine	305.4	NOGA	80			
n-Octyl-β-D-gluco pyranoside	292	octylglucoside, OG	25	84	-	-
n-Octyl-β-D-thio glucoside	308	octylthioglucoside, OSG	9.0	-	-	-
6-O-(N-heptyl carbamoyl)-methyl-α-D-gluco pyranoside)	335.4	Hecameg	16.5			
n-Undecyl- β-D-maltoside	496.6		0.59			

Where cmc is the critical micelle concentration, HLB is the hydrophile-lipophile balance number, cp is the cloud point and N is the aggregation number.

Helenius, A., and Simons, K. Solubilization of membranes by detergents. *Biochim. Biophys. Acta*. 1975, 415, 29-79 [109].

Tanford, C., and Reynolds, J. A. Characterization of membrane proteins in detergent solution. *Biochim. Biophys. Acta*. 1976, 457, 133-170 [110].

1.5. N-Alkyl-2-Pyrrolidinones

N-Alkyl-2-pyrrolidinones (*N*-2-ethylhexyl-(C2,6P), *N*-octyl-(C8P), *N*-decyl-(C10P), and *N*-dodecyl-(C12P) 2-pyrrolidinone) are highly surface-active molecules which possess relatively small hydrophilic head groups. They are nonionic surfactants and show some of the properties of zwitterionics due to their dipolar resonance form (Figure 1C). The physical properties of these surfactants have been well studied [1-6]. They have limited solubility in water at 25ºC (room temperature) and consequently never reach a cmc value. Solubility limits have been reported for C2,6P (1.3×10^{-2} M) and C8P (5.2×10^{-3} M) in pure water. Molar absorptivities at 191 nm have been measured for C2,6P (8.11×10^{3} $M^{-1}.cm^{-1}$) and C8P (7.94×10^{3} $M^{-1}.cm^{-1}$) in distilled water [1].

In addition, preliminary effects of N-Alkyl-2-pyrrolidones on the mating of *Chlamydomonas rheinhardii* have been investigated by Forest [7]. These surfactants appear to inhibit gamete fusion in *Chlamydomonas rheinhardii* while allowing the gametes to retain their ability to specifically adhere to each other through their activated mating structures, mimicking the phenotype of fusion-defective mutants.

The interfacial properties (maximum surface (or interfacial) excess concentration, Γ_{max}; minimum area/molecule at the interface, A_{min}; efficiency of interfacial tension reduction, pC_{20}; effectiveness of interfacial tension reduction, Π_{max}; standard free energy of adsorption, ΔG^{0}_{ad}) of highly purified C2,6P and C8P have been investigated at the aqueous solution-air, Parafilm, Teflon, and hexadecane interfaces [1]. The results are summarized in Table 2.

At the aqueous solution/air interface, the effectiveness of the interfacial tension reduction (Π_{max}) for the N-alkyl-2-pyrrolidinones is greater than 40 mN/m, and compares favorably with other surfactants with a small hydrophilic head group. From the pC_{20} (efficiency of interfacial tension reduction) it appears that C8P is equivalent in surface activity and hydrophobic character to n-$C_8H_{17}OCH_2H_4OH$, whereas the ΔG^0_{ad} (standard free energy of adsorption) values for the two isomeric surfactants (C8P and C2,6P) are almost identical [1].

As expected from their chemical structure, a resonance hybrid of the nonionic and zwitterionic forms may exist for the N-alkyl-2-pyrrolidinones (Figure 1C), which has the potential to interact synergistically with anionic surfactants. Indeed, mixtures of the N-alkyl-2-pyrrolidinones (C2,6P, C8P, C10P and C12P) with commercially available linear alkylbenzenesulfonate (LAS) have been investigated [2]. The molecular interaction parameters, β^{σ} for mixed monolayer formation and β^{M} for mixed micelle formation with mixtures of the first three compounds of the N-alkyl-2-pyrrolidinone series: C2,6P; C8P; and C10P showed synergism in surface tension reduction efficiencies. All four compounds show synergism in the effectiveness of the surface tension reduction, when mixed in the proper proportions with LAS. However, C8P showed the greatest degree of synergism in surface tension reduction effectiveness and the greatest potential for foaming effectiveness.

Table 2

Interfacial Properties of N-Alkyl-2-pyrrolidones in Water and Aqueous 0.1 M NaCl at 25°C (From Ref.1)

Surfactant	*Interface*	Γ_{max}, (mol/cm^2× 10^{10})	A_{min} *(nm^2× 100)*	pC_{20}	Π_{max}, mN/m	ΔG^0_{ad}, kJ mol^{-1}
C2,6P	H_2O-air	3.57	46.5	3.00	42.9	-32.7
C2,6P	H_2O-Parafilm	3.30	50.3	3.09	42.8	-33.6
C2,6P	H_2O-Teflon	3.14	52.8	2.88	38.2	-32.7
C8P	H_2O-air	4.38	37.9	3.14	41.6	-32.4
C8P	H_2O-Parafilm	4.07	40.8	3.24	41.7	-33.3
C8P	H_2O-Teflon	3.72	44.6	3.04	36.0	-32.5
C8P	H_2O-hexadecane	3.92	42.4	2.99	44.9	-34.6
C8P	0.1M NaCl(aq)-air	4.27	38.9	3.21	41.1	-32.9
C8P	0.1M NaCl(aq)-Parafilm	4.14	40.3	3.23	40.6	-33.2
C8P	0.1M NaCl(aq)-Teflon	3.79	43.8	3.04	34.5	-32.6
C8P	0.1M NaCl(aq)-hexadecane	3.65	45.5	3.22	48.5	-36.5
n-$C_8H_{17}O$ C_2H_4OH	H_2O-air	5.2	32	3.17	45.0	-31.8
n-C_8H_{17}CH-OH-CH_2OH	H_2O-air	5.1	33	3.63	48.6	-34.3

Rosen, M. J., Zhu, Z. H., Gu, B., and Murphy, D.S. Relationship of structure to properties of surfactants. 14. Some N-Alkyl-2-pyrrolidinones at various interfaces. *Langmuir*. 1988, 4(6), 1273-1277 [1].

In alternate study Rosen *et al.,* investigated the interactions of C2,6P, C8P, C10P, and C12P with LAS and sodium dodecanesulfonate (C12SNa) [3]. Mixtures of C8P and C12SNa showed synergism in the surface or interfacial tension reduction efficiency at the aqueous/air, aqueous/parafilm, aqueous/Teflon, and aqueous/hexadecane interfaces, both in pure water and in 0.1M NaCl. C8P-C12SNa mixtures in 0.1 M NaCl provided the greatest degree of synergism at the aqueous solution/air interface of this type of all the C8P-C12SNa mixtures studied at various interfaces. C8P-LAS mixture also showed the greatest degree of synergism of all the N-alkyl-2-pyrrolidinone-LAS mixtures investigated.

N-alkyl-2-pyrrolidinones form mixed micelles with LAS and C12SNa, which increase their water solubility and permit them to reduce the surface tension of the solution to lower values at 25 ºC. Such behavior may be predicted for their interactions with lipid bilayers.

Interfacial and micellar properties of mixtures of N-Alkyl-2-pyrrolidinones and dimyristoylphosphatidylcholine (DMPC) have not been investigated. Phospholipids belong to another category of biological surface active compounds, which are involved in numerous biological activities e.g., membrane solubilization, DNA extraction, drug delivery [98, 101, 111-118]. Industry is always in need of novel and more surface active compounds, so that better performance can be achieved in more economical ways. N-alkyl-2-pyyrrolidinones have a very high surface activity and interact synergistically with other surfactants to increase their foaming and wetting properties. The basic mechanism involved in such interactions is related to the mixed micellization effect between the surfactant and phospholipid monomers. Such

behavior is expected with the interaction of lipid bilayers with N-alkyl-2-pyrrolidones, which provides the motivation for this work.

1.6. Lipid Bilayer and Lipid Vesicles

1.6.1. Lipids

There is no strict definition of the term lipid that is generally accepted [119]. A good definition was recently proposed by Christie: “Lipids are fatty acids and their derivatives, and substances related biosynthetically or functionally to these compounds” [120]. Lipid molecules, primarily phospholipid molecules, are the basis from which cells and cell organelles are constructed. These small cellular bodies derive their function through the operations of protein molecules. All of the lipid molecules in the plasma membrane are amphiphilic. They have a hydrophilic (“water-loving” or polar) head and a hydrophobic (“water-hating” or nonpolar) tail (Figure 5). Polar head groups can range chemically from carboxyl groups in single-chain surfactants to alcohols, amino acids, or amines esterified to the phosphate group in biological lipids. The head groups can be charged (positively or negatively), zwitterionic, or non-charged polyhydroxylated moieties. Here the polar character is also due to hydroxyl groups which can form many hydrogen bonds with water. The water insoluble part consists normally of one or two fatty acid chains. Chain lengths in these diacyl lipids range from 8 to 24, mostly from 14 to 18 carbon atoms, and they can be fully saturated (all carbon-carbon bonds are single bonds) or unsaturated with one to four double bonds. The double bonds found in fatty acids are most normally in the *cis* configuration although the *trans* configuration has been identified. Natural

lipids, compared with pure synthetic lipids, exhibit a greater diversity in the composition of the fatty acid chains.

The three major kinds of membrane lipids are phospholipids, glycolipids, and cholesterol. The most abundant are the phospholipids. The platform on which phospholipids are built may be glycerol, a 3-carbon alcohol (phosphoglycerides) or sphingosine, a more complex alcohol (sphingolipids) [98]. The term phospholipid is generally understood to mean a lipid containing a phosphate moiety. As used in this thesis, the term phospholipid, unless otherwise indicated is intended to denote a phosphoglyceride; i.e, a phospholipid contains a glycerol-phosphate moiety. For phosphoglycerides, a glycerol group provides a bridge that covalently links the fatty acid chains and a negatively charged phosphate group. This is bound further to a characterizing headgroup moiety that defines the different classes of phosphoglycerides. Two major classes of phosphoglycerides that can be found in common animal cells are phosphatidylcholines (PC), i.e. or lecithins, and phosphatidylethanolamines (PE). Phosphatidylcholines have a tertiary amine as the polar head group whereas phosphatidylethanolamines have an ethanolamine (primary amine) head group. Phospholipids usually have one acyl chain with one or more *cis*-double bonds (unsaturated), while the other lipid tail is saturated. Differences in the length and saturation of the fatty acid chains are important because they influence the ability of phospholipid molecules to pack with one another, and can affect the fluidity and ordering of the membrane.

The amphiphilic nature of lipid molecules defines their ability to form different aggregates in water or water solutions. Simple mixing of lipid and water results in

lipid assembly in the solution and at interfaces (Figure 4). At the air-water interface the lipids form a monolayer. In solution, amphiphiles form aggregates starting from monomers, sometimes aggregating into dimers and trimers, leading to micelles and bilayers [101]. The lipid aggregates are stabilized primarily by hydrophobic interactions, which are driven by the inability of lipid hydrocarbon chains to hydrogen bond with water. In terms of free energy, the mixing of hydrocarbon chains and water causes a decrease in entropy (the entropy of water is decreased at the interface between hydrocarbon and water). Other stabilizing forces are van der Waals interactions between the hydrocarbon chains, electrostatic interactions and hydrogen bonds between the polar heads. At the interface between the hydrocarbon chains and water, there exists a higher energy state because hydrogen bonds are lost. It is energetically favorable for the hydrocarbon chains to associate with each other and so minimize the surface area of contact with water. The other major forces: hydrophilic; ionic; or steric repulsion of the headgroups impose the opposite requirement that they remain in contact with water. These two interactions compete giving rise to 'opposing forces' [121] acting mainly in the interfacial region: one interaction tending to decrease and the other tending to increase the interfacial area per molecule exposed to the aqueous phase. The opposing forces of headgroup repulsion and interfacial hydrophobic attraction are balanced at the optimal lipid headgroup area, a_0.

It has been shown previously [122] that for lipids of optimal area (a_0), hydrocarbon volume (v), and critical chain length (l_c), the value of the dimensionless packing parameter or shape factor, $v / a_0 l_c$, will determine whether lipids form spherical micelles $\left(v/a_0 l_c < 1/3\right)$, non-spherical micelles

$(1/3 < v/a_0 l_c < 1/2)$, vesicles or bilayers $(1/2 < v/a_0 l_c < 1)$, or 'inverted' structures $(v/a_0 l_c > 1)$. Each of these structures corresponds to the minimum-sized aggregate. Lipids that form bilayers do not pack into micellar structures due to their small headgroup area a_0, or because their hydrocarbon chains are too bulky to fit into such small aggregates while maintaining the surface area at its optimal value. Therefore, lipids with two chains are likely to form bilayers, and indeed most of them do, such as di-C_{14} and di-C_{16} lecithins. Also, increasing hydrophobicity lowers the cmc of the lipids. The cmc of the micelle-forming lipids are in range of 10^{-2}-10^{-5} M whereas bilayer-forming lipids the cmc range is of 10^{-6}-10^{-10} M.

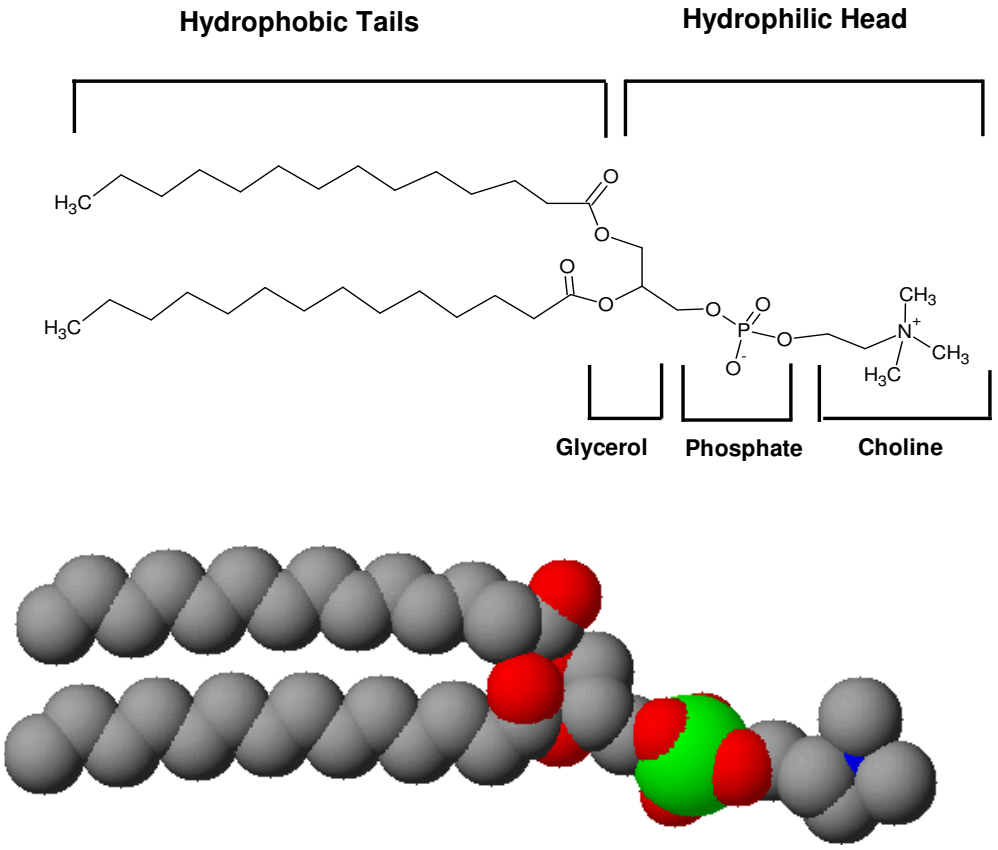

Figure 5: A) Structural features of lipids, using dimyristoylphosphatidylcholine (DMPC) as an example. B) Space-filling model of dimyristoylphosphatidylcholine (DMPC)

1.6.2. Lipid Vesicles

Amphiphilic molecules, including lipids, can be used to form hydrophobic and hydrophilic compartments within an aqueous environment. As such, the term 'liposome' was first introduced by Bangham and Horne [123] in the early 1960s to define a lipid bilayer structure which encloses an aqueous volume protected by a membrane. Vesicles have been used extensively as model systems to try to understand more complicated membrane mediated cellular processes. Vesicle size can range from nanometers to tens of microns in diameter. As such they are useful tools for studying critical biological questions including: membrane permeability; cellular transport; endo- or exocytosis; mechanical or rheological properties; and fusion of membranes. Versatility of the vesicle size is one advantage to using vesicles, and a main reason they are used as model systems. In particular, depending on the preparation technique used, it is possible to create a range of vesicles with both different sizes and lamellarities.

Vesicles can be unilamellar or multilamellar, depending on the number of bilayer shells. Small unilamellar vesicles (SUV), large unilamellar vesicles (LUV) and large multilamellar vesicles (MLV) or multivesicular vesicles (MVV) exist as discrete and differentiated self assembled systems (Figure 6). Vesicles enclosing a number of smaller vesicles are called multivesicular vesicles. SUVs can range in diameter from 20 to approximately 100 nm. LUVs, MLVs, and MVVs range in size from a few hundred nanometers to several microns. The term giant unilamellar vesicles (GUV) with diameters ranging from 1-20 μm [124-125] are also used as large vesicles with a single bilayer surrounding entrapped solvent for optical microscopy studies.

The thickness of the membrane (phospholipid bilayer) measures approximately 5 to 6nm. It is important to note that there are chemical differences between micelles and vesicles. As shown in Figure 7, a vesicle in aqueous solution displays nine different regions for solute interaction [126]. These regions include the outer bulk water region, the hydration sphere, the hydrophobic membrane close to the outer head groups, the similar four inner regions in the water pool direction, and the hydrophobic core of the vesicle. In contrast, micelles provide less available sites for solute localization/solubilization. Interaction of a given solute with normal micelles is restricted to the first four regions mentioned above and in some cases the hydrophobic core of the micelle itself [127].

1.6.3. Gel to Liquid-Crystalline Phase Transition in Model Bilayers

Biological membranes consist of numerous lipid, protein, and carbohydrate-containing molecular species that undergo various interactions with each other and with elements of the extra-and intracellular environment of the membrane. Due to this complexity, the properties of membrane phospholipids have most often been studied using model bilayers, such as liposomes, in which the phospholipid composition can be manipulated in a well–defined manner. One feature of model bilayers that has attracted the attention of membrane biophysicists is the thermally induced gel to liquid-crystalline phase transition (T_m). In the bilayer gel phase, the phospholipid hydrocarbon chains assume a nearly all-trans conformation and are closely packed. On passing through the phase transition (by increasing the temperature), the phospholipid hydrocarbon chains cooperatively “melt” at a characteristic temperature, T_m, in an endothermic event caused by the introduction of gauche conformations into

the hydrocarbon chains, with concomitant weakening of van der Waals chain contacts, and changes in the hydration and polar interactions of the phospholipid headgroups. These processes result in a lateral expansion within the plane of the bilayer on melting that is accompanied by a thinning of the membrane in the liquid-crystalline phase (Figure 8). It is well established [128] that the phase transition behavior of phosphoglycerides is dependent on the length(s) of the two lipid hydrocarbon chains, the degree of unsaturation of the chains, the positions of the unsaturated carbon bonds in the chain, the nature of the chain linkages to the glycerol moiety of the phospholipid, and the chemical nature of the phospholipid headgroup.

For charged phosphoglyceride headgroups, the thermotropic behavior of the bilayer is coupled to the pH, ionic strength, and ionic composition of the aqueous phase [129]. A series of T_m values for amphiphiles that have been determined for differing lipid vesicle preparations are summarized in Table 3 [128]. These values have been obtained experimentally and T_m values depend to some extent, on the experimental conditions particularly if the amphiphiles used have polar head groups that can undergo protonation-deprotonation (e.g. phosphatidic acid) [130]. The presence of cholesterol can lead to a drop in T_m (reduced cooperativity of the transition), as cholesterol interacts with the membrane lipids in a complex manner [124], thereby disturbing the intermolecular interactions resulting in an inhibition of the formation of the crystalline-analog state in the case of DPPC [124], or formation of cholesterol-rich and lipid-rich domains [131]. In addition, T_m values also depend to some extent on the curvature of the bilayer [130]. In analogy to the case of cholesterol, the use of lipid mixtures may result in the formation of domains within

the bilayers, which are enriched with one of the lipids, resulting typically in multiple peaks in T_m measurements [132-135]. In some cases, e.g., with phosphatidylcholines, the major phase transition is preceded by a lipid pretransition, which is associated with changes in orientation of the hydrocarbon chains [98]. These changes have been studied extensively by a variety of physical techniques, including X-ray diffraction [136], nuclear magnetic resonance [137-138], electron paramagnetic resonance [139-141], differential scanning calorimetry [132-135, 141-149], and fluorescence spectroscopy [142-144, 146-156].

Studies of phospholipid phase transitions in model bilayers have enriched our understanding of the thermodynamics that govern lipid interactions in bilayers and how they are affected by the chemical composition and molecular geometry of the lipids. This knowledge, in turn, provides a framework for understanding how the physical properties of lipids could be coupled to biomembrane processes in the physiological state. More directly, the relationship of the chemical composition of membrane lipids to their thermotropic properties has provided a basis for understanding how prokaryotes, such as microorganisms, modulate the lipid composition of their membranes in response to changes in the temperature and pressure of their environment (adaptive response) so as to maintain the membrane in a functional fluid state [157]. Additionally, many biological membranes exhibit a thermally broad and poorly cooperative phase transition arising from the heterogeneous lipid fraction of the membrane. In many instances the normal physiological temperature of the organism lies within, or near, the temperature range encompassed by this broad phase transition. Several studies suggest that membrane

protein function could be coupled to the properties of the lipid bilayer through the fluctuation behavior of the lipids or through lipid compositional lateral phase separation: two phenomena associated with the lipid phase transition. Finally, the study of bilayer phase transitions is of practical value in the burgeoning field of liposome technology [129].

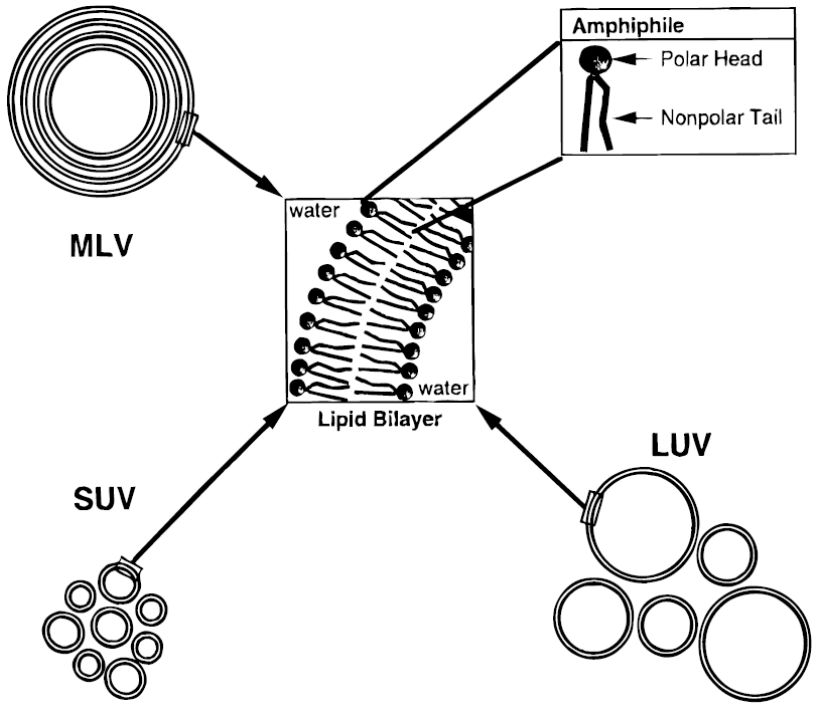

Figure 6: Schematic illustration of liposomes of different size and number of lamellae. SUV: Small unilamellar vesicles; LUV: Large unilamellar vesicles; MLV: Multilamellar vesicles. (Taken from http://www.avantilipids.com)

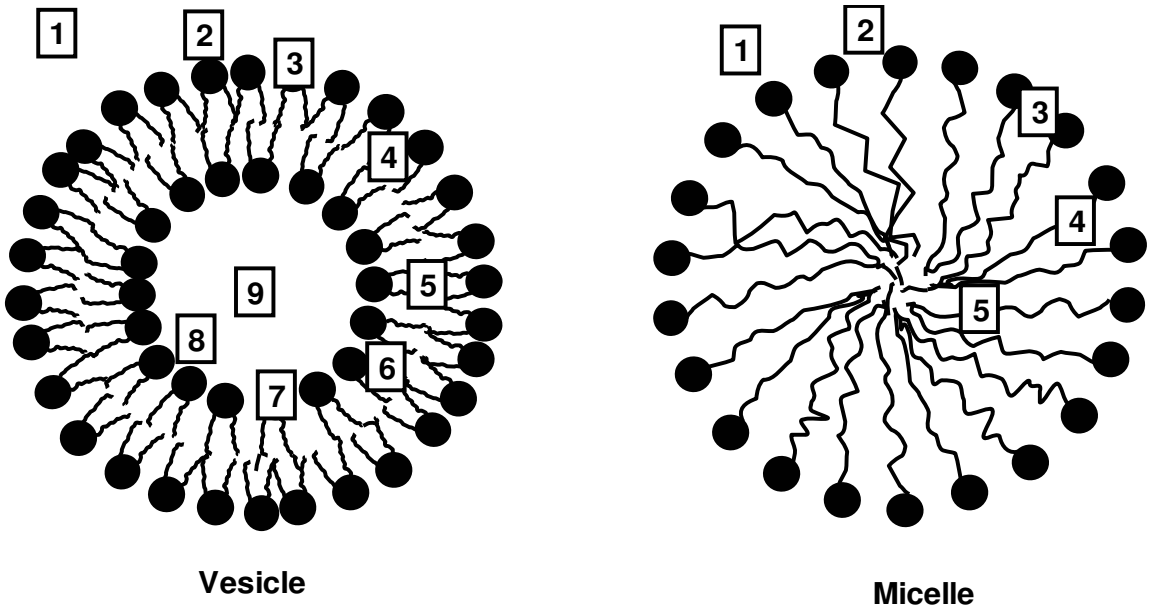

Figure 7: Available sites for solute interaction/solubilization in vesicles and micelles.

Adapted from Ref. 126. Fuhrhop, J-H., and Mathieu, J. Routes to functional vesicle membranes without proteins. *Angew. Chem. Int. Ed. Engl*. 1984, 23, 100-113.

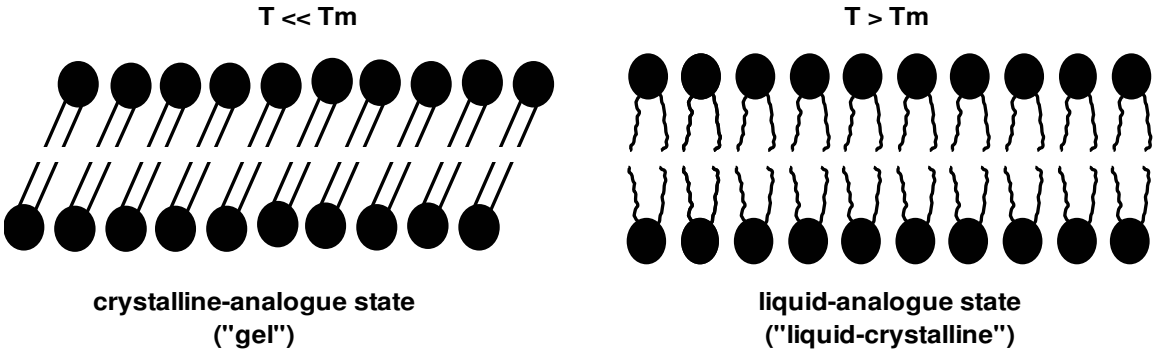

Figure 8: Schematic representation of the gel and liquid-crystalline phases of a bilayer. The transformation occurs at the temperature T_m.

Adapted from Ref. 129. Mason, J. T. Ackers, G. K., and Johnson, M. L. (Eds.). Investigation of phase transitions in bilayer membranes. *Methods in Enzymology*, 1998, 295, 468-494.

Table 3
Selected Physical Properties of Diacyl Phosphatidylcholine-Water Systems
(From Ref. 128)

Acyl chain length	*PC name*	*State in water*	T_m (°C)	*Heat absorbed at* T_m *(kcal/mol) phospholipid*
12	dilauryl PC (DLPC)	bilayer	0	-
14	dimyristoyl PC (DMPC)	bilayer	23	6.65
16	dipalmitoyl PC (DPPC)	bilayer	41	8.65
18	distearoyl PC (DSPC)	bilayer	58	10.70
22	dibehenoyl PC (DBPC)	bilayer	75	14.90
18:1	dioleoyl PC (DOPC)	bilayer	-22	7.6
mixture	egg PC	bilayer	-11	-

Taken from Chapman, D., Williams, R. M., and Ladbrooke, B. D. Physical studies of phospholipids. VI. Thermotropic and lyotropic mesomorphism of some 1, 2 diacylphosphatidylcholines (lecithins). *Chem. Phys. Lipids*. 1967, 1, 445. [128].

1.6.4. Vesicle Applications

The applications of vesicles are widespread. They are important in many areas of science and technology. In basic research, phospholipid vesicles serve as models for cell membranes and their fusion, transport studies, and investigations of membrane proteins that can be reconstituted in vesicles. Eye-catching applications are found in the medical field, including specific drug delivery to e.g., cancer cells [111]. Hydrophilic drugs can be encapsulated in the hydrophilic core of the vesicles whereas hydrophobic drugs can be sorbed in the alkyl/acyl chain region. Amphiphilic drugs are sorbed in both regions. Vesicles may seem to have a bright future ahead as drug vehicles. However, despite the extensive research, major deficiencies are still faced: limited encapsulation capacity, lack of control of drug release, lack of means to override biological barriers such as the blood-brain barrier, immuno activity, and often inefficient active targeting [112-113]. Only in 1990, was the vesicle-sorbed amphotericin approved in medicine as the first vesicle-based product [114]. Higher amphotericin doses could be administered as toxicity was reduced considerably without loss of efficacy against fungal infections [112, 115]. Several vesicle-formulated drug products are now commercially available. Delivery of DNA to cells using cationic vesicles has been studied intensively [116], as replacement for viral vectors, which are limited in terms of size of the foreign gene that can be introduced and which may possibly lead to infections or cancer [117]. DNA delivery by vesicles still suffers from a lack of target specificity. Nevertheless, several gene delivery applications of vesicles have been clinically tested [112].

Although the vast majority of patents have been granted in the biomedical field, other important vesicle applications exist. A vesicle technique that increases chroma and edge acuity of dye based inks was patented by Kabalnov [158]. Vesicles are also used in cosmetic products [159] such as ointments or toothpastes [160]. Further, several commercial fabric softeners comprise multilamellar cationic vesicle dispersions [161].

1.7. Interaction of Surfactants with Vesicles

Surfactant micelles have the ability to solubilize insoluble or only sparingly soluble materials in aqueous media by incorporating them within the micellar interior to form mixed micelles. Phospholipids and other constituents of biomembranes can also be solubilized by surfactant micelles. Due to solubilization properties, surfactants are widely used as molecular tools in membranelogy. One of their applications is disintegration of biomembranes to mixed micelles for the purpose of isolation and purification of membrane proteins. A reverse course for solubilization is also possible; the removal of surfactant molecules from the solution of surfactant/phospholipid micelles by appropriate methods, such as gel filtration or dialysis, leads to the formation of phospholipid vesicles. Thus, surfactants are utilized in reconstitution of functional membrane systems, as well as in preparation of phospholipid vesicles of homogeneous and controlled size.

According to Lichtenberg's three-stage model [108, 162-163]: Stage 1) Starting at low surfactant concentrations, the first step is a partitioning of the surfactant into the membrane bilayer which affects various membrane properties such as membrane

fluidity, membrane permeability, and bilayer phase transition; Stage 2) With increasing partitioning of surfactant within the bilayer, a point of saturation is reached (Re^{sat}), marking the conversion of surfactant-saturated bilayers into mixed micelles. Here mixed surfactant/lipid bilayers coexist with mixed micelles. At a critical molecular ratio of surfactant to lipid (Re^{sol}), the onset of membrane solubilization occurs. Increasing the surfactant concentration beyond this critical limit produces a gradual disruption of the bilayer until all vesicles are transformed into micelles; Stage 3) Only micelles exist.

Most of the physiologically active agents, including various drugs, are amphiphilic molecules or ions. Due to their amphiphilicity, they can interact with biomembranes and exhibit their bioactivity. It is believed that perturbation of membrane properties induced by a foreign molecule can be relevant to certain biological functions of the bioactive agents. Hence, the investigation of the interactions between a small amphiphilic molecule and model membrane is useful for understanding the mechanism of action of drugs on the molecular or supramolecular level. Surfactants are also typical amphiphiles, and the amphiphilicity can be readily controlled by combining various types of head groups and hydrocarbon tails. Thus, the surfactant/vesicle system may serve as a favorable model system for the systematic study of the interaction between amphiphilic ligands and phospholipid bilayer membranes.

In practice, application of vesicles as a tool of drug delivery requires that they act as a tight container for a given drug, and can release their contents under desired conditions. The efficiency of the membrane barrier of vesicles can be influenced by

their interaction with amphiphilic molecules, particularly when the vesicles are introduced into physiological fluids. Thus, it is important to know the manner in which the vesicular content is released in the presence of foreign molecules [8] for efficient drug delivery systems. Studies of surfactant on the barrier efficiency (or permeability) of vesicle membranes can provide useful information about this problem.

In general, the nonionic surfactants are suited for disrupting lipid-lipid and lipid-protein interactions of membranes, as they are essentially ineffective in breaking interactions between proteins. The non-denaturing properties of these surfactants have resulted in their wide use for the isolation of membrane proteins in biologically active forms [9]. In particular, Triton X-100 and other surfactants of the polyoxyethylene series (Lubrol and Tween type) are widely used in membrane biology for solubilization and reconstitution of membrane-bound receptors, enzymes and antibodies in order to analyze protein conformation and functional activity [109, 164]. Members of the alkyl polyoxyethylene ether non-ionic surfactant class have the general formula C_nH_{2n+1} $(OCH_2CH_2)_xOH$, abbreviated C_nE_x. For those ethers which contain a phenyl ring between the alkyl group and the polyoxyethylene chain (abbreviated $C_n\phi E_x$) such as the Tritons, the polar group is generally larger than the hydrophobic tail. As a result, the solution properties of these detergents are quite different from those of the ionic surfactants for which classical micellar behavior and structure are derived. This property provides many advantages for membrane solubilization [33, 38-39, 44, 52, 83, 102, 105, 108, 165-173], although their

bulkiness can limit the surface activity since close packing of the surfactant molecules at the interface is not possible.

Another nonionic surfactant which is particularly useful for membrane solubilization and reconstitution studies is octyl glucoside (OG) which, due to its very high cmc of about 25 mM, facilitates its rapid removal from mixed micellar complexes and does not denature membrane proteins easily [9, 27, 29-31, 40, 45, 74, 174].

In contrast, alkyl ionic surfactants, such as the commonly used sodium dodecyl sulfate (SDS), are usually denaturants at the concentrations and temperatures that are typically used for complete solubilization of membranes. Furthermore, they usually dissociate complex proteins into their constituent polypeptide chains. SDS, an anionic surfactant, is the standard surfactant used for complete membrane disruption and separation of multimeric proteins to their monomeric form [9, 41, 43, 46-48, 51, 85, 168-169, 175]. Other alkyl anionic surfactants (the alkyl and alkyl aryl sulfates and sulfonates; the alkyl sarcosinates, etc.) and cationic surfactants (the alkylamines, the quaternary amines, the alkyl pyridinium derivatives, etc.) are often not as effective denaturants as SDS, but must be treated with caution if the intact protein structure is to be retained. Thus ionic surfactants are useful for breaking protein-protein interactions.

Membrane proteins with high hydrophobicity have a tendency to associate non-specifically with other proteins when solubilized. In such cases, non-ionic surfactants are often not able to prevent protein aggregation. In contrast, ionic surfactants, while preventing aggregation, are often too harsh, resulting in denaturation and inactivation

of the proteins. In such cases, zwitterionic surfactants such as CHAPS or N-decyl-N, N,-dimethyl-3-ammonio-1-propanesulfonate may be used for solubilization of proteins of high hydrophobicity, while maintaining a non-denatured form [46, 104, 176].

Since all surfactants have an amphiphathic structure, the question arises as to why ionic surfactants denature most proteins while nonionics do not? The answer clearly must lie in the nature of the headgroup interactions.

Ionic surfactants contain a head group with a net charge that can be either anionic or cationic. They also contain a hydrophobic hydrocarbon chain or steroidal backbone. The cmc of an ionic surfactant is determined by the combined effect of the head group repulsive forces and hydrophobic interactions of the tails. Anionic surfactants will bind to cationic sites (lysyl, histidyl, and arginyl residues), while cationic surfactants will bind to anionic sites (glutamyl and aspartyl residues). While headgroup interactions with charged sites on the protein surface are electrostatic, the surfactants alkyl chains interact hydrophobically with hydrophobic patches on the protein. In general, at concentrations lower than the cmc, monomeric surfactant binds to the protein, while at higher concentrations they form micelles that denature proteins by electrostatic and hydrophobic interactions [10, 177].

Nonionic surfactants contain uncharged head groups. The binding of nonionic surfactant can only involve relatively weak head group interactions, such as hydrogen bonding, so that the predominant interactions will be hydrophobic, involving the alkyl chains.These interactions are insufficiently strong to bring about protein unfolding. In fact, in the case of globular proteins there is considerable disagreement as to whether

nonionic surfactants such as OG bind to globular proteins at all, although there is no doubt that they can bind hydrophobically to membrane proteins [10, 177].

Hence, there is a great interest in identifying surfactants with predictable solubilization and reconstitution characteristics for use in membrane research and pharmacological applications. The choice of a particular surfactant molecule for such applications is based on non-evasive chemical and physical properties, including surfactant solubility and critical micelle concentration. Various techniques such as fluorescence spectroscopy [27-55, 178] turbidity [165-168, 174, 179-181], dynamic light scattering [102-105, 169, 175], NMR [104-105, 169-172], X-ray diffraction [173, 182-184], isothermal titration calorimetry [74-92], and surface tension [106, 176, 185-190] have been used to analyze the surfactant partitioning into lipid bilayers and surfactant induced solubilization of lipid vesicles.

1.8. Methods Used in this Study to Investigate Interactions of Surfactants with Phospholipid Vesicles

1.8.1. Surface Tension

The thermodynamic definition of wetting is rooted in the concept of surface energy or surface tension. Surface tension is a measurement of the cohesive energy present at an interface. At the surface of a liquid, the molecules are attracted to each other and create forces that pull themselves together. Molecules on the surface of a liquid experience an imbalance of forces. The net effect of this situation is the presence of free energy at the surface. The excess energy is called surface free energy and can be quantified as a measurement of energy per area. Alternatively, the

interface may be described as having a line tension or surface tension which is quantified as a force per length measurement. The common units for surface tension are mN/m in SI units which are equal to dynes/cm in the older cgs units. The surface tension either decreases, or is unaffected to any great extent, but it never increases greatly. High surface tension indicates that the molecules at the interface tend to interact strongly, such as in water which has a high degree of hydrogen bonding. Organic molecules have weaker bonds and consequently lower the surface tension. Substances that lower the surface tension also lower the free energy of the surface. Thus such substances will concentrate at the surface and can give rise to large decreases in surface tension; substances that increase the surface tension will avoid surfaces and consequently give only small increases in surface tension.

A number of techniques have been developed for determining surface tension, including methods that involve measurements of capillary height, maximum bubble pressure, drop weight, sessile drop, spinning drop, stalagmometer, and vibrating jets. However, the most prevalent techniques are the force methods: Wilhelmy plate and du Nouy ring methods. In these methods, the time dependence of the surface tension is followed until one is satisfied that equilibrium is reached. The method used in this study is the Wilhelmy plate method. The method developed by L. Wilhelmy in 1863 [191], is especially suited to the measurement of surface tension over long time intervals. It employs a thin vertical plate, usually a platinum blade of known perimeter, attached to a microbalance. The surface tension of the liquid, assuming a zero contact angle (complete wetting of the plate), is determined by direct measurement of the weight of the meniscus formed on the perimeter of the plate

divided by the plate's perimeter [192]. The corresponding equation for the vertical force, (F) is:

$$F = \gamma P Cos\theta_r \qquad (2)$$

Where P is the perimeter and θ_r is the receding contact angle.

When surfactant molecules are dissolved in solvent (usually in water) they can arrange themselves in two different ways at the air-liquid interface: 1) The adsorption process occurs at low surfactant concentration, in which surfactant molecules migrate toward the interface and orient their hydrophobic groups away from solvent water, avoiding contact between water molecules and surfactant hydrophobic groups to minimize the free energy increase. 2) At higher surfactant concentration, micellization process occurs as the surface becomes crowded with surfactant and molecules arrange themselves into micelles or vesicles to minimize the free energy (maximize the entropy) of the system (Figure 9).

The dependence of surface or interfacial tension on the amount of surfactant in the solution phase is described by the Gibbs adsorption equation:

$$d\gamma = -\sum_i \Gamma_i d\mu_i \qquad (3)$$

Where:

$d\gamma$ is the change in surface or interfacial tension of the solvent, Γ_i is the surface excess concentration of any component of the system, $d\mu_i$ is the change in chemical potential of any component of the system.

At equilibrium between the interfacial and bulk phase concentrations,

$$d\mu_i = RTdlna_i \qquad (4)$$

Where:

a_i is the activity of any component in the bulk (liquid) phase, *R* is the gas constant, and *T* is the absolute temperature.

A typical equilibrium surface tension (γ) versus log bulk surfactant molar concentration (C) plot is shown in Figure 3. From this curve, several key surfactant properties can be determined. The difference between solute concentration in the bulk and that at the interface is the surface excess concentration (Γ) and related to surface and interfacial tension by the Gibbs Adsorption Equations (3-4), which in its practical form, is as follows:

$$\Gamma = -\frac{1}{2.303nRT}\left(\frac{\partial\gamma}{\partial logC}\right)_T \qquad (5)$$

Where:

$(\partial\gamma/\partial\ log\ C)_T$ is the slope in the γ vs. *log C* plot; *T* is the absolute temperature and R is the universal gas constant (8.314 J•mol^{-1}•K$^{-1)}$.

The factor n, an integer, is a constant depending on the number of species/ surfactant adsorbing at the interface. For a non-ionic or a uni-univalent ionic surfactant in the presence of excess electrolyte as the counterion, n=1. For a univalent ionic surfactant in the absence of supporting electrolyte, n=2 is used. For bis(quaternary ammonium) surfactants, one should use n=3. It has been argued,

however, that for bis(quaternary ammonium) surfactants, one counterion is associated with one ionic head, and thus a value of n=2 should be used [192]. For the surfactant mixtures, $n = n_1X_1 + n_2X_2$, where n_1 and n_2 are the number of species of surfactant 1 and 2, respectively, whose interfacial concentration changes with the change in surfactant bulk phase concentration; X_1 and X_2 are the molar fractions (on a surfactant only basis) of surfactants 1 and 2, respectively, at the interface.

Once the surface excess concentration (Γ) is known, the area per molecule of adsorbed surfactant (A_{min}) in Å^2 can be calculated using the following equation [99(d)]:

$$A_{min} = \frac{10^{16}}{N\Gamma} \qquad (6)$$

Where:

N is the Avogadro's number (6.023×12^{23} molecules per mole). The area per molecule at the interface provides information on the degree of packing.

The break point in the curve (Figure 3) indicates the concentration at which surfactant molecules begin to aggregate and form colloidal-sized clusters known as micelles (cmc). The corresponding surface tension at this concentration, symbolized by Π_{cmc}, indicates the effectiveness of surface tension reduction by this surfactant. The concentration, at which the surface tension has been reduced by 20 mN/m compared to pure solvent, is defined as C_{20} (Figure 3). When the surface tension is decreased by 20, the air/aqueous solution interface is expected to (normally) be 80-

100% covered by surfactant molecules. Thus C_{20} indicates the efficiency of surface tension reduction by a surfactant.

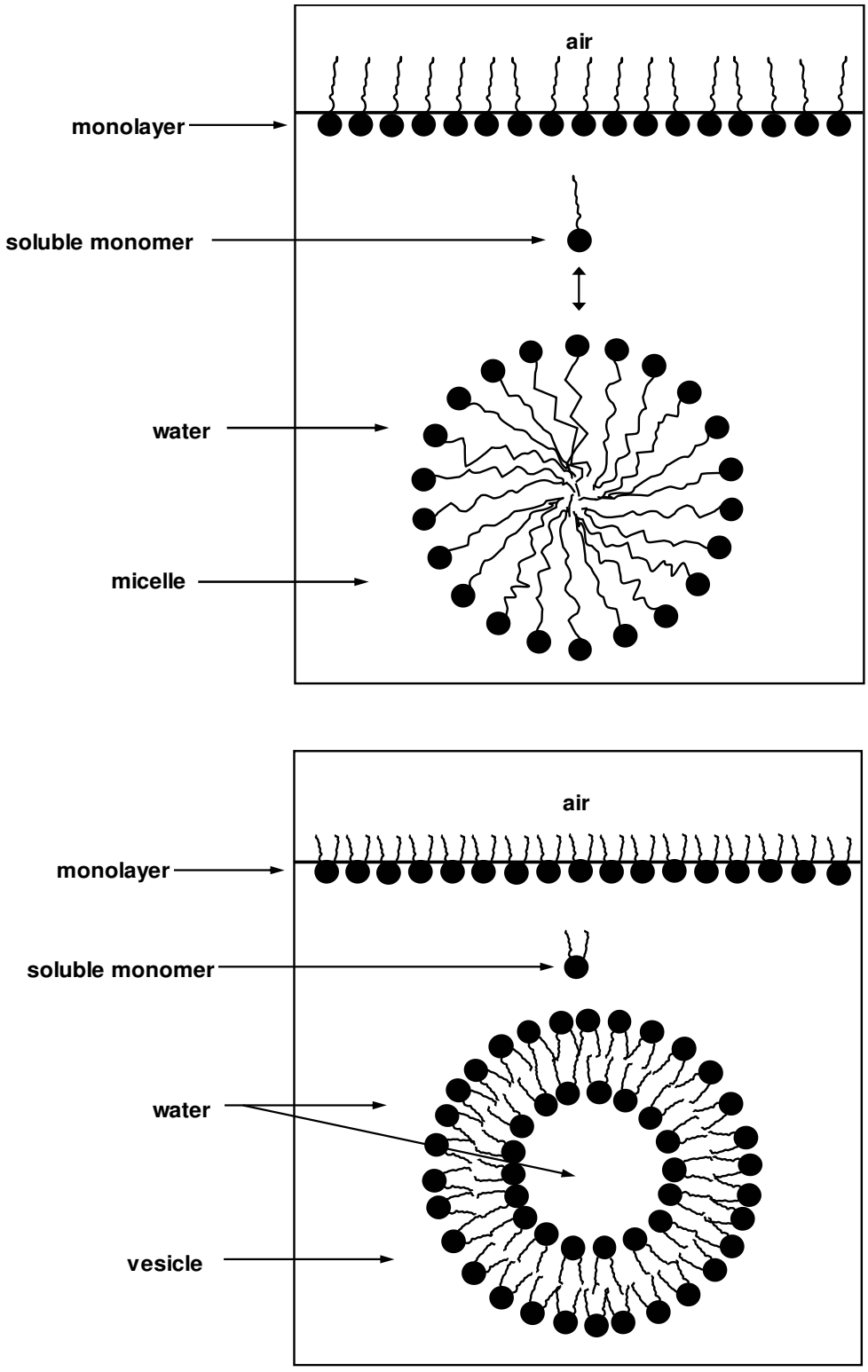

Figure 9: Schematic representation of the surfactant and lipid adsorption at air/aqueous interface.

1.8.1.1. Molecular Interactions and Synergism in Mixtures of Two Surfactants

In the last two decades, numerous reports have appeared in the field of mixed micelles using a variety of surfactants including cationic-anionic [11], nonionic-nonionic [12-16], nonionic-zwitterionic [15], cationic-nonionic [12-13, 15-16, 22-23], anionic-nonionic [2-3, 11-19], cationic-cationic [20-21], anionic-zwitterionic [11, 24], anionic-anionic [25], and cationic-zwitterionic [26] mixtures. The need for so much research in this particular area probably arises from the wide applications. Industry is always in need of novel and more surface active chemical compounds, so that better performance can be achieved in more economical ways. Mixed-micelle formation has considerable importance compared with single-surfactant micelle formation for various reasons. Generally, if a mixture of two or more surfactants shows better performance properties than those measured for the individual components, this relates to the existence of synergy between the surfactants. Synergy is defined here as the conditions under which the properties of the mixture, at some ratio of the two surfactants, are better than those attainable by the individual components alone.

Molecular interactions between two surfactants at an interface or as micelles are commonly measured by the so-called beta parameters: β^{σ} and β^{M}, respectively [2-3, 13, 15, 19-21, 23, 193-194] and conveniently obtained from surface (or interfacial) tension or from critical micelle concentration data.

The nature and the strength of the interaction between two surfactants in their mixed monolayer at the air/aqueous solution interface (β^{σ}), can be determined by calculating their β parameter from surface tension (γ) vs. concentration (C) plots

of aqueous solutions of the individual surfactants and at least one mixture of them, as illustrated in Figure 10. The interaction parameter (β^{σ}) is calculated by use of equations 7 and 8,

$$\frac{X_1^2 \ln\left(\alpha_1 C_{12} / X_1 C_1^0\right)}{(1-X_1)^2 \ln\left[(1-\alpha_1) C_{12} / (1-X_1) C_2^0\right]} = 1 \qquad (7)$$

$$\beta^{\sigma} = \frac{\ln\left(\alpha_1 C_{12} / X_1 C_1^0\right)}{(1-X_1)^2} \qquad (8)$$

where X_1 is the mole fraction of surfactant *1* in the total mixed monolayer (on a surfactant-only basis); C_1^0, C_2^0, and C_{12} are the molar concentrations in the solution phase of surfactant *1,* surfactant *2*, and their mixture, respectively, at the mole fraction α_1 of surfactant *1* (on a surfactant-only basis), required to produce a given surface or interfacial tension (γ) value. To calculate β^{σ} equation 7 is solved numerically for X_1, which is then substituted into equation 8.

The value of β^{M} , the interaction parameter for mixed micelle formation in an aqueous medium, is calculated from equations 9 and 10,

$$\frac{(X_1^M)^2 \ln\left(\alpha_1 C_{12}^M / X_1^M C_1^M\right)}{(1-X_1^M)^2 \ln\left[(1-\alpha_1) C_{12}^M / (1-X_1^M) C_2^M\right]} = 1 \qquad (9)$$

$$\beta^M = \frac{ln\left(\alpha_1 C_{12}^M / X_1^M C_1^M\right)}{(1-X_1^M)^2} \qquad (10)$$

Where X_1^M is the mole fraction of surfactant *1* of the total surfactant in the mixed micelle; C_1^M, C_2^M and C_{12}^M are the critical micelle concentrations (cmc) for surfactant *1*, surfactant *2*, and their mixture, respectively, at the mole fraction α_1.

In order to obtain valid β^σ or β^M parameters, several conditions must be met [99(e)]: 1) the two surfactants must be molecularly homogeneous and free of surface-active impurities; 2) since equations 7-10 neglect counterion effects, all solutions containing ionic surfactants should have the same total ionic strength, with a swamping excess of any counterions; 3) it is advisable to determine β^σ using C_1^0, C_2^0 and C_{12} values taken from the γ-log C plots at such a value of γ where the slopes are all linear or almost so, and preferably at the lowest possible γ value; and 4) since equations 7 and 9 contain the terms $((X_1)^2/ (1-X_1)^2)$ or $((X_1^M)^2/ (1-X_1^M)^2)$, respectively, which change rapidly in value when X approaches 1 or 0, it is advisable to use α values for the surfactant mixtures that yield X_1 or X_1^M values between 0.2 and 0.8.

Under these conditions, the values of β^σ and β^M are essentially constant with changing in the values of X_1 and X_1^M [99(e)].

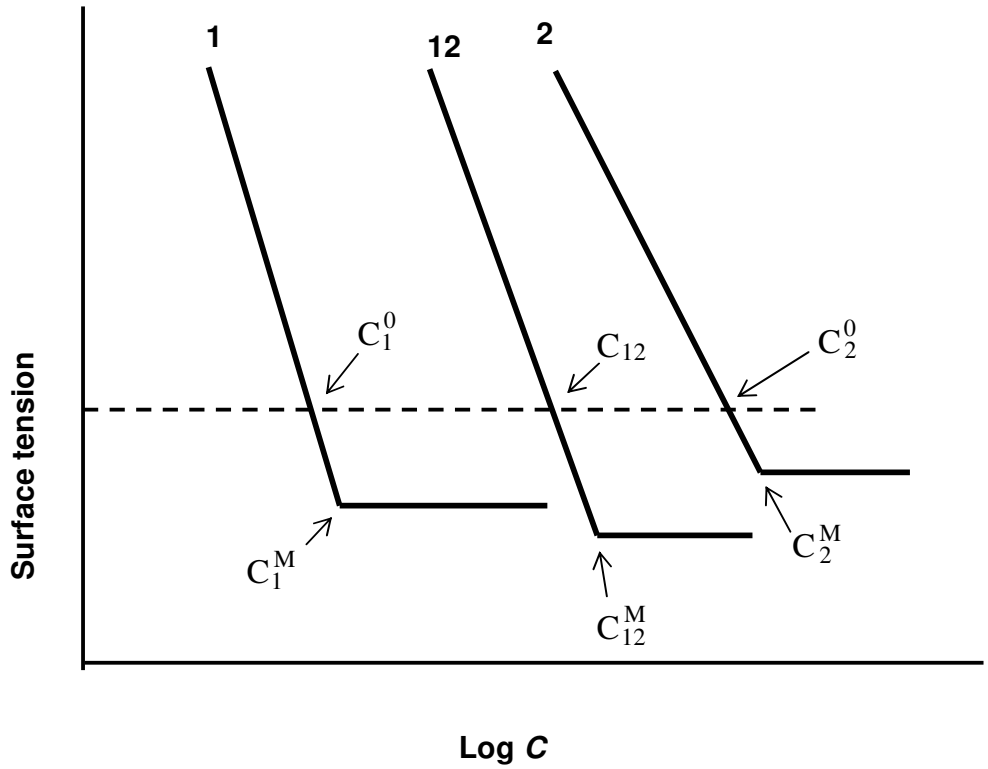

Figure 10: Equilibrium surface tension (γ) versus log bulk surfactant molar concentration (C) plots. Experimental evaluation of β^{σ} or β^{M}. (C_1) individual surfactant 1; (C_2) individual surfactant 2; (C_{12}) mixture of surfactants 1 and 2 at a fixed mole fraction α in solution.

Adapted from Ref. 99 p.381. Rosen, M.J. *Surfactants and Interfacial Phenomena*, 3rd. Edition, John Wiley & Sons, Inc. 2004.

1.8.1.2. Properties of Interaction Parameters (β)

Since the value of the β parameter is proportional to the free energy of mixing of the system, a negative value of β means that the attractive interaction between the two different surfactants after mixing is stronger than the attractive interaction of the two individual surfactants with themselves before mixing, or that the repulsive interaction between the two different surfactants after mixing is weaker than the self-repulsion of the two individual surfactants before mixing. A positive value of β indicates that the attractive interaction of the two different surfactants with each other after mixing is weaker than the attractive interaction of the two individual surfactants for themselves before mixing, or that the repulsive interaction between the two different surfactants after mixing is stronger than the self-repulsion of the two individual surfactants before mixing. When the value of the β parameter is close to zero, it indicates almost ideal mixing of the two surfactants.

Usually the interactions, and consequently the values of the β parameters, are dominated by the electrostatic interactions between the hydrophilic head groups of the two different surfactants [193]. The strength of the interaction between the two surfactants in a mixed monolayer at the surface depends on the nature of the surface and the molecular environment, for example, temperature, and ionic strength of the solution phase. From the β parameters, and from relevant properties of the individual surfactant components of the mixture, the existence of synergism can be predicted.

Three kinds of synergy have been investigated [2-3, 13, 15, 19, 21, 99, 194-196]: synergism in surface tension reduction effectiveness; synergism in surface tension reduction efficiency; and synergism in mixed micelle formation in aqueous medium.

The conditions for the existence of these synergisms are listed as following [99(f)]: 1) synergism in surface tension reduction efficiency for monolayers: (a) β^{σ} must be negative, (b) $| \beta^{\sigma} | > | \ln(C_1^0 / C_2^0) |$; and 2) synergism in mixed micelle formation in aqueous medium: (a) β^{M} must be negative, (b) $| \beta^{M} | > | \ln(C_1^M / C_2^M) |$; and 3) synergism in surface tension reduction effectiveness: (a) $\beta^{\sigma} - \beta^{M}$ must be negative, (b) $| \beta^{\sigma} - \beta^{M} | > | \ln((C_1^{0,CMC} * C_2^M) / (C_2^{0,CMC} * C_1^M)) |$; where $C_1^{0,CMC}$, $C_2^{0,CMC}$ are the molar concentrations of surfactant 1 and 2, respectively, required to yield a surface tension equal to that of any mixture at its cmc.

The value of β^{σ} (the interaction parameter for mixed monolayer formation at the air/solution interface) is generally not the same as the value of β^{M} (the interaction in mixed micelle formation in the solution phase) for the same two surfactants under the same conditions. Generally, interactions of mixed monolayer are stronger than in the mixed micelle, for the same two surfactants under the same conditions. But there are some situations where there are relatively stronger interactions in the mixed micelle over the mixed monolayer system.

1.8.1.3. Previous Studies Using Surface Tension to Investigate Surfactant-Lipid Interactions

Phospholipids are known amphiphiles owing to their zwitterionic polar head group. Several studies have been undertaken to explore micelle formation between surfactant and phospholipid momomers and to study their interfacial and bulk micellar behavior using surface tension methods [55, 106, 185, 188, 190].

Sehgal *et al*., have studied mixed micellar formation between zwitterionic surfactant dimethyl-dodecylaminopropane sulfonate (DPS) and 1, 2-diheptanoyl-sn-glycero-3-phosphocholine (DHPC) monomers in different proportions in an aqueous medium at the air/water interface. From surface tension data, they showed that a mixed monolayer is formed at the air/water interface by the adsorption of surfactant and phospholipid monomers. Interfacial parameters showed nonideal mixing for DPS/DHPC with negative β values over the entire mole fraction range [188].

Yaseen *et al.,* have investigated the adsorption of n-dodecyl phosphocholine ($C_{12}PC$) and n-hexadecyl phosphocholine ($C_{16}PC$), using surface tension methods. They found that an increase in the alkyl chain length of the PC surfactants combined with changes in temperature, salt and pH conditions had only small effects on surface tension, area per molecule and cmc values [190].

In this study, in order to determine whether mixtures of the N-alkyl-2-pyrrolidinones (nonionic surfactants) with DMPC (zwitterionic) would show synergism in their surface properties, molecular interaction parameters, β^{σ} for mixed monolayer formation at the aqueous solution/air interface and β^{M} for mixed micelle formation in aqueous solution, were calculated from the surface tension-concentration curves for the individual surfactants, DMPC and two DMPC/surfactant mixtures. Also, the interfacial properties (maximum surface excess concentration, Γ_{max}; minimum area/molecule at the interface, A_{min}; efficiency of interfacial tension reduction, pC_{20}; effectiveness of interfacial tension reduction, Π_{max}; standard free energy of adsorption, ΔG_{ad}^{0}) were determined from the surface tension-concentration data.

1.8. 2. Fluorescence Spectroscopy

Due to the inherent sensitivity and ease of detection, fluorescence spectroscopic methods are widely used in industry, science and medicine. Fluorescence is defined as the radiative emission of a photon during relaxation of a molecule from its singlet excited singlet-state to the singlet ground-state ($S_1 \rightarrow S_0$). In order for this to occur, the molecule must first undergo an absorption process. The transition of an electron from the singlet ground-state (S_0) to an upper excited-singlet state (S_x) level may be depicted using a Jablonski energy level diagram (Figure 11), as a vertical line to illustrate the instantaneous nature of light absorption which occurs within 10^{-15} s. The paired electrons of the ground, first, and second electronic singlet states (denoted as S_0, S_1, S_2, respectively) exist in orbitals of opposite spin. There is no change in electron spin during the singlet-singlet absorption process.

Each of the electronic singlet energy levels comprise a number of vibrational energy levels, denoted by v_0, v_1, v_2, etc. In general the energy of absorption ($E = h.\nu$) for fluorescence studies, corresponds to wavelengths in the near ultraviolet and visible wavelength range (190-650 nm). As a consequence, the fluorophore is promoted usually to a higher vibrational level of either the S_1 or S_2 excited-state electronic energy levels. With a few rare exceptions, excited-state molecules in condensed phases rapidly relax to the lowest vibrational level of S_1. This process, called internal conversion, is generally complete prior to emission and occurs in 10^{-12} s or less. Return of the molecule back to its ground state is spin-allowed and occurs rapidly either by emission of a photon (fluorescence), thermal deactivation (exothermic solvent warming), *via* solvent relaxation, chemical reaction (excimer

formation or proton transfer) or non-radiative (Förster) energy transfer. Alternatively, the electron may undergo inter-system crossing (ISC) to the triplet state (T_1), with a corresponding flip in electron spin. Deactivation from the triplet state back to the ground-state ($T_1 \rightarrow S_0$) gives rise to radiative phosphorescence emission occurring on a millisecond to second time scale. In contrast, the emission rates (k_f) for fluorescence ($S_1 \rightarrow S_0$) are typically 10^8 s^{-1}, so that a typical fluorescence lifetime (where: $\tau \equiv k_f^{-1}$) is near 10 ns. The fluorescence lifetime for a fluorophore is thus defined as the average decay time between instantaneous excitation and its return back to the ground state [197].

Additionally, the response of the fluorescence emission signal to the local environment around the fluorophore can provide important information about molecular conformation and cellular interactions [197]. As a result, the development of instrumentation, data analysis methods, and fluorescence probe technologies, has been rapid over the last thirty-five years [197].

1.8.2.1. Fluorescence Emission Quenching

Quenchers decrease the fluorescence intensity of a fluorophore. They include a variety of substances that interact with the fluorophore in the ground (static quenching) or the excited states (collisional (or dynamic) quenching, e.g. molecular oxygen, acrylamide, iodide, amines) [197].

To determine the location of flurophores in bilayer, one approach is to use quenchers, which are either water soluble or can partitition into the membranes. Information about the location of the flurophore can be obtained from the amount of

quenching by water-soluble (e.g. acrylamide, N-methylnicotin-amide, iodide) or membrane-soluble quenchers (e.g. dimethylaniline) [197].

Another approach is to use fluorescence quenchers which are covalently linked to the phospholipids and thus restricted to particular depths in the lipid bilayers. The most widely used lipid quenchers are the brominated phosphatidylcholines (bromo-PCs) and nitroxide-labeled PCs or fatty acids [197]. Such probes have been used to determine the location of fluorophores in bilayers based on the comparative amounts of quenching when the probe and quencher are at various depths in the membrane [197].

The quenching of the fluorescence intensity may be described by the linear Stern-Volmer equation [197]:

$$\frac{F_0}{F} = 1 + K_{SV}[Q] \qquad (11)$$

where F and F_0 are the fluorescence intensities in the presence and absence of quencher Q, respectively, and K_{SV} is the Stern-Volmer quenching constant.

Static quenching arises from ground state interactions between the fluorophore and quencher to form a complex that is non-fluorescent [197]. In such cases, the Stern-Volmer quenching constant, K_{SV} is equivalent to the association constant, K_A, for complex formation between the fluorophore and quencher.

Collisional (or dynamic) quenching arises from excited state interactions between the quencher and fluorophore to form an excited state complex that returns to the

ground state without emitting a photon [197]. For the collisional quenching of fluorescence, the Stern-Volmer equation (11) can be reexpressed as:

$$\frac{F_0}{F} = 1 + k_q \tau_0 [Q] = 1 + K_{SV} [Q] \qquad (12)$$

where F and F_0 are the fluorescence intensities in the presence and absence of quencher Q, respectively, k_q is the biomolecular quenching constant, τ_0 is the lifetime of the fluorophore in the absence of quencher, and [Q] is the concentration of quencher.

1.8.2.2. Fluorescence Emission Spectrum

Fluorescence spectral data are generally presented as emission spectra. A fluorescence emission spectrum is a plot of the fluorescence intensity (in arbitrary units) *versus* wavelength (nanometers) or wavenumber (cm^{-1}) for a fixed wavelength of absorption (excitation). The fluorescence intensity is related to the absorptivity of the sample in arbitrary unit:

$$F = \Phi I_0 \varepsilon c l \qquad (13)$$

Where Φ represents the quantum yield for the fluorophore, I_0 is the incident light intensity, ε is the molar absorptivity coefficient ($M^{-1}cm^{-1}$), c is the fluorophore concentration (M) and l is the pathlength of the cuvette (cm).

Since the fluorescence emission almost always occurs from the lowest vibrational level of the S_1 energy level, the fluorescence emission spectrum is independent of the excitation wavelength. In addition, the emission spectrum for a fluorophore is typically a mirror image of its absorption spectrum, representing the $S_0 \rightarrow S_1$ transition. This similarity occurs when the electronic excitation does not greatly alter the nuclear geometry. Hence, the spacings of the vibrational energy levels of the excited state fluorophore are similar to that of its ground state. As a result, the vibronic detail of the observed measured absorption and the emission spectra are similar [197].

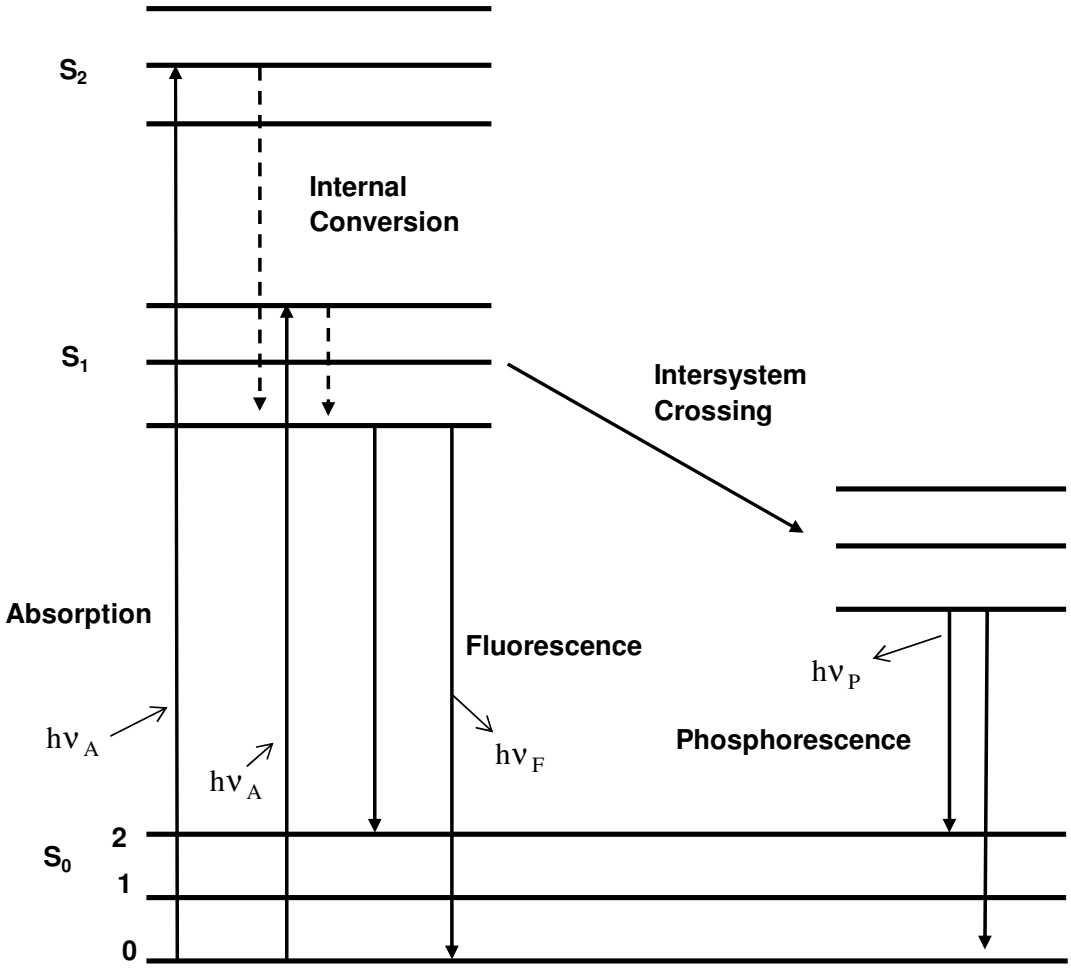

Figure 11: Jabłoński diagram. S_0, S_1, S_2 are the different electronic levels and 0, 1, and 2 are the different vibrational energy levels within each electronic level.

Adapted from Ref. 197, p.5. Lakowicz, R.J. *Principles of Fluorescence Spectroscopy*, 2nd Edition, Kluwer Academic/ Plenum Publishers, New York, 1999.

1.8.2.3. Fluorescence Emission Anisotropy

The fluorescence emission anisotropy (EA) technique is based on excitation photoselection. Excitation with polarized light excites only those molecules that are oriented with their absorption dipole moment close to the angle of incident light.

The rotational motions of a fluorophore from the original photoselected orientation may be characterized by the steady-state emission anisotropy parameter, <r>, (where <> represents an average of all rotational motions). The emission anisotropy of a fluorophore following excitation using polarized light, is calculated from the difference (<D>) divided by the sum (<S>) of the observed four polarized emission intensity components (I_{VV}, I_{VH}, I_{HH}, I_{HV}) [197]:

$$< r >= \frac{< D >}{< S >} = \frac{G \bullet I_{VV} - I_{VH}}{G \bullet I_{VV} + 2 \bullet I_{VH}} = \frac{R - 1}{R + 2} \qquad (14)$$

Where:

$$R = G \bullet \frac{I_{VV}}{I_{VH}} \; ; \; G = \frac{I_{HV}}{I_{HH}} \qquad (15)$$

and subscripts V (vertical) and H (horizontal) refer to the direction of the excitation (first) and emission (second) polarizers (Figure 12). The “G” or grating factor is an instrumental factor [198] that corrects for inequalities in the sensitivity of the detection system for horizontal and vertically polarized emissions [56-62, 69, 197].

For a fluorophore with colinear absorption and emission dipoles, and in a rigid environment, the maximum anisotropy value that can be obtained (r_0) is 0.4. An r_0

value of -0.2 is obtained when the absorption and emission dipoles are at right angles to each other [197]. The value of the limiting anisotropy (r_0) thus reflects the angle (β) between the absorption and emission dipoles for a fluorophore in a restricted/glass medium. For rod-shaped fluorophores DPH and TMA-DPH the measured r_0 value is about 0.395 (λ_{ex}=355 nm) and 0.390 (λ_{ex}=353 nm), respectively [69] when β is close to zero [184] and r_0 is 0 when β is 54.7 (deg). Measured values for r_0 in a rigid matrix are often less than the expected theoretical value because of fast intrinsic depolarizing motions of the fluorophore [197]. For DPH and TMA-DPH fluorophores embedded in a lipid matrix, the measured anisotropy values (<r>) thus fall within the range: $0 \leq (<r>) \leq 0.4$, where zero represents unhindered, isotropic rotation of the molecule, and 0.4 represents complete restriction of rotational freedom.

Fluorescence emission anisotropy (EA) measurements have been used to examine and quantify protein denaturation, protein association with other macromolecules, and the internal dynamics of proteins. In addition, the anisotropy of membrane-bound fluorophores has been used to estimate the internal viscosities of membranes and the effects of lipid composition upon the membrane phase-transition temperatures (T_m) [69].

For a non-spherical fluorophore, the microviscosity (η) of the surrounding microenvironment can be estimated from the measured emission anisotropy values (<r>) through the Perrin equation:

$$\frac{r_0}{< r >} = 1 + C(r)\frac{T\tau}{\eta} \qquad (16)$$

where <r> and r_0 are the measured emission anisotropy and limiting anisotropy values, respectively, T is the absolute temperature, τ is the excited state lifetime lifetime and η is the "microviscosity" of the system. $C(r)$ is a structural parameter of the fluorophore related to its effective rotational volume and is equal to 8.6×10^5 poise $deg^{-1}s^{-1}$ for DPH [57] and 15.3×10^5 poise $deg^{-1}s^{-1}$ for TMA-DPH [199].

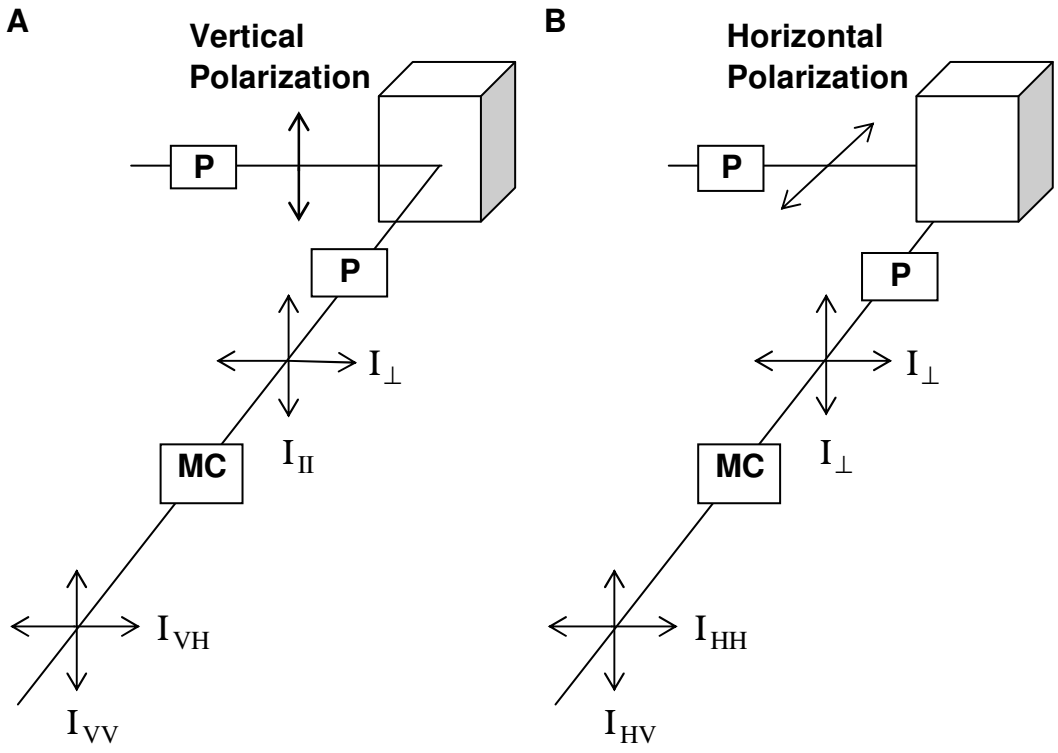

Figure 12: Measurement of steady-state fluorescence anisotropy with the L-format instrumentation. Vertical (A) or horizontal (B) polarized light excites the sample and the parallel and perpendicular emissions are detected through the monochromator (MC) by a photomultiplier.

Adapted from Ref. 197, p.292. Lakowicz, R.J. *Principles of Fluorescence Spectroscopy*, 2nd Edition, Kluwer Academic/ Plenum Publishers, New York, 1999.

1.8.2.4. General Spectroscopic Properties of Fluorophores Used in This Study

Fluorescence usually arises from molecules that are aromatic or demonstrate a high degree of conjugated π and n-electron bonding [197]. In the current work, 1,6-diphenyl-1,3,5-hexatriene (DPH) and its cationic analog, 1-(4-trimethylammoniumphenyl)-6-diphenyl-1,3,5-hexatriene) (TMA-DPH) are employed as fluorophores for monitoring surfactant effects on lipid bilayers.

Labeling of membranes is often accomplished by simple partitioning of the water-insoluble probes into the nonpolar regions of membranes. Typical molar labeling ratios of probe to phospholipid lie in the range 1:500 to 1:2000. Probe-induced "local" perturbation effects are minimized because of the low molar labeling ratios used for fluorescence studies (typically 0.05 to 0.50 mol %). For a probe to phospholipid molar labeling ratio of 1:500 (as used in these studies), if it is assumed that an SUV (with diameter of 250-300Å) comprises about 3500 phospholipid molecules, then the 1:500 labeling ratio corresponds to, on average, about 7 probe molecules per vesicle [69, 200]. The lipid-water partition coefficients have been reported for both DPH ($1.3x10^6$) and TMA-DPH ($2.4x10^5$) [72]. The value for TMA-DPH is lower than DPH reflecting the increased water solubility attributed to its polar substituent.

DPH has a rod-like structure and possesses cylindrical symmetry around its long axis (Figure 13). DPH aligns with the fatty acyl chains and reports on the more hydrophobic acyl chain region of the bilayer. Studies have also shown that DPH may also reside within the center of the lipid bilayer, lying parallel to the membrane surface [56-69]. The DPH fluorophore can also be attached to fatty acid chains or

directly to the 2'-position of the glycerol backbone of the phosphoglycerides [66]. The high extinction coefficient and fluorescence quantum yield of DPH in non-aqueous solvents make it possible to label bilayers with low concentrations, thus minimizing potential membrane perturbations, and making DPH a particularly attractive probe for obtaining dynamic and structural information about membrane bilayers. In contrast, TMA-DPH, as a consequence of its positive charge, is expected to reside at the polar headgroup region of the bilayer and probe that region. TMA-DPH is oriented in the bilayer with its symmetry axis oriented normal to the plane of the bilayer [66, 68].

Both DPH and TMA-DPH have the feature that they are virtually non fluorescent in water, and that the fluorescence intensity increases about 10,000 fold on permeation within the membrane bilayer. As a consequence the observed fluorescence signals arise only from those probes that are membrane associated and any potential background signal from non-incorporated probe is thus negligible. Attachment of the trimethylammonium moiety to the fluorophore results in a marked reduction in absorptivity with ε = 53,000 $M^{-1}.cm^{-1}$ (in methanol) [69] for TMA-DPH versus 80,000 $M^{-1}.cm^{-1}$(in methanol) [69] for DPH. Both DPH and TMA-DPH have high fluorescence quantum yield values (Φ). The quantum yields for DPH (in hexane) [56] and TMA-DPH (in membranes) [201] are reported to be 0.8 and 0.7, respectively. The absorption and emission bands are well separated with little spectral overlap [56]. Cundall *et al*., [73] have reported that the absorption spectra, fluorescence emission spectra, quantum yields and fluorescence lifetimes for several DPH derivatives (excluding TMA-DPH) are somewhat quenched compared to the parent DPH molecule. In contrast, the very short fluorescence lifetime of TMA-DPH

in different solvents varies from 0.14 ns to 0.37 ns and lifetime of TMA-DPH increases to 7 ns when the probe is embedded in lipid bilayers at temperatures less than the phase transition temperature of the lipid [66]. In general, the lifetime of TMA-DPH is shorter than DPH. Indeed, Zolese *et al.,* [202] have investigated fluorescence lifetimes of DPH and TMA-DPH in DMPC MLVs. They have shown that fluorescence lifetimes of DPH decreased from 9.96 ns to 8.13 ns with increasing temperature from 7.7 ºC to 27 ºC and fluorescence lifetimes values for TMA-DPH decreased from 8.75 ns to 5.52 ns with increasing temperature from 5.7 ºC to 30.5 ºC. These studies suggest that the fluorescence lifetimes of these two probes are sensitive to the gel-fluid membrane transitions.

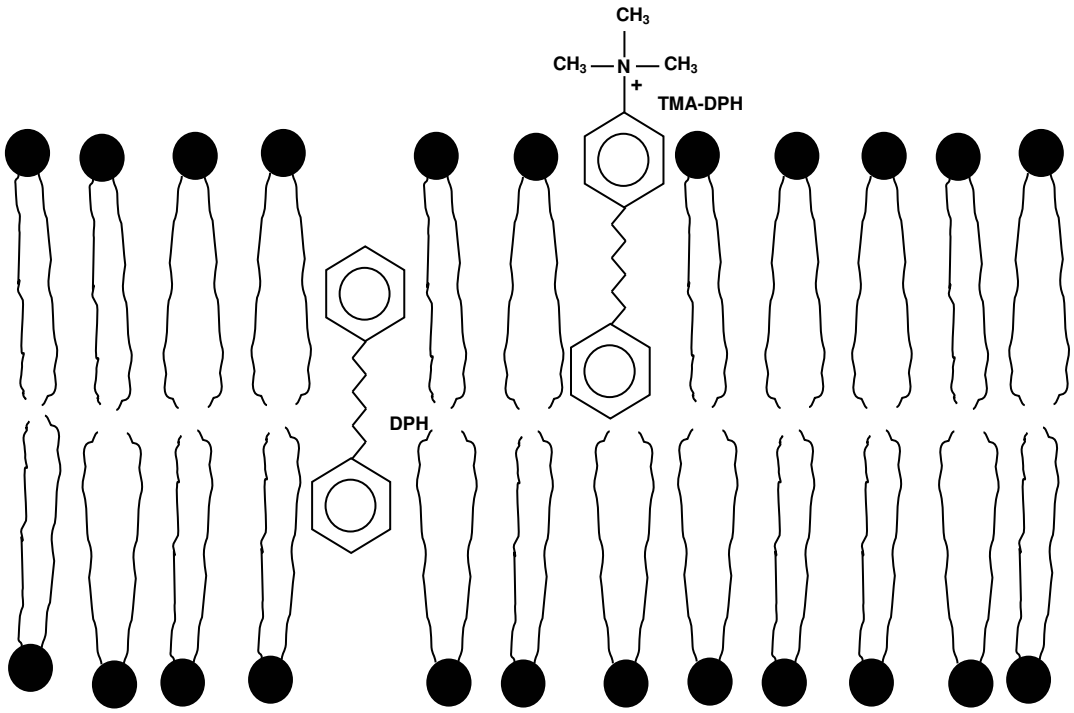

Figure 13: Possible location and orientation of DPH and TMA-DPH in the membrane bilayers.

Adapted from Ref. 68. Kitagawa, S., Matsubayashi, M., Kotani, K., Usui, K., and Kametani, F. Asymmetry of membrane fluidity in the lipid bilayer of blood platelets: Fluorescence study with diphenylhexatriene and analogs. *J. Membrane Biol*. 1991, 119, 221-227.

1.8.2.5. Previous Studies Using DPH and TMA-DPH in Lipid Membranes

1.8.2.5.1. Fluorescence Membrane Fluidity Probes DPH and TMA-DPH

Fluorescent probes are widely used in the study of the molecular order and dynamics of both natural and model membrane systems. A wide range of probes have been used for determination of membrane fluidity including perylene, pyrene, 2-methylanthracene, fluorescein, rhodamine, parinaric acid, and Texas red [56, 197, 203]. However, DPH and its more polar analog, TMA-DPH, are often chosen because of their favorable photophysical properties, as discussed above [56-73].

DPH was first introduced by Shinitzky and Barenholz [56] to monitor the fluidity of the hydrocarbon region of the bilayer and to detect fluidity changes that accompany the gel-liquid crystalline phase transition in a series of liposomes of lecithin and sphingomyelin containing different concentrations of dicetylphosphate systems.

Determination of membrane fluidity has been important for several clinical studies such as Down's syndrome [204-207], diabetes [208-212], and malignancy [213-215] where there are significant differences in fluidity between the normal and diseased state.

Przybylska *et al* have studied the fluorescence anisotropy of TMA-DPH and 12-(9-anthroyloxy)-stearic acid (12-AS) as a tool to determine the fluidities of Down's syndrome (DS) cell membranes *versus* normal cells. TMA-DPH and 12-AS, which are located with different regions of the bilayer, yield information about the the rigidity of the cell membrane near the lipid polar heads (TMA-DPH) and within the hydrophobic lipid core (12-AS). From emission anisotropy measurements they

showed that the membrane fluidity of the polar region of the DS cell membrane was decreased (more viscous) in comparison with normal cells [216].

1.8.2.5.2. DPH and TMA-DPH in Surfactant Studies

The estimation of cmc values for surfactants has been studied by many physicochemical techniques including light scattering, surface tension, hydrodynamic properties and changes in the absorbance or fluorescence signals upon probe solubilization. Methods based upon altered fluorescence intensities of a probe on incorporation into micelles are among the most sensitive and convenient assays. However, as might be expected, cmc assays employing charged fluorescent probes are unreliable if the probe and surfactant have specific interactions [217-219]. Chattopadhyay and London [220] have shown that this problem can be avoided when neutral DPH is used. Upon mixing surfactant solutions with DPH (no quencher present) a large increase in fluorescence signal is observed when the surfactant concentration exceeds the cmc. This property has been used to determine the cmc values of Triton X-100, OG, CHAPS, SDS, Sodium Cholate and cetyltrimethylammonium bromide (CTAB). Results were comparable with the literature values obtained by varying biophysical methods. Therefore, the method is relatively simple and reliable. Indeed, Jackson *et al.,* [27] have used DPH to determine the cmc of octyl glucoside (OG), and to characterize the solubilization of egg phosphatidylcholine vesicles (egg-PC) by surfactant in 50 mM KCl. Using both the total polarized emission intensities (<S>) and EA (<r>) of DPH, they reported a cmc value of 22mM for OG. Chattopadhyay *et al*., [221] have investigated the dependence of the cmc for CHAPS with ionic strength using changes in the

fluorescence intensity of DPH and reported a cmc value of 6.41 mM in the absence of any salt. These results again compare favorably with cmc values determined by other methods (25 mM for OG and 6.5 mM for CHAPS) [109-110], and demonstrate the versatility and applicability of DPH as a fluorescent probe for determining accurate cmc values of surfactants.

Similar studies, as proposed here have been performed by Koga *et al*., [38, 222] using DPH and TMA-DPH to investigate the effects of Span- and Tween-type surfactants and glycerol esters on the membrane lipid fluidity. They found that the emission anisotropy of DPH-labeled membranes decreased with increasing surfactant concentration, however, TMA-DPH labeled membranes differed with the type of surfactant [38].

1.8.3. Isothermal Titration Calorimetry

Calorimetry has made an enormous contribution to our understanding of chemical reactions and the properties of chemical substances. Many different calorimeters have been described, each requiring characteristic methods for data analysis. Isothermal titration calorimetry (ITC) allows direct determination of the molar enthalpy change (ΔH) for a reaction. ITC is the most direct method for measuring the heat change based on complex formation at a constant temperature.

Almost all chemical and physical processes entail changes in heat, and thus can be measured with ITC. The two different sample and reference cells (both 1.433 ml volume) are housed in an adiabatic (no heat exchange) jacket (Figure 14). The contents of two solutions of interest are then mixed in the sample cell using precise

injections (± 0.1 µl) through a motorized injection syringe (volume 0.3 ml). Temperature differences between the two cells are measured *via* the differential power needed to equilibrate and maintain temperature equilibrium of the two cells. The raw signal has units of power, and integration of the signal with respect to time yields a measurement of thermal energy. In this way, the ITC method provides information about the heat evolved in a reaction which is released proportional to the amount, or number of moles, of binding that occurs. The apparatus is extremely sensitive and measures heats of reaction of ~1 µcal (10^{-6}K) temperature change for a 1 mL cell, and it is thus possible to measure small amounts of dilute reactants. This allows very precise characterization of energies involved in formation of bimolecular complexes. With such sensitivity one is able to determine binding affinities with a great degree of accuracy [93-96].

The heat absorbed or evolved during a calorimetric titration is proportional to the fraction of bound ligand. Thus, it is important to determine accurately the initial concentrations of both the macromolecule and the ligand. For the initial injections, all or most of the added ligand is bound to the macromolecule, resulting in large endothermic or exothermic signals depending on the nature of the association. As the ligand concentration increases, the macromolecule becomes saturated and subsequently less heat is evolved or absorbed on further addition of ligand. The amount of heat evolved on addition of ligand can be represented by the equation 17:

$$Q = \frac{V_0 \Delta H_b [M]_t K_a [L]}{1 + K_a [L]} \qquad (17)$$

where V_0 is the volume of the cell, ΔH_b is the enthalpy of binding per mole of ligand, $[M]_t$ is the total macromolecule concentration including bound and free fractions, K_a is the binding constant, and $[L]$ is the free ligand concentration.

For a more general model of binding, (the multiple independent sites model), the macromolecule contains multiple ligand binding sites that are noninteracting. The cumulative heat of binding can be described by the equation 18:

$$Q = \frac{V_0[M]_t \sum(n_i \Delta H_i K_{ai}[L])}{1 + K_{ai}[L]} \tag{18}$$

where i is the number of titration.

To determine n (stoichiometry of the binding, $\frac{[L]_t}{[M]_t}$), K_a, and ΔH_b equation 18 is represented in terms of the binding constant and total ligand concentration $[L]_t$ by the quadratic equation 19:

$$Q = \frac{(n[M]_t \Delta H V_0)}{2}\left[1 + \frac{[L]_t}{n[M]_t} + \frac{1}{nK_a[M]_t} - \sqrt{\left(1 + \frac{[L]_t}{n[M]_t} + \frac{1}{nK_a[M]_t}\right)^2 - \frac{4[L]_t}{n[M]_t}}\right] \tag{19}$$

The value of Q from above can be calculated (for any designated values of n, K_a and ΔH_b) at the end of the i^{th} titration and designated $Q(i)$, the change in heat content from the completion of the i-1 titration to completion of the i titration. The expression for

Q in equation 19 only applies to the liquid contained in volume V_0. Therefore, after completing a titration, it is obvious that a correction must be made for displaced volume (i.e., ΔV_i = titration volume) as some of the liquid in V_0 after *i-1* titration will no longer be in V_0 after the i^{th} titration, even though it will contribute to the heat effect (assuming the kinetics of reaction and mixing are fast) before it passes out of the working volume V_0. The liquid in the displaced volume contributes about 50% as much heat effect as an equivalent volume remaining in V_0. The correct expression then for heat released, $\Delta Q(i)$, from the ith titration is

$$\Delta Q(i) = Q(i) + \frac{dV_i}{V_0}\left[\frac{Q(i) + Q(i-1)}{2}\right] - Q(i-1) \qquad (20)$$

The process of fitting experimental data then involves: 1) initial guesses of n, K_a and ΔH_b which most often can be made accurately by the instrumental data analysis (ORIGIN) software and a simple single site binding model (multiple independent sites) fit to the ITC data; 2) calculation of $\Delta Q(i)$ for each titration and comparison of these values with the measured heat for the corresponding experimental titration; 3) improvement in the initial values of n, K_a and ΔH_b by standard Marquardt methods; and 4) iteration of the above procedure until no further significant improvement in fit occurs with continued iteration.

The magnitudes of ΔG and ΔS are then obtained from the relationship,

$$\Delta G = \Delta H - T\Delta S = -RTlnK_a \qquad (21)$$

where R is the molar gas constant and T is the experimental temperature. Binding is described as exothermic if ΔH is negative (heat is released) and endothermic if the value is positive (heat is taken up). A process with a negative ΔG is described as exergonic, whereas a positive value characterizes an endergonic change [97-223].

$K_d (= 1/K_a)$ is the equilibrium constant for dissociation (free ligand concentration where 50% of the binding sites are occupied) whereas the other thermodynamic parameters relate to association. K_d can be more easily understood than its inverse, the association constant K_a, because it gives a measure of the free ligand concentration required for half-saturation [94-95].

ITC has proven extremely useful for the study of surfactant-membrane equilibria and four types of experiments can be distinguished broadly: 1) Measurement of the critical micellar concentration (cmc) [81, 84-85, 91]; 2) The partition equilibrium between monomeric surfactant and the lipid membrane [74-77, 80-82, 84, 86, 88, 91]; 3) Membrane solubilization at high concentration of surfactant [75-78, 82, 85, 88, 91]; and 4) Membrane formation upon dilution of mixed lipid-surfactant micelles [78-79, 83, 85, 88, 91].

In general, a number of technical details must be taken into account when analyzing ITC data. First, in order for measurable and reproducible signals, the ligand (the sample to be placed in the injection syringe) should be at a concentration at least 10 times higher than the concentration of the macromolecule (the sample to be placed in the sample cell). Secondly, the ITC experiment usually consists of injections of ligand into macromolecule, where both solutions are in exactly the same buffer. The observed heat changes therefore contain heat effects from several sources: the heat of

binding (to be measured); the heat of dilution of macromolecule; and the heat of dilution of ligand. Even small heat changes are measured for a buffer-into-buffer injection due to temperature differences between the injection syringe and the sample cell. Strictly, control experiments are therefore needed to correct for unwanted heat effects. This involves a further three titrations to measure the required heat controls. However, the initial macromolecule solution is usually diluted by around ~20%, leading to only small heat effects that can be neglected. The dilution of the ligand on the other hand, is always larger because the starting concentration in the sample cell is zero, and the ligand is added from a high concentration in the injection syringe until the final concentration in the cell is several times the final macromolecule concentration. This usually leads to heats of dilution for ligands that cannot be neglected. Therefore, the heat of dilution of the ligand into buffer, at least, should be subtracted from the overall heat effect measured in the experiment. Finally, the filling and mounting of the syringe may cause a slight inaccuracy of the volume of the first injection. Therefore, a first injection of a small volume (2μL) is often made and the corresponding heat change is not included in the evaluation [82].

1.8.3.1. Previous Studies Using ITC to Investigate Partitioning of Surfactants into Lipid Vesicles

Many studies have been performed using ITC to monitor the partitioning of surfactants into lipid vesicles, and solubilization of lipid vesicles by the addition of surfactants [74-81, 83, 85-86, 88, 91, 183, 224]. Similar studies, as proposed here have been performed by several groups to investigate the thermodynamics of nonionic surfactant partitioning into lipid vesicles [74-81, 83, 86, 91, 184].

Wenk *et al.,* have investigated the interaction of octyl-*β*-*D*-glucopyranoside (OG) surfactant with lipid vesicles composed of 1-palmitoyl-2-oleoyl-*sn*-glycero-3-phosphocholine (POPC), either in pure form or in mixture with DMPC, negatively charged 1-palmitoyl-2-oleoyl-sn-glycero-3-phosphoglycerol (POPG), or cholesterol using ITC. They measured the heat of binding (ΔH_b) and the partition constant (K). For POPC vesicles, they report that K=120 M^{-1} and ΔH_b = +1.30 kcal/mol and found that mixing of POPC with POPG, DMPC, or cholesterol reduces the partition constant for OG by about 30% to K $\approx$100 M^{-1}, and increases the binding enthalpy [74].

In another study, Keller *et al.,* have used ITC to determine the partitioning of octylglucoside (OG) monomers into DPPC or DMPC vesicles at two different temperatures (27°C and 70°C). They showed that the partition coefficient from aqueous to lipid bilayers decreases from 5570 at 27°C to 3805 at 70°C. The enthalpy of the reaction is positive (3.1 kcal/mol) at 27°C and negative (-2.4 kcal/mol) at 70°C [77].

No thermodynamic parameters are available for the partitioning of the nonionic surfactants C8P and C2,6P into DMPC SUVs. In the current study we have used ITC to determine the complete set of thermodynamic parameters for these two surfactant systems.

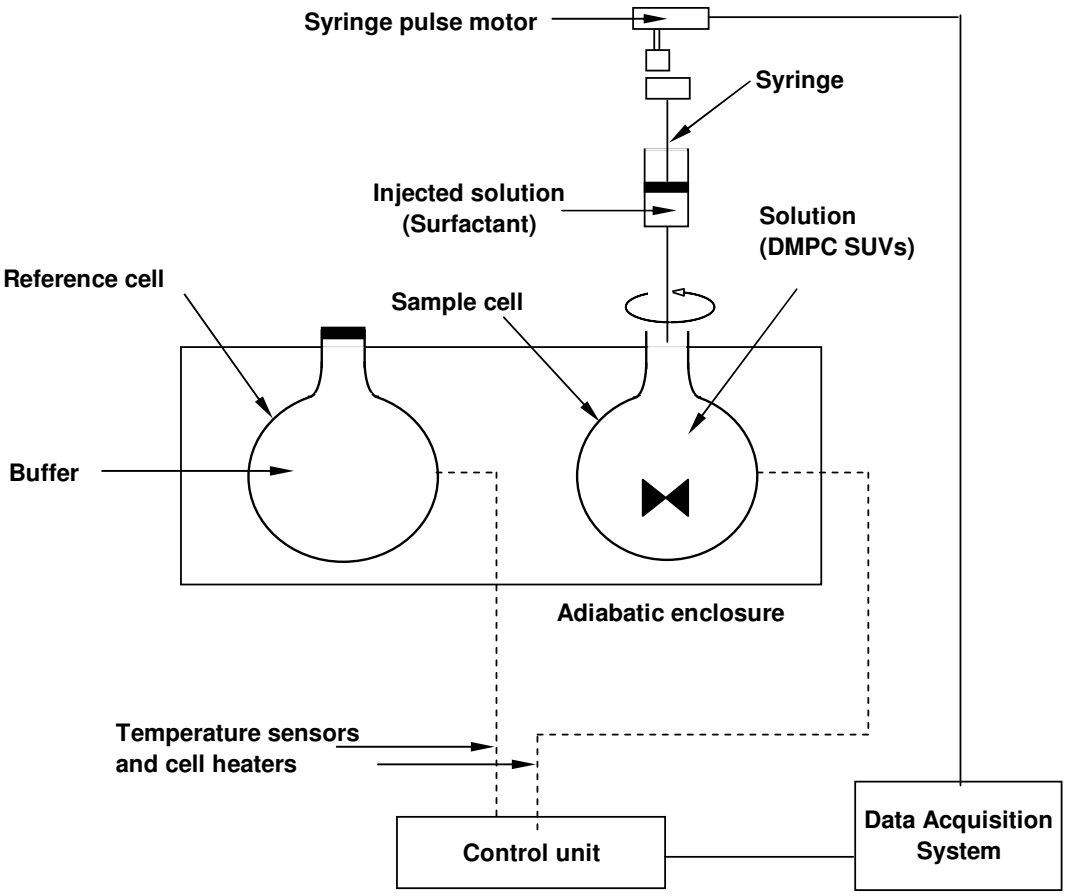

Figure 14: A schematic diagram of the isothermal titration calorimeter. The temperature is maintained *via* a differential electrical feedback system that works to keep both sample and reference cells at a constant temperature. In addition a separate feedback system maintains an equilibrium temperature between the reference cell and the external environment. In this way one has an apparatus operating in an isothermal, adiabatic environment.

Adapted from Ref. 93. Blandamer, M. J., Cullis, P. M., and Engberts, J. B. F. N. Titration calorimetry. *J.Chem.Soc., Fraday Trans*. 1998, 94(16), 2261-2267.

CHAPTER 2: EXPERIMENTAL PROCEDURES

2.1. Materials

L-α-Dimyristoylphosphatidylcholine (DMPC) (P7331), and 1,6-diphenyl-1,3,5-hexatriene (DPH) (D-4380) were obtained from Sigma Chemical Co., (MO). 1-(4-trimethylammoniumphenyl)-6-diphenyl-1,3,5-hexatriene (TMA-DPH) (T-204) was obtained from Molecular Probes, Inc. (OR). All fluorescent probes and lipids were received more than 99% pure and used as received. Stock solutions of DMPC in chloroform ($10 mg.mL^{-1}$), DPH in tetrahydrofuran (1 mM), and TMA-DPH in methanol (1 mM) were prepared. All stock solutions were stored in glass vials at -10°C and protected from uv light using aluminum foil. Ammonium molybdate tetrahydrate (A-7302), L-Ascorbic acid (A-0278), and Trizma hydrochloride (T3253-2506) were obtained from Sigma Chemical Co., (MO) and received more than 99% pure and were used as received. Well-purified pyrolidinones, N-octyl-2-pyrrolidone (C8P) and N-(2-ethylhexyl)-2-pyrrolidone (C2,6P) surfactants from ISP Technologies, Inc. (Wayne, NJ) were provided by Professor Milton J. Rosen, (Surfactant Research Institute , Brooklyn College, CUNY) and used as received.

2.2. Methods

2.2.1. Preparation of Model Membrane Vesicles

In a glass vial, DMPC stock solution (1 mL) was deposited as a thin layer by evaporation of the solvent using a gentle stream of nitrogen. The vial was covered with a filter paper cap, placed in vacuum dessicator and dried under vacuum for 60

minutes in order to remove any traces of organic solvent. To the dried lipid film, 0.01 M Tris.HCl buffer containing 0.1 M NaCl (pH 8.3) was added and mixed by vortexing until a milky suspension was obtained. The suspension was then sonicated for 20 minutes (intermediate output), using a Heat Systems probe sonifier (Farmingdale, NY). The sample was continuously flushed using a gentle stream of nitrogen to prevent lipid oxidation and held at 35°C (above the phase transition temperature), using a water bath during the vesicle preparation process. Small unilamellar vesicles were formed when an opalescent suspension was observed. Fractionation of SUVs from multilamellar lipid and titanium fragments from the sonicator probe was achieved using ultracentrifugation. The sample was centrifuged at 100,000g for one hour at room temperature using a Beckman Airfuge. The desired SUV preparation was isolated from the supernatant as the central core and removed carefully using a Pasteur pipette and placed in to a clean glass vial. The vial was covered with aluminum foil, protected from light and stored at 35°C until required for studies [142]. Previous electron microscopy studies performed in our laboratory have shown that SUVs with diameters 250-300 Å are formed using this method.

2.2.2. Determination of Lipid Phosphorus

The concentration of SUVs was determined as lipid phosphate using the procedure of McClare [225]. The method described as the "phosphorus assay" provides a sensitive method for determination of phosphorus content of phospholipid samples. The sensitivity range of the assay is 0 - 14 µg inorganic phosphorus.

Anhydrous disodium hydrogen phosphate (Na_2HPO_4; Fisher Scientific Company) was further dried under vacuum for two hours. In a volumetric flask, Na_2HPO_4

(80.20 mgs) was dissolved in Millipore water (specific resistance 18.2 $M\Omega cm^{-1}$) (250 mLs) to provide a stock phosphorus solution containing 7µg/100 µL. Aliquots of the phosphorus stock solution (0.1; 0.2; 0.3; 0.5; 1.0; 2.0; 3.0; 4.0; and 5.0 mLs) were pipetted into 9 different volumetric flasks and made up to the 25 mL mark with Millipore water. These dilutions resulted in standard phosphorus solutions corresponding to 0.28; 0.56; 0.84; 1.4; 2.8; 5.6; 8.4; 11.2; and 14.0 $\mu g.mL^{-1}$, respectively. These solutions were stored for subsequent phosphorus assays.

For preparation of the phosphorus assay calibration plot, aliquots (1 mL) of each of the phosphorus standard solutions were pipetted into 9 different Pyrex test tubes. A blank sample was prepared which contained Millipore water (1 mL). All samples were evaporated to dryness using a Bunsen burner, leaving a faint white deposit of solid Na_2HPO_4 residue in the bottom of the test tubes. The tubes were cooled to room temperature and concentrated perchloric acid (0.5mL) was added to each, mixed thoroughly using the vortex mixer, and covered with glass marbles. The samples were refluxed at 210±5 °C for 45 minutes until solutions turned from pale yellow to colorless.

The colorimetric reagent was prepared fresh by mixing ammonium molybdate (2.5g) with perchloric acid (20 mL) and Millipore water in the bottom of a 250 mL volumetric flask. A bath sonicator was utilized to aid dissolution of the ammonium molybdate. Ascorbic acid (0.5g) was dissolved in a little Millipore water and added to the molybdate solution. The resultant bright yellow solution was made up to the 250 mL mark with Millipore water and mixed thoroughly by inversion.

To each of the phosphorus containing test tubes, the molybdate reagent (9.5 mLs) was added and then sealed with a rubber stopper. Tubes were mixed thoroughly by inversion and placed in a water bath at 50 °C for 40 minutes. The resultant blue complex formed with phosphate was measured at 825 nm against the prepared (water) blank using a Perkin Elmer Lambda 3B UV-visible spectrophotometer. The assay calibration plot of A_{825} *versus* phosphorus concentration was constructed. The results are shown in Figure 15. Subsequent phosphorus assays were performed and errors in the absorption values were typically less than 3%.

For determination of SUV concentrations, aliquots (50µL) of the lipid sample were pipetted into two separate Pyrex test tubes and evaporated to dryness using a Bunsen burner. Complexation of the lipid sample phosphorus with molybdate was performed exactly as described above. The lipid concentration was determined from the standard calibration plot.

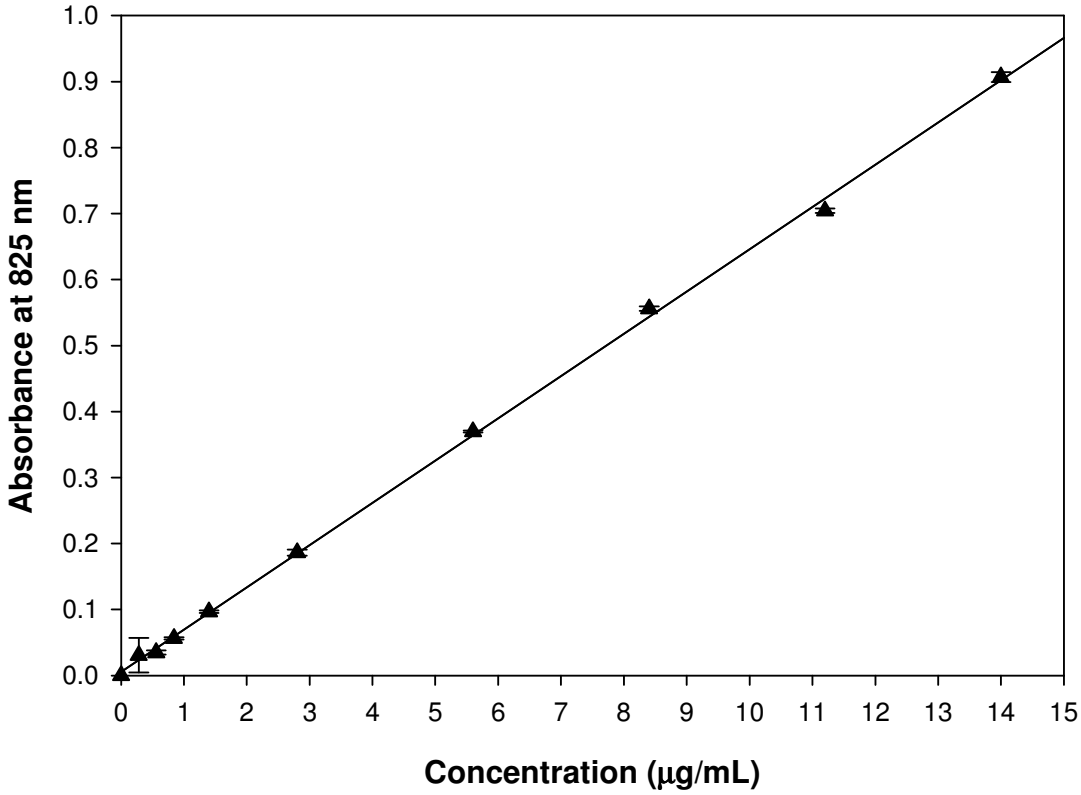

Figure 15: Calibration plot for the "phosphorus" assay at room temperature ($m=6.41\pm0.02 \times 10^{-2}$), $R^2= 0.999$).

2.2.3. Preparation of Fluorescently Labeled DMPC SUVs

Labeling of DMPC SUVs with fluorescent probes was accomplished by addition of 1.0 μL of the DPH (1mM in THF) or TMA-DPH (1mM in methanol) stock solutions into 2 mLs of a vortexing vesicle suspensions (0.25 mM DMPC by phosphorus) providing a final probe-to-phospholipid molar labeling ratio of 1:500. Samples containing fluorescent probes were incubated in the dark above the phase transition temperature of the lipid for two hours prior to fluorescence measurements.

2.2.4. Addition of Surfactant to Lipid Bilayer

The concentrations of the surfactants in 0.01 M Tris.HCl buffer containing 0.1 M NaCl (pH 8.3) were determined from their extinction coefficients, reading absorbance values at 190 nm against the blank (buffer) using a Perkin Elmer Lambda 3B UV-visible spectrophotometer. For the individual pyrrolidinone surfactant solutions (C8P and C2,6P), though not having a maximal wavelength in the UV-vis range, show UV absorbance values that follow Beer's Law, as shown in Figure 16. The molar extinction coefficients from two separate experiments were determined for C2,6P ($7.77\pm0.03\times10^3$ $M^{-1}.cm^{-1}$) and C8P ($7.91\pm0.04\times10^3$ $M^{-1}.cm^{-1}$) in the Tris.HCl buffer. The extinction coefficients at 191 nm have been reported for C2,6P (8.11×10^3 $M^{-1}.cm^{-1}$) and C8P (7.94×10^3 $M^{-1}.cm^{-1}$) in distilled water [1].

Surfactant solutions of a defined concentration were prepared by weighing out a certain amount of C8P and C2,6P and dissolving them in buffer. For lipid-surfactant mixtures, concentrated solutions of surfactant and DMPC SUVs were prepared separately. The solutions were mixed at the desired molar ratio and diluted with buffer to the final desired concentration of components.

The addition of surfactant to DMPC SUVs was monitored by uv absorbance at 350 nm *versus* time. No change in absorbance values was observed following a few minutes from the addition of surfactant. Therefore, fluorescence and isothermal titration calorimetry experiments were performed after 15 minute equilibration times.

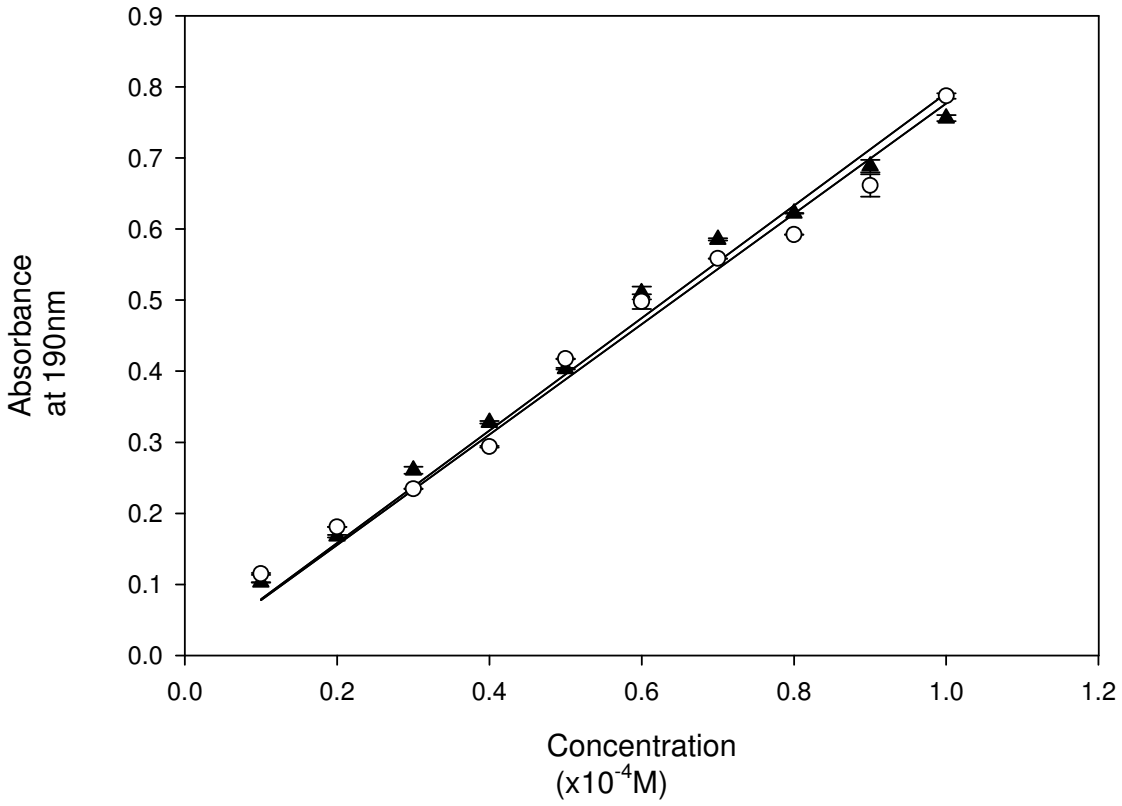

Figure 16: Absorbance calibration curves for the C8P (▲) and C2,6P(○) at 190 nm.

2.2.5. Surface Tension Measurements

Equilibrium surface tension measurements were performed using the Wilhelmy plate technique with a Krüss K-12 tensiometer (Krüss GmbH, Hamburg). The plate is made of platinum-iridium with a length of 19.9 mm and thickness of 0.2 mm. The instrument was calibrated each day at 25°C against quartz-condensed, double-distilled water (the last distillation stage from alkaline permanganate through a 1-m-high Vigreaux column equipped with quartz condenser and receiver). The surface tension of the quartz-condensed water at 25°C is 71.97 mN/m. Sets of measurements were recorded every 15 minutes until the change in surface tension was less than 0.08mN/m. For the mixtures and DMPC alone, the surface tension equilibrium was reached after about 8 hours for concentrated solutions and more than a day was required for the dilute solutions to reach equilibrium. The temperature of the measurement cell (25°C) was controlled by a water thermostat and values were within ±0.1°C. Surfactants were prepared in 0.01 M Tris.HCl buffer containing 0.1 M NaCl (pH 8.3). The standard deviation for surface tension measurements was less than 0.4 mN/m.

The stock solutions of DMPC SUVs plus surfactant were prepared first by weighing the appropriate amounts of surfactants in a clean volumetric flasks and then adding the desired amount of DMPC SUVs. This solution was stirred for 1 hour to ensure complete mixing and was incubated overnight in order to attain equilibrium before performing the surface tension measurements. The composition of the solution was expressed as the molar fraction (α_{DMPC}) of the lipid, and defined as:

$$\alpha DMPC = \frac{[DMPC]}{[surfactant]+[DMPC]} \quad (22)$$

where [surfactant] and [DMPC] are the molar concentrations of the surfactant and DMPC SUVs in the mixed solution, respectively.

2.2.6. Steady State Fluorescence Studies

Steady-state fluorescence measurements were carried out using a Spex Fluorolog Tau 2 fluorimeter (SPEX-Horiba Instruments, Inc., New Jersey) equipped with a thermostatted sample cuvette holder. Desired temperatures were achieved using a VWR Scientific 1167 circulating water bath equipped with a computer controlled temperature feedback from the sample chamber. Excitation and emission wavelengths used for DPH and TMA-DPH were set to 355 and 430 nm, respectively, with corresponding bandwidths of 4 nm each. Using standard right-angle emission optics, steady-state fluorescence intensity measurements were recorded using the photon counting mode and corrected for any fluctuations of the 450-Watt Xenon arc lamp source by deflecting a portion of the excitation signal on to a separate photodiode. The measured intensity signals are thus reported in the ratio mode (S/R) as counts per second (S) measured on the emission photomultiplier over the photodiode current (R). Measurements were performed using quartz fluorescence cuvettes with path-lengths of 10 mm. For all fluorescence studies, samples were adjusted to provide an absorbance value at the excitation wavelength of less than 0.1. Under such conditions, possible inner filter effects [226] are minimized and the fluorescence signal is proportional to concentration.

Fluorescence intensity experiments were carried out by adding aliquots of 5 mM surfactants into 2mL (0.25 mM) DPH or TMA-DPH labeled DMPC SUVs at 15 min

intervals. Control experiments were carried out by adding an equivalent volume of buffer solution (as added with surfactant) into the same concentration and volume of DPH or TMA-DPH labeled DMPC SUVs. Samples containing bilayers and no fluorophore were used as a blank and titrated with the buffer solution (same volume as added for the surfactants) and subtracted from the corresponding fluorescence intensity values for both the sample and control. Reported fluorescence intensity data represents the mean of at least three measurements of separately prepared SUVs. All data were collected at 30°C, where the phospholipid exists above its lipid phase transition in the fluid phase.

To determine steady-state emission anisotropy values (which reflects changes in fluorescence polarization), parallel and perpendicular fluorescence emission intensity components were measured for all four possible excitation and emission polarizer combinations of vertical (v, 0°) or horizontal (h, 90°) alignments: I_{VV}, I_{VH}, I_{HV}, and I_{HH}, using a photon counting integration time of 10 s for each orientation. The emission anisotropy was calculated according to equation:

$$< r >= \frac{I_{VV} - G \bullet I_{VH}}{I_{VV} + G \bullet 2I_{VH}} \qquad (14)$$

Where I_{VV} is the vertical emission intensity, I_{VH} is horizontal emission intensity using vertical excitation light, and G is the grating factor which corrects the instrument emission detection system for differences in sensitivity to vertical and horizontal polarizations [198].

$$G = \frac{I_{HV}}{I_{HH}} \qquad (15)$$

Polarized intensities were collected for both the surfactant/DMPC SUVs sample of interest and the control solution. Samples containing bilayers and no fluorophore were used as a blank for these studies. Polarized intensity values for the blank were subtracted from the corresponding polarized intensity value for the sample (e.g. $I_{VV} = I_{VV(sample)} - I_{VV(blank)}$) before calculation of the emission anisotropy according to Equation 3.

The effects of surfactants on transition temperature (T_m) of DMPC SUVs labeled with DPH or TMA-DPH were obtained from measurement of <r> values *versus* temperature. The temperature was increased from 10°C to 40°C in increments of 2±0.1 °C. Data were recorded 15 minutes after the temperature was changed so that the samples had reached equilibrium. Reported anisotropy values represent the mean of at least three separate vesicle measurements.

2.2.7. Isothermal Titration Calorimetry

The thermodynamic quantities involved in surfactant binding (C8P and C2,6P) to DMPC SUVs was measured with high-sensitivity isothermal titration calorimetry using a MicroCal VP ITC calorimeter (Microcal, Northampton, MA, USA) with a sample cell volume of V_{cell}= 1.43 mL at 30°C . DMPC SUVs were prepared in 0.01 M Tris.HCl buffer containing 0.1 M NaCl (pH 8.3). Ligand (surfactant) solutions (C8P and C2,6P) were prepared in the same buffer to ensure minimal background from buffer mismatch. Prior to the experiment the surfactants as well as the cell content were degassed for 10 minutes to prevent air bubbles. The surfactant was

injected in to the sample cell *via* a syringe driven by a stepping motor. The tip of the syringe is flat and acts as a stirrer, rotating at a speed of 300 rpm. A preliminary injection of 5μL of ligand was used to cover the enhanced error of the first injection, which is due to a possible slight loss of titrant upon mounting the syringe. The material injected preliminarily is considered to contribute to the concentration scale, but not to the measured reaction heat. Titration data were obtained using 0.25 mM DMPC SUVs (C_M^0) in the sample cell (1.43mL) and 5mM surfactants (C_L^0) in the ligand delivery syringe. This provides surfactant to lipid molar ratios of 4.21 at the end of the titration. Typically, 28 injections (V_{inj}=10 μL, per injection) were made at 15 minutes intervals. With each injection, the total surfactant concentration in the calorimeter chamber increased by δC=3.5x10^{-5}M. The increase of the total reaction volume was also taken into account for determining the DMPC SUV concentration, and the following correction factor was applied:

$$C_{i,M} = C_M^0 \frac{V_{cell}}{\left(V_{cell} + n_i V_{inj}\right)} \tag{23}$$

where $C_{i,M}$ is the DMPC SUV concentration after n_i injections. For the surfactant solution the corresponding concentration factor was:

$$C_{i,L} = \mathrm{C_L^0} n_i \frac{V_{inj}}{\left(V_{cell} + n_i V_{inj}\right)} \tag{24}$$

where $C_{i,L}$ is the surfactant concentration in the sample cell, after n_i injections.

Correction for displaced volume effects which occur with each injection (using expressions $C_{i,M}$ and $C_{i,L}$), baseline correction, peak integration, and dilution corrections were performed using the ORIGIN analysis software supplied with the ITC instrument. The heats of reaction per injection (micro calories per second) were determined by integration of the peak areas. The heat of dilution of the surfactants was determined separately from injection of surfactants into buffer only and was subtracted from the observed heat of binding prior to data analysis. The ORIGIN software provided the best-fit values of ΔH^0 (enthalpy of binding in cal/mole), the stoichiometry of binding *(n)* (surfactant to lipid molar ratio), the binding constant (K_a in M^{-1}) and entropy change *(ΔS* in cal/mole/deg) from plots of heat evolved (in kilocalories) per mole of substrate injected (surfactant) *versus* the surfactant/DMPC SUVs molar ratio. *ΔG* was also obtained for the binding process which is related to the enthalpy of binding by the following expression:

$$\Delta G = \Delta H - T\Delta S = -RTlnK_a \qquad (21)$$

Where, T is the experimental temperature, 303 K. Reported ITC data represents the mean of at least four experiments of separately prepared SUVs.

CHAPTER 3: RESULTS and DISCUSSION

The interactions of non-ionic surfactants, C2,6P and C8P, with DMPC lipid bilayers were assessed using surface tension, steady-state fluorescence spectroscopy (in the presence of DPH and TMA-DPH), and isothermal titration calorimetry (ITC).

3.1. Surface Tension Data

Surface tension methods were used to explore the mixed monolayer and mixed micelle formation of surfactant and phospholipids monomers and to study their interfacial and bulk micellar behavior. Measurements were performed using DMPC SUVs. However, for surface tension studies, it is expected that only the monomeric form of the phospholipids will contribute to the surface activity measurements. This was verified in a separate experiment where monomeric DMPC (not SUVs) solutions were measured.

3.1.1. Surfactant-Lipid Interactions in Mixed Monolayer at the Air/Aqueous Solution Interface

3.1.1.1. Adsorption at the Air/Aqueous Interface

An abrupt slope change in the surface tension *versus* log (C) plot occurs at the cmc (Figure 3). Above the cmc, the equilibrium surface tension of the solution remains essentially constant, because only the monomeric form of the surfactant contributes to the surfactant activity or chemical potential, and hence to the tension reduction. For surfactant concentrations below the cmc, therefore, the absorption of surfactant (Γ_{LA}) (surface excess concentration) at the air/aqueous solution interface can be obtained from the slope of the plot of surface tension *versus* log (C) through

use of equation (5). Where n=1, for the non-ionic surfactants, Figure 17 shows the equilibrium surface tension (γ) *versus* log bulk surfactant molar concentration (C) plots of DMPC, C8P, and C2,6P in 0.01M Tris.HCl buffer containing 0.1 M NaCl (pH 8.3) at 25°C. After calculating surface excess concentrations, the minimum areas per molecule at the air/aqueous solution can be calculated using equation (6). Calculated results for DMPC, C8P, and C2,6P are listed in Table 4. Values obtained for C8P (42.8±0.64 Å^2) and C2,6P (47.1±0.55 Å^2) are in good agreement with published results (Table 2). The value obtained for DMPC (57.5±0.53 Å^2) is also in good agreement with the published value 59.5 Å^2 [227].

Table 4 also lists the pC_{20} values (the negative log of the surfactant molar fraction, C_{20}, that reduces the surface tension of the solvent by 20 mN/m and a measure of the efficiency of adsorption of the surfactant at the interface) and ΔG^0_{ad} values, the standard free energy of adsorption, calculated from equation:

$$\Delta G^0_{ad}(J/mol) = -5710\, pC_{20} - 120.5\, A_{min} - 9962 \qquad (25)$$

based on the relationship

$$\Delta G^0_{ad} = RT\ln(C_\pi)/\omega - \pi A^s_m \qquad (26)$$

where C_π is the molar concentration of surfactant in the aqueous phase at a surface pressure of π, and ω is the number of moles of water per liter of water. At π=20

mN/m and $A_m^s = A_{min}$, equation 21 is obtained, where R=8.314 J mol^{-1} K^{-1}, T=298.2 K, and ω=55.6 mol/L [5, 99].

As shown in Table 4, the effectiveness of adsorption at the interface (Γ_{LA}) of the individual surfactant at the air/aqueous solution interface decreases in the order C8P>C2,6P>DMPC. The smaller effectiveness of adsorption of DMPC presumably arises because of its large area per molecule. However, DMPC has the greatest tendency and efficiency of adsorption (-ΔG_{ad}^0 and pC_{20} values, respectively). Even though C2,6P exhibits less effectiveness of adsorption and occupies the larger area per molecule than C8P, it exhibits reduced efficiency of adsorption (pC_{20} for C2,6P<C8P) over C8P. pC_{20} values increase with increasing number of carbon atoms in the hydrophobic chain, but also for a straight alkyl chain as the hydrophobic group rather than a branched alkyl chain containing the same number of carbon [89]. These values are comparable with previous published data for N-alkyl-2-pyrrolidinones (Table 2).

Figures 18 and Figure 19 show the equilibrium surface tension (γ) *versus* log bulk surfactant molar concentration (C) plots for C8P, DMPC, and a mixture of these two components in 0.01M Tris.HCl buffer containing 0.1 M NaCl (pH 8.3) at 25°C with $\alpha_{DMPC} = 0.05$ and $\alpha_{DMPC} = 0.10$, respectively. Figures 20 and Figure 21 show similar plots for C2,6P, DMPC, and a mixture of these two components also in 0.01M Tris.HCl buffer containing 0.1 M NaCl (pH 8.3) at 25°C with $\alpha_{DMPC} = 0.05$ and $\alpha_{DMPC} = 0.10$, respectively. The total adsorption values , Γ_{LA}^{mix}, of DMPC and the pyrrolidinones separately (C8P and C2,6P) and in DMPC-pyrrolidinone mixtures at

different mole fraction of DMPC were obtained from the slopes shown in Figures 18, 19, 20, and 21, and through use of equation (5). Data are summarized in Table 4. For mixtures of C2,6P with DMPC, the total surfactant adsorption of the mixture, Γ_{LA}^{mix}, increases with an increase in the mole fraction of C2,6P (from 0.90 to 0.95) reflects the higher adsorption value, Γ_{LA}, of the C2,6P over DMPC. A greater total surfactant adsorption, Γ_{LA}^{mix}, for DMPC-C8P mixtures with smaller area per molecule ($A_{min,\ mix}$) was observed over the DMPC-C2,6P mixtures. However, similar tendencies and efficiency of adsorption ($-\Delta G_{mix}^{0}$ and pC_{20} values, respectively) were observed for both DMPC/C8P and DMPC/C2,6P mixtures. The effectiveness of adsorption, Γ_{LA}, is related to the interfacial area occupied by the surfactant molecule; the smaller the effective cross-sectional area of the surfactant at the interface, the greater its effectiveness of adsorption. Effectiveness of adsorption, therefore, depends on the structural groupings of the surfactant molecule and its orientation at the interface. C8P/DMPC mixtures have more surface excess concentration (Γ) (the difference between the solute concentration in the bulk and that at the interface) than C2,6P/DMPC mixtures because the straight alkyl chains of C8P/DMPC mixtures at the interface results in strong attractive hydrophobic interactions. On the other hand, C2,6P/DMPC mixtures, exhibit less surface excess concentration, probably because the C2,6P/DMPC mixtures may not pack as effectively at the interface, due to their branched chains. We believe that our data presented here, are the first available in the literature on adsorption of non-ionic surfactant-zwitterionic lipid mixture at the air/water interface.

3.1.2. Interaction Parameters (β^{σ} , β^{M})

In order to determine whether mixtures of the DMPC-C8P and DMPC- C2,6P would show synergism in their surface properties, molecular interaction parameters, β^{σ} for mixed monolayer formation at the aqueous solution/air interface and β^{M} for mixed micelle formation in aqueous solution, were calculated from the surface tension (γ) versus log bulk surfactant molar concentration (C) plots for the component surfactants and their mixtures. The interaction parameters can be used to predict whether synergism will exist in mixtures of pyrrolidinones with DMPC.

3.1.2.1. Synergism in Surface Tension Reduction Efficiency, β^{σ} Values

Figures 18, 19, 20, and 21 show the equilibrium surface tension (γ) versus log bulk surfactant molar concentration (C) plots for DMPC-C8P and DMPC-C2,6P systems. Values for C_1^0 , C_2^0 and C_{12} were determined from the plots, respectively at a value of γ= 33 mN/m where the slopes are all linear. From the data in Figures 18-21, β^{σ} values were obtained for the four systems investigated by use of equations (7) and (8). All the parameters required for input into the equations and the final results that were obtained are listed in Table 5. Negative β^{σ} values are observed for all surfactant/lipid systems, which indicate that there are very strong interactions at air/aqueous interface. The negative value of β^{σ} implies that the attractive interactions between the two different surfactants (DMPC and C8P, or DMPC and C2,6P) after mixing are stronger than the attractive interactions of the individual surfactants with themselves before mixing. Alternatively, the repulsive interactions between the two

surfactants after mixing are weaker than the self-repulsion before mixing. Negative β^{σ} values and $\left|\beta^{0}\right| > \left|ln\left(C_1^0 / C_2^0\right)\right|$ values indicate synergism in surface tension reduction efficiency. DMPC-C2,6P mixtures show greater synergism in surface tension reduction efficiency compared with DMPC-C8P mixtures. It is unexpected that β^{σ} values for DMPC-C2,6P would be more negative than for DMPC-C8P, since branching near the hydrophilic head group is expected to decrease the synergism and hence the negative values of β^{σ}**.** However, it is important to note that the β^{σ} values obtained from this study represent interaction parameters for mixed monolayer formation of DMPC monomers (not bilayers) with the N-alkyl-2-pyrrolidinones.

3.1.2.2. Synergism in Mixed Micelle Formation in Aqueous Medium, β^{M} Values

Figures 18, 19, 20, and 21 show the equilibrium surface tension (γ) *versus* log bulk surfactant molar concentration (C) plots for DMPC-C8P and DMPC-C2,6P systems. The N-alkyl-2-pyrrolidinones investigated here do not reach their cmc values because of their limited solubility in water at 25°C (Figure 17). Therefore, the molar concentration of the N-alkyl-2-pyrrolidinone at its maximum solubility in water (C_M^2) was used rather than a cmc value in order to determine the approximate synergism for mixed micelle formation in aqueous medium.

From the data in Figures 18-21, β^{M} values were obtained for the four systems investigated using equations 9 and 10. All the parameters needed to input into the equations and the final results are listed in Table 6. High negative β^{M} values observed for all systems, suggest that in general, there are very strong interactions

between DMPC and surfactants in aqueous medium. The negative value of β^M suggests that the attractive interactions between the two different surfactants (DMPC and C8P or DMPC and C2,6P) after mixing is stronger than the attractive interactions of the two component surfactants or alternatively that the repulsive interactions between the two different surfactants after mixing are weaker than the self-repulsion of the individual surfactants. Negative β^M values and $|\beta^M| > |ln(C_1^M / C_2^M)|$ values estimate synergism effects for surface tension reduction efficiency. DMPC-C2,6P systems show greater synergism for mixed micelle formation in aqueous medium compared with DMPC-C8P systems.

The absolute values of the β parameters indicate the strength of the interaction between the two surfactants upon mixing and also the extent of the deviation of the mixture solution from the ideal behavior. A value close to zero indicates little or no change in interactions upon mixing of two surfactants (almost ideal mixing of the 2 surfactants). Also, steric effects contribute to the value of the β parameter when there are variations in the size of the hydrophilic head group or in the branching of the hydrophobic groups of the two surfactants. Thus the more negative β values obtained for C2,6P -DMPC mixtures compared to C8P (straight chain)-DMPC mixtures, may arise from its branched chain structure.

Usually the interactions and consequently the values of β are dominated by electrostatic interactions between the hydrophilic head groups of the two different surfactants. Larger β parameters have been reported between anionic and cationic mixtures with β^σ values between -5.5 to -35.6 and β^M values between -3.9 to -25.5

[99(g)]. Similarly, for anionic-zwitterionic mixtures β parameters exhibit ranges of β^{σ} values between -2.5 to -15.7 and β^{M} values between -1.2 to -15.5 [99(g)]. However, only limited data is available for nonionic-zwitterionic mixtures; their β^{σ} values are in the range between -0.6 to -2.7, with β^{M} values between -0.3 to -2.7 [99(g)].

The attractive interactions (high β values) obtained in this study, between N-alkyl-2-pyrrolidinones and DMPC may result from electrostatic interactions between the phosphocholine group of DMPC (Figure 2 C) and the zwitterionic head group of the N-alkyl-2-pyrrolidinones (due to their resonance form, Figure 1C).

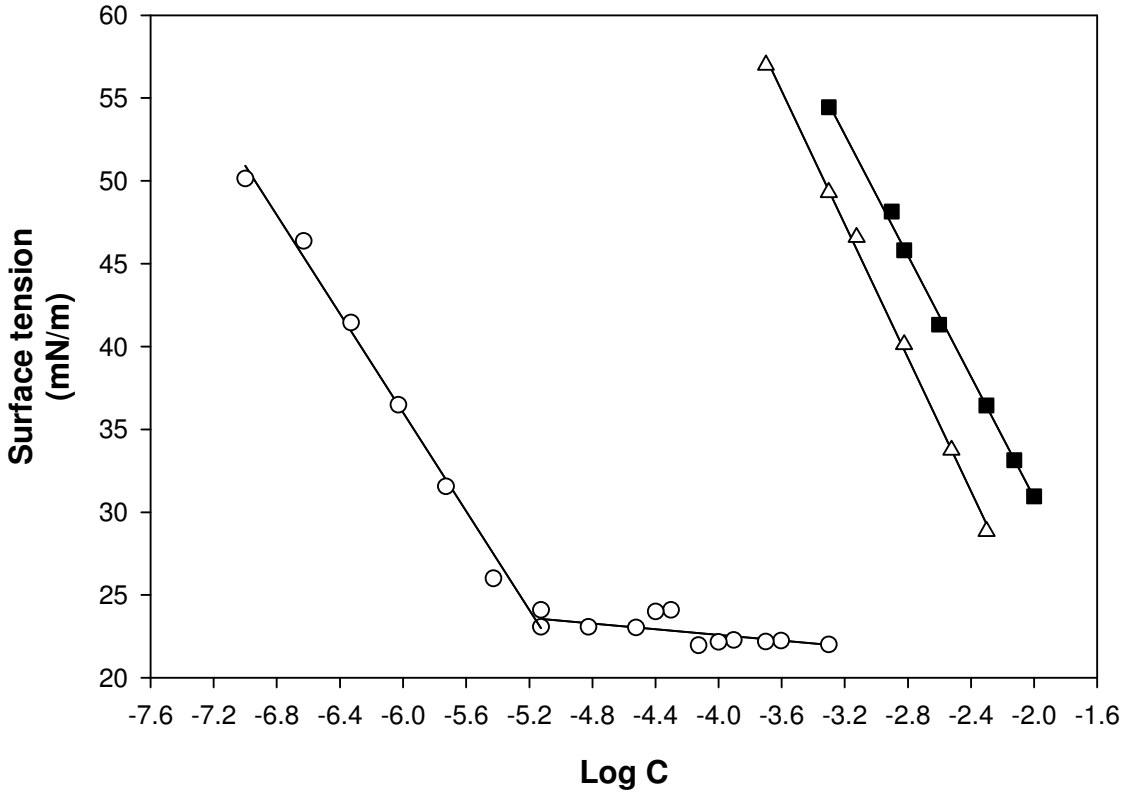

Figure 17: Surface tension (γ) versus log *C* curves for (○) DMPC; (Δ) C8P; and (■) C2,6P in 0.01M Tris.HCl buffer containing 0.1 M NaCl (pH 8.3) at 25°C. Data represent an average of 3 trials for each with standard deviation less than 0.4 mN/m.

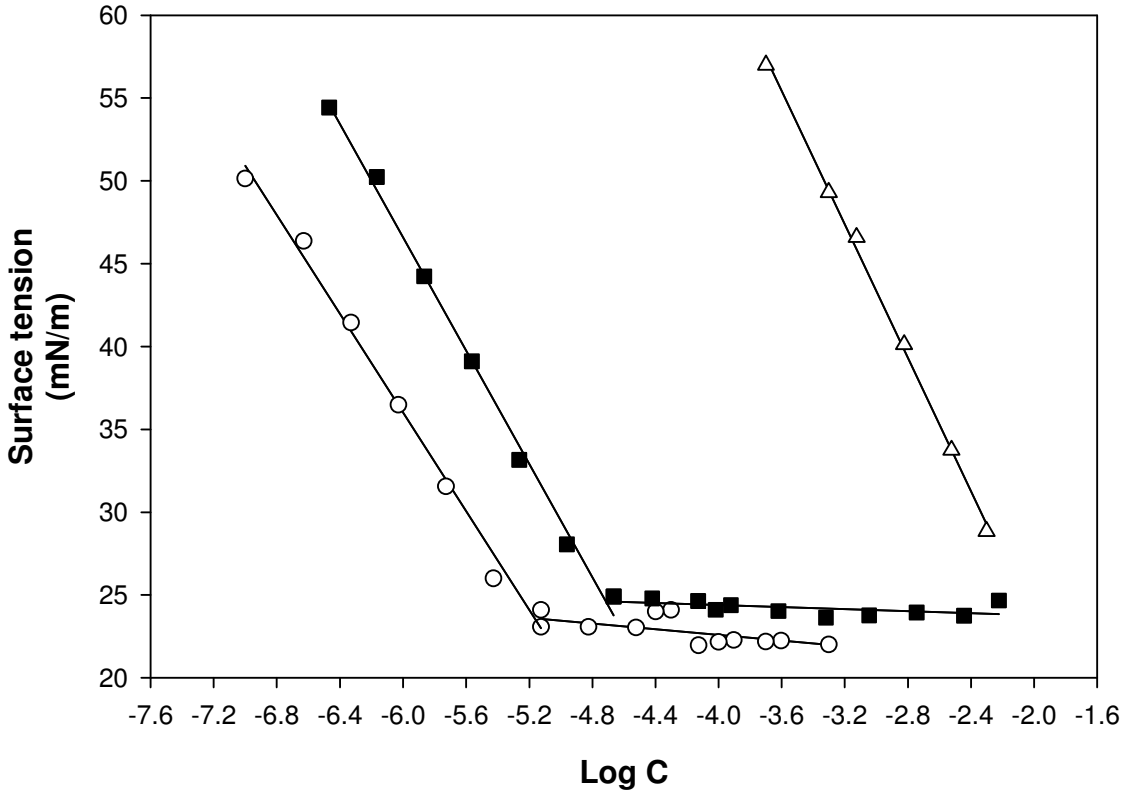

Figure 18: Surface tension (γ) versus Log *C* curves for (■) DMPC / C8P, (○) DMPC; and (Δ) C8P in 0.01M Tris.HCl buffer containing 0.1 M NaCl (pH 8.3) at 25°C. $\alpha_{DMPC} = 0.05$ (mole fraction of DMPC of the total surfactant in the bulk phase). Data represent an average of 3 trials for each with standard deviation less than 0.4 mN/m.

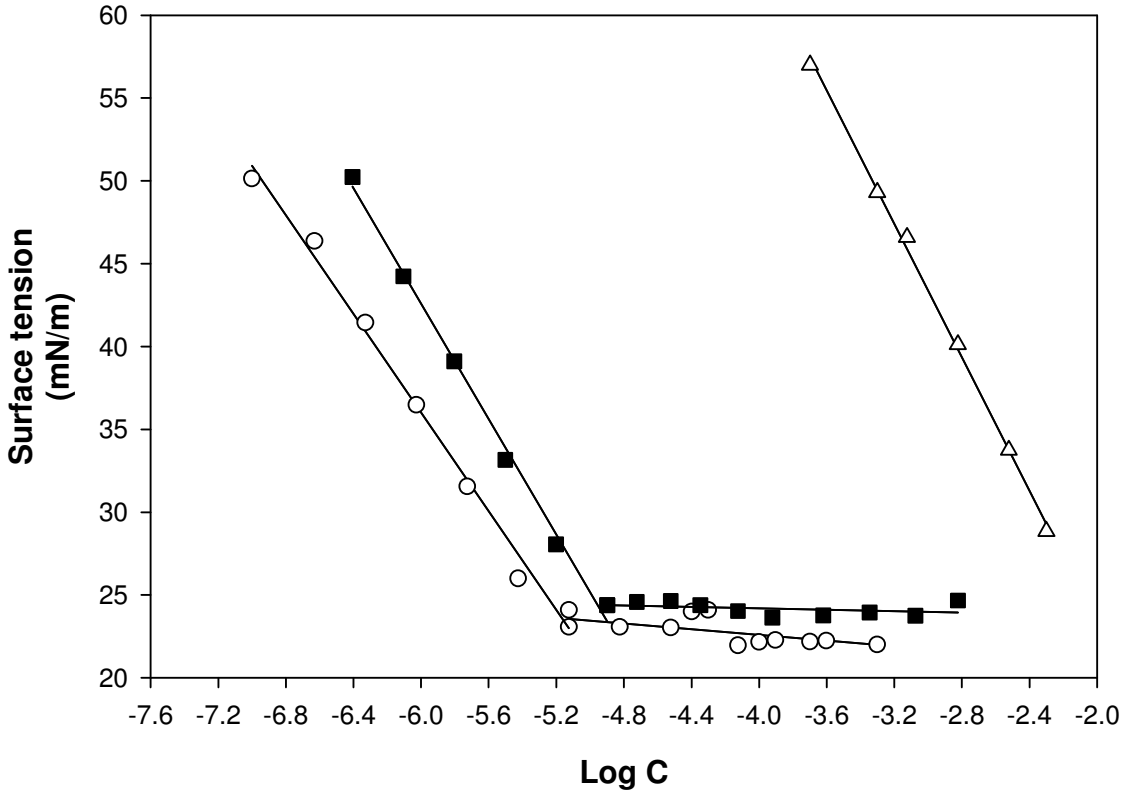

Figure 19: Surface tension (γ) versus Log *C* curves for (■) DMPC / C8P, (○) DMPC; and (Δ) C8P in 0.01M Tris.HCl buffer containing 0.1 M NaCl (pH 8.3) at 25°C. $\alpha_{DMPC} = 0.1$ (mole fraction of DMPC of the total surfactant in the bulk phase). Data represent an average of 3 trials for each with standard deviation less than 0.4 mN/m.

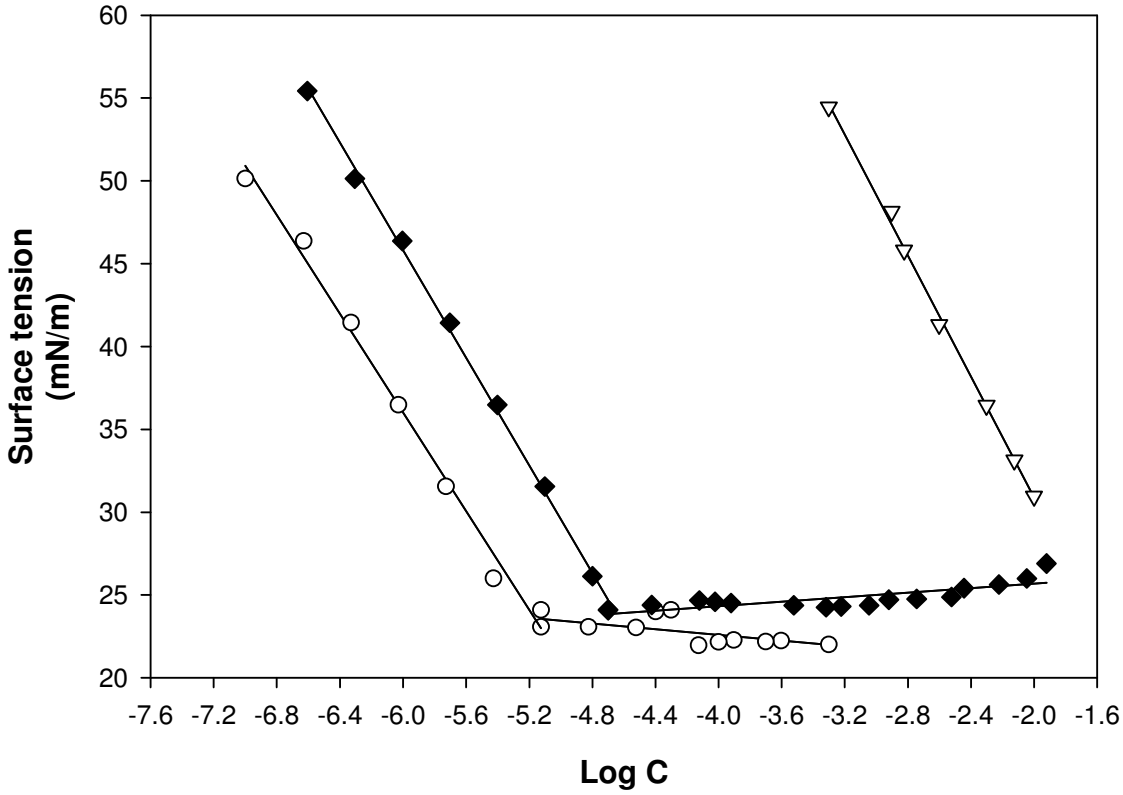

Figure 20: Surface tension (γ) versus Log *C* curves for (♦) DMPC / C2,6P, (○) DMPC; and (∇) C2,6P in 0.01M Tris.HCl buffer containing 0.1 M NaCl (pH 8.3) at 25°C.

$\alpha_{DMPC} = 0.05$ (mole fraction of DMPC of the total surfactant in the bulk phase). Data represent an average of 3 trials for each with standard deviation less than 0.4 mN/m.

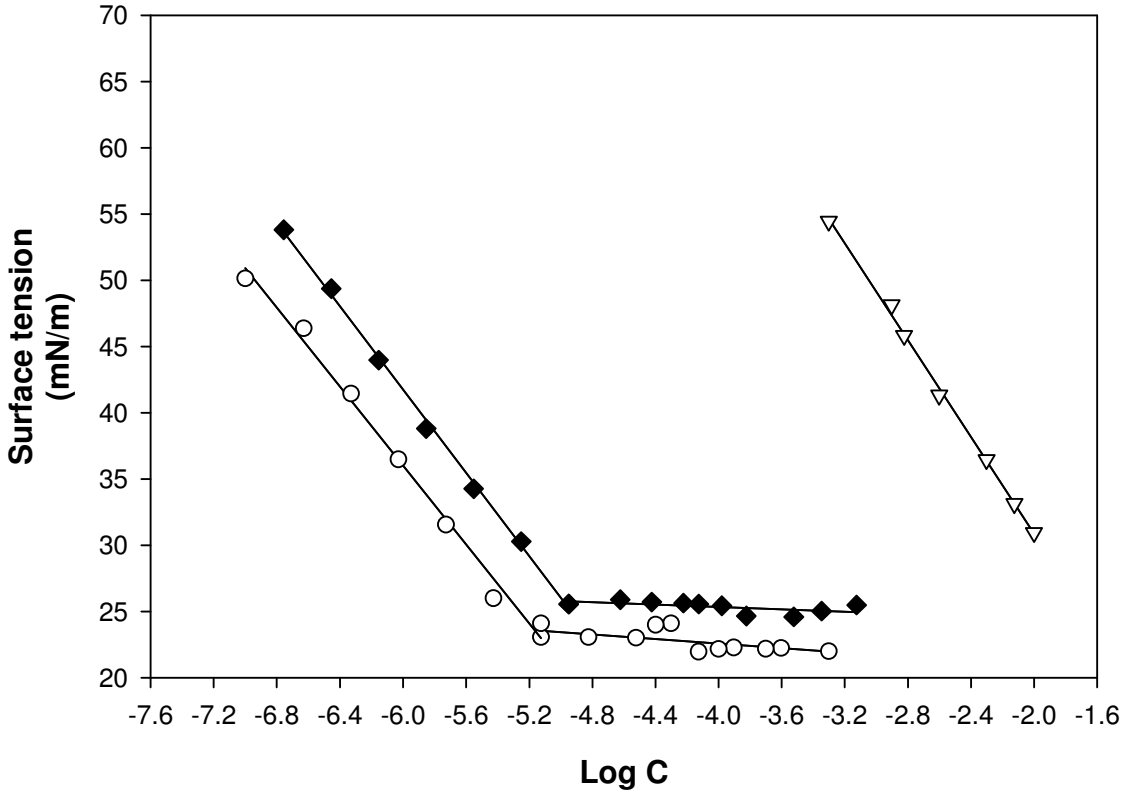

Figure 21: Surface tension (γ) versus Log *C* curves for (♦) DMPC / C2,6P, (○) DMPC; and (∇) C2,6P in 0.01M Tris.HCl buffer containing 0.1 M NaCl (pH 8.3) at 25°C.

$\alpha_{DMPC} = 0.1$ (mole fraction of DMPC of the total surfactant in the bulk phase). Data represent an average of 3 trials for each with standard deviation less than 0.4 mN/m.

Table 4
Interfacial properties of DMPC, N-Alkyl-2-Pyrrolidinones (C8P and C2,6P), and their mixtures at air/aqueous interface in 0.01M Tris.HCl buffer containing 0.1 M NaCl (pH 8.3) at 25°C. Data represent an average of 3 trials for each measurement.

System	$\Gamma_{LA} \times 10^{10}$ (mol/cm^2)	A_{min} (Å^2)	pC_{20}	ΔG^0_{ad} (kJ/mol)
DMPC	2.63±0.03	57.5±0.53	6.55±0.02	-54.3±0.20
C8P	3.53±0.05	42.8±0.64	3.04±0.02	-32.4±0.15
**C8P* (in H_2O)	4.38	37.9	3.14	-32.4
C2,6P	3.21±0.03	47.1±0.55	2.73±0.01	-31.2±0.15
**C2,6P* (in H_2O)	3.57	46.5	3.00	-32.7

* literature values from Table 2.

System	α_{DMPC}	$\Gamma^{mix}_{LA} \times 10^{10}$ (mol/cm^2)	$A_{min,mix}$ (Å^2)	pC_{20}	ΔG^0_{mix} (kJ/mol)
DMPC / C8P	0.05	3.00±0.04	50.4±0.64	5.86±0.01	-49.5±0.12
DMPC / C8P	0.1	3.05±0.03	49.4±0.49	6.09±0.01	-50.7±0.10
DMPC / C2,6P	0.05	2.85±0.02	53.0±0.38	5.90±0.01	-50.0±0.06
DMPC / C2,6P	0.1	2.76±0.04	54.8±0.76	6.16±0.01	-51.7±0.12

Table 5

Interaction parameters for mixed monolayer formation at the air/aqueous solution for DMPC /C8P and DMPC /C2,6P mixtures in 0.01M Tris.HCl buffer containing 0.1 M NaCl (pH 8.3) at 25°C. Molar concentrations to yield γ= 33 mN/m. Data represent an average of 3 trials for each measurement.

System	α_{DMPC}	X_1	β^{σ}	*Average*	$\left\|ln\left(C_1^0/C_2^0\right)\right\|$
DMPC/C8P	0.05	0.67	-11.5		7.6
				-11.8± 0.4	
DMPC/C8P	0.10	0.69	-12.0		7.6
DMPC/C2,6P	0.05	0.69	-12.8		8.5
				-13.0±0.3	
DMPC/C2,6P	0.10	0.71	-13.2		8.5

System	α_{DMPC}	C_1^0 (M)	C_2^0 (M)	C_{12} (M)
DMPC/C8P	0.05	1.598×10^{-6}	3.276×10^{-3}	6.244×10^{-6}
DMPC/C8P	0.10	1.598×10^{-6}	3.276×10^{-3}	3.559×10^{-6}
DMPC/C2,6P	0.05	1.598×10^{-6}	7.647×10^{-3}	6.140×10^{-6}
DMPC/C2,6P	0.10	1.598×10^{-6}	7.647×10^{-3}	3.600×10^{-6}

Table 6

Interaction parameters for mixed micelle formation in aqueous medium for DMPC /C8P and DMPC /C2,6P mixtures in 0.01M Tris.HCl buffer containing 0.1 M NaCl (pH 8.3) at 25°C. Data represent an average of 3 trials for each.

System	α_{DMPC}	X_1	β^M	*Average*	$\left\|ln\left(C_1^M / C_2^M\right)\right\|$
DMPC/C8P	0.05	0.64	-11.5		6.7
				-11.7±0.3	
DMPC/C8P	0.10	0.66	-11.9		6.7
DMPC/C2,6P	0.05	0.66	-12.5		7.6
				-12.9±0.5	
DMPC/C2,6P	0.10	0.68	-13.2		7.6

System	α_{DMPC}	C_1^M (M)	C_2^M (M)	C_{12}^M (M)
DMPC/C8P	0.05	6.752×10^{-6}	5.2×10^{-3}	1.865×10^{-5}
DMPC/C8P	0.10	6.752×10^{-6}	5.2×10^{-3}	1.108×10^{-5}
DMPC/C2,6P	0.05	6.752×10^{-6}	1.3×10^{-2}	2.080×10^{-5}
DMPC/C2,6P	0.10	6.752×10^{-6}	1.3×10^{-2}	1.145×10^{-5}

3.2. Characterization of Surfactant Effects on DMPC SUVs by Fluorescence Spectroscopy

The effects of the non-ionic surfactants, C2,6P and C8P, on the physical structure of DMPC lipid bilayers was assessed using steady-state fluorescence spectroscopy in the presence of extrinsic fluorophores (DPH and TMA-DPH). The surfactant to lipid molar ratio used was typically 0 to 5 because in most previously studied cases, solubilization of vesicles with surfactants has been found to occur within the 0.5 to 3.0 molar range (Re^{sol}) [108]. These membrane-bound probes are nonfluorescent in aqueous media but partition readily into membranes and lipid assemblies accompanied by strong fluorescence enhancement. DPH is located in the membrane interior; whereas its derivative TMA-DPH is anchored to the membrane-water interface by the attachment of quarternary ammonium group to one of the phenyl rings (Figure 13). Fluorescence emission from DPH or TMA-DPH arises only from DPH or TMA-DPH embedded within the membrane microenvironment [197]. From control experiments, no evidence for specific interactions between TMA-DPH and surfactants were determined.

3.2.1. Fluorescence Spectral Analysis

Fluorescence emission spectra are sensitive to the fluorophore's local environment. Hence the spectra of DPH and TMA-DPH probes can provide information on its immediate bilayer environment through fluorescence intensity changes and fluorescence emission wavelength shifts.

3.2.1.1. DPH Data

The effects of increasing the C8P and C2,6P surfactant concentrations on fluorescence emission intensity of DPH in DMPC SUVs are shown in Figures 22 and Figure 23, respectively (uncorrected for dilution). All measurements were performed at 30°C where DMPC exists in the liquid crystalline state. Both surfactants examined resulted in a decrease of the fluorescence emission intensity with increasing C8P and C2,6P concentrations from 0 to 0.83 mM, corresponding to a surfactant to lipid molar ratio ([S]/[L]) from 0 to 4 within the bilayer. However, since the the total volume increases by 16.7% for each titration experiment, Figure 24 shows the control experiments carried out by the titration of DPH labeled DMPC vesicles with buffer solution (using the same volumes as added for the surfactant studies). Changes in fluorescence intensities due to dilution effects are significant, and data were subsequently corrected for decreased fluorescence due to dilution. For all cases, the spectra (Figure 22, 23, and 24) showed no shift of the fluorescence λmax for DPH.

From separate experiments, the emission spectra of DPH labeled DMPC vesicles were recorded after each titration with surfactant. Raw fluorescence intensities at λmax (426 nm) were obtained and F_0/F (surfactant free / bound surfactant) data were calculated and plotted as a function of increasing molar ratio S/L (surfactant to DMPC SUVs) as shown in Figure 25.

Data represented in Figure 25 were corrected for titration dilution effects by first subtracting the intensities from the control samples as described above. Results are shown in Figure 26. Since DPH is located within the acyl chain region of the bilayer, the observed spectral signals report on any changes occurring within the membrane

interior. The emission data represented in Figure 26 suggest that introduction of C8P into the bilayer results in a significant effect on the lipid packing within the bilayer compared with data observed for C2,6P. It would appear that after correction of the data, the observed initial quenching of DPH fluorescence intensities in the presence of the C2,6P surfactant is due simply to a dilution effect.

Such results may be explained by considering three associated models: a) C8P can extend/penetrate (larger permeability coefficient) further into the acyl chain region of the bilayer *versus* the branched chain C2,6P, b) the binding coefficient for C8P is more favorable than for C2,6P (i.e. more surfactant bound to the membrane), and c) a combination of both can be occurring.

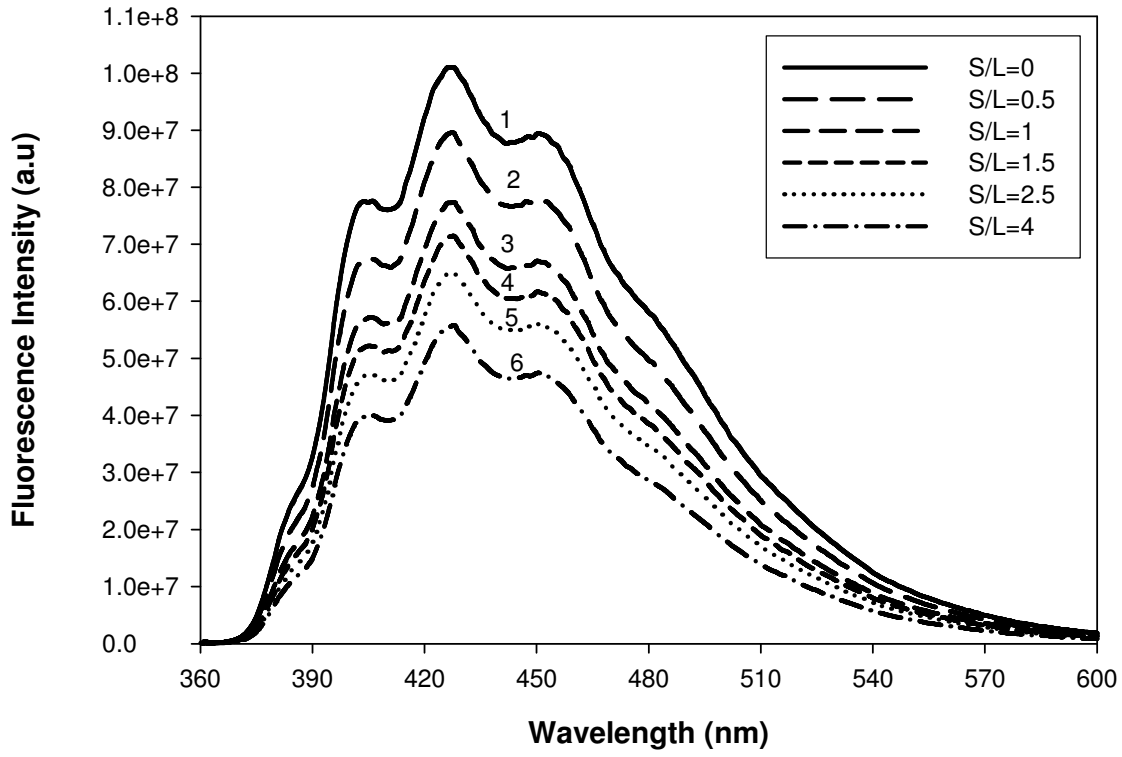

Figure 22: Fluorescence emission spectra: Titration of DPH labeled DMPC SUVs with C8P at 30°C, obtained with excitation at 355 nm and emission at 430 nm. Excitation and emission bandwidths were each 4 nm, respectively. [L]= DMPC SUVconcentration. $[S]_{tot}$ = Total surfactant concentration.

Spectrum 1: [L] = 0.25 mM, $[S]_{tot}$= 0 mM; 2: [L] = 0.24 mM, $[S]_{tot}$= 0.12 mM; 3: [L] = 0.24mM, $[S]_{tot}$= 0.24 mM; 4: [L] = 0.23 mM, $[S]_{tot}$= 0.35 mM; 5: [L] = 0.22 mM, $[S]_{tot}$= 0.56 mM; 6: [L] = 0.21 mM, $[S]_{tot}$= 0.83 mM.

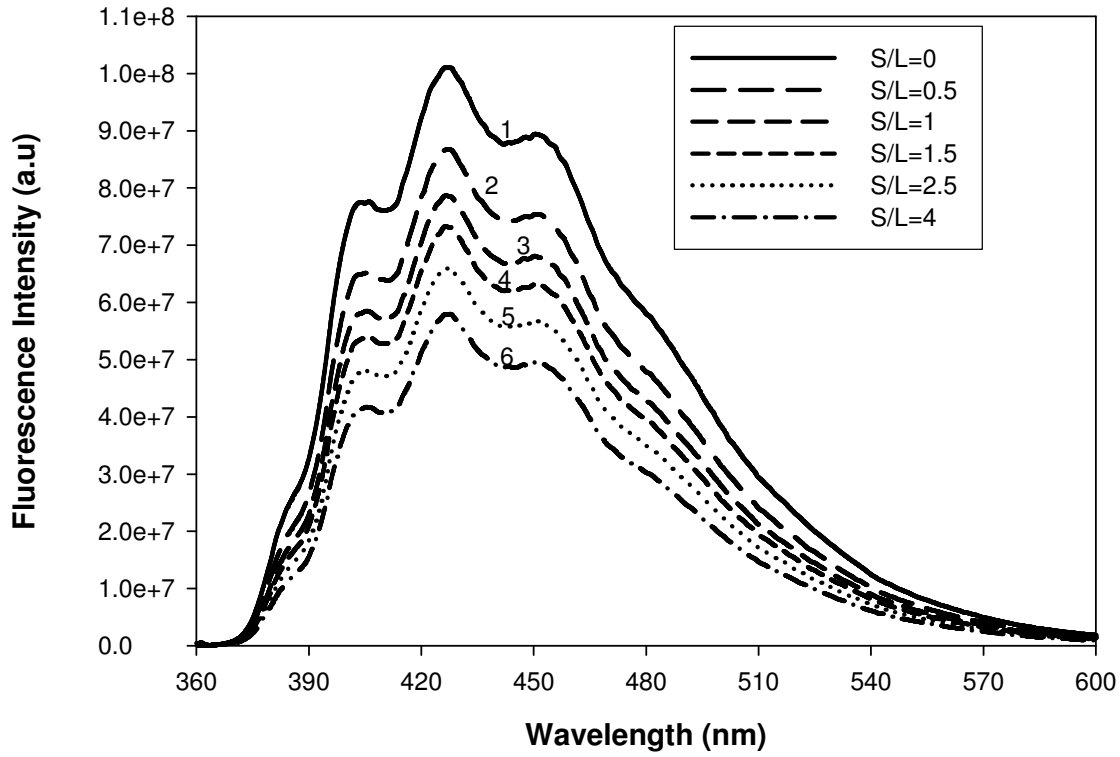

Figure 23: Fluorescence emission spectra: Titration of DPH labeled DMPC SUVs with C2,6P at 30°C, obtained with excitation at 355 nm and emission at 430 nm. Excitation and emission bandwidths were each 4 nm, respectively. [L]= DMPC SUVconcentration. $[S]_{tot}$ = Total surfactant concentration.

Spectrum 1: [L] = 0.25 mM, $[S]_{tot}$= 0 mM; 2: [L] = 0.24 mM, $[S]_{tot}$= 0.12 mM; 3: [L] = 0.24mM, $[S]_{tot}$= 0.24 mM; 4: [L] = 0.23 mM, $[S]_{tot}$= 0.35 mM; 5: [L] = 0.22 mM, $[S]_{tot}$= 0.56 mM; 6: [L] = 0.21 mM, $[S]_{tot}$= 0.83 mM.

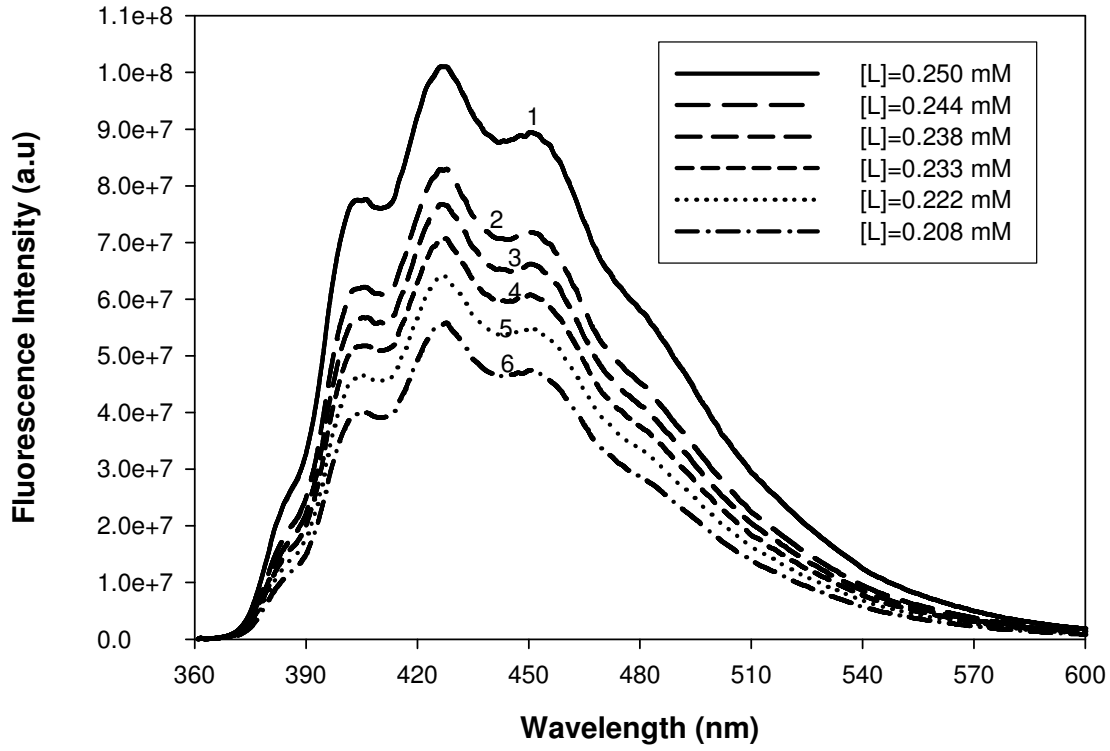

Figure 24: Fluorescence emission spectra: Titration of DPH labeled DMPC SUVs with buffer at 30°C, obtained with excitation at 355 nm and emission at 430 nm. Excitation and emission bandwidths were each 4 nm, respectively. [L]= DMPC SUVconcentration. $[S]_{tot}$ = Total surfactant concentration.

Spectrum 1: [L] = 0.25 mM, $[S]_{tot}$= 0 mM; 2: [L] = 0.24 mM, $[S]_{tot}$= 0 mM; 3: [L] = 0.24 mM, $[S]_{tot}$= 0 mM; 4: [L] = 0.23 mM, $[S]_{tot}$= 0 mM; 5: [L] = 0.22 mM, $[S]_{tot}$= 0 mM; 6: [L] = 0.21 mM, $[S]_{tot}$= 0 mM.

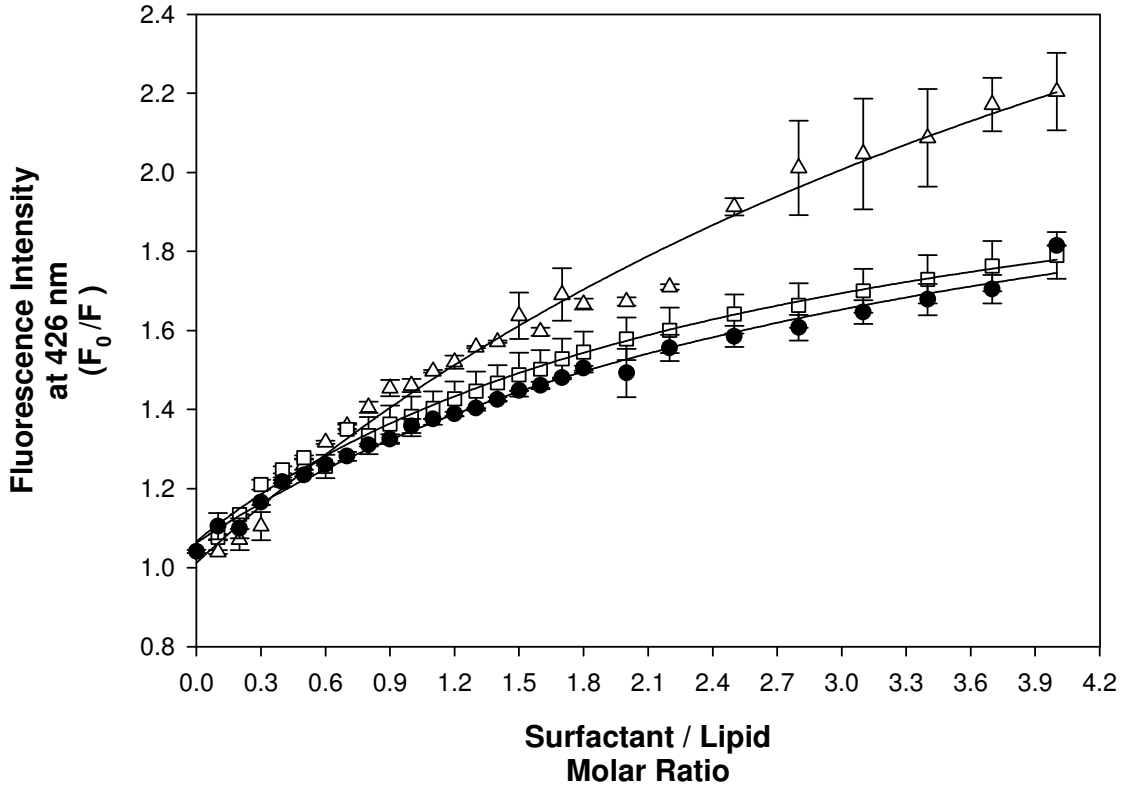

Figure 25: Titration of DPH labeled DMPC SUVs with surfactants at 30°C, obtained with excitation at 355 nm and emission at 430 nm. Excitation and emission bandwidths were each 4 nm, respectively. The absence of surfactant (control) (●) and presence of C2,6P (□) and C8P (Δ) at λ_{max} = 426 nm. The standard deviations reflect 3 trials for each sample studied. The continuous lines are drawn only to guide the eye.

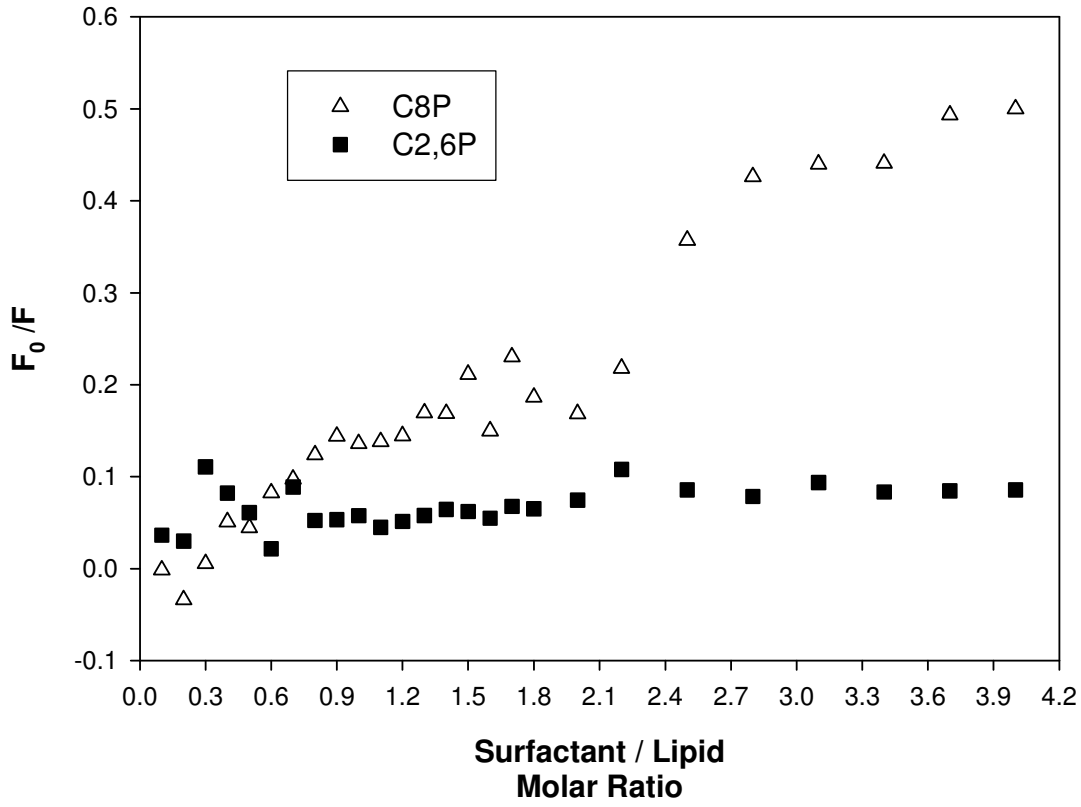

Figure 26: DPH embedded in DMPC SUVs, correction of Figure 25 for dilution effect by subtraction of control from samples. In presence of C2,6P (■) and C8P (Δ).

3.2.1.2. TMA- DPH Data

Fluoresence emission intensity studies were also obtained for TMA-DPH labeled DMPC samples. In these studies, the fluorescence probe is reporting specifically about packing affects occurring as a result of surfactant interactions at the head group region of the bilayer.

Figures 27 and Figure 28 show the uncorrected fluorescence intensity changes on titration of TMA-DPH labeled DMPC vesicles with C8P and C2,6P, respectively. As previously shown for DPH, both surfactants examined result in a decrease of the fluorescence emission intensities with increasing C8P and C2,6P concentration from 0 to 0.83 mM, corresponding to a surfactant to lipid molar ratio ([S]/[L]) from 0 to 4 within the bilayer. Again, the total volume increased 16.7% for each titration experiment and Figure 29 shows the decrease in fluorescence intensity for TMA-DPH labeled control experiments carried out by the titration of DMPC vesicles with buffer solution (using the same volumes as added for the surfactant studies). For all cases, the spectra (Figure 27, 28, and 29) showed no shift of the wavelength of maximum fluorescence emission, λmax, for TMA-DPH.

From separate experiments, the emission spectra of TMA-DPH labeled DMPC vesicles were taken after each titration with surfactant (15 minute incubation periods). Raw fluorescence intensities at λmax (426 nm) were measured and ploted as F_0/F (surfactant free / bound surfactant) as a function of increasing molar ratio [S]/[L] (surfactant to DMPC SUVs) as shown in Figure 30. Intensities were corrected for dilution effects by first subtraction of the intensities determined for control samples (control SUV/ TMA-DPH) and due to dilution effects. The results are shown in

Figure 31. Clearly, addition of C8P to DMPC SUVs appears to have a greater effect on bilayer packing at the head group region compared with C2,6P. It would appear that the fluorescence quenching effects observed for TMA-DPH with addition of C2,6P surfactant also arises from simple dilution effects. Decreasing fluorescence intensity trend compares favorably with the previously discussed DPH/surfactant/DMPC SUVs data.

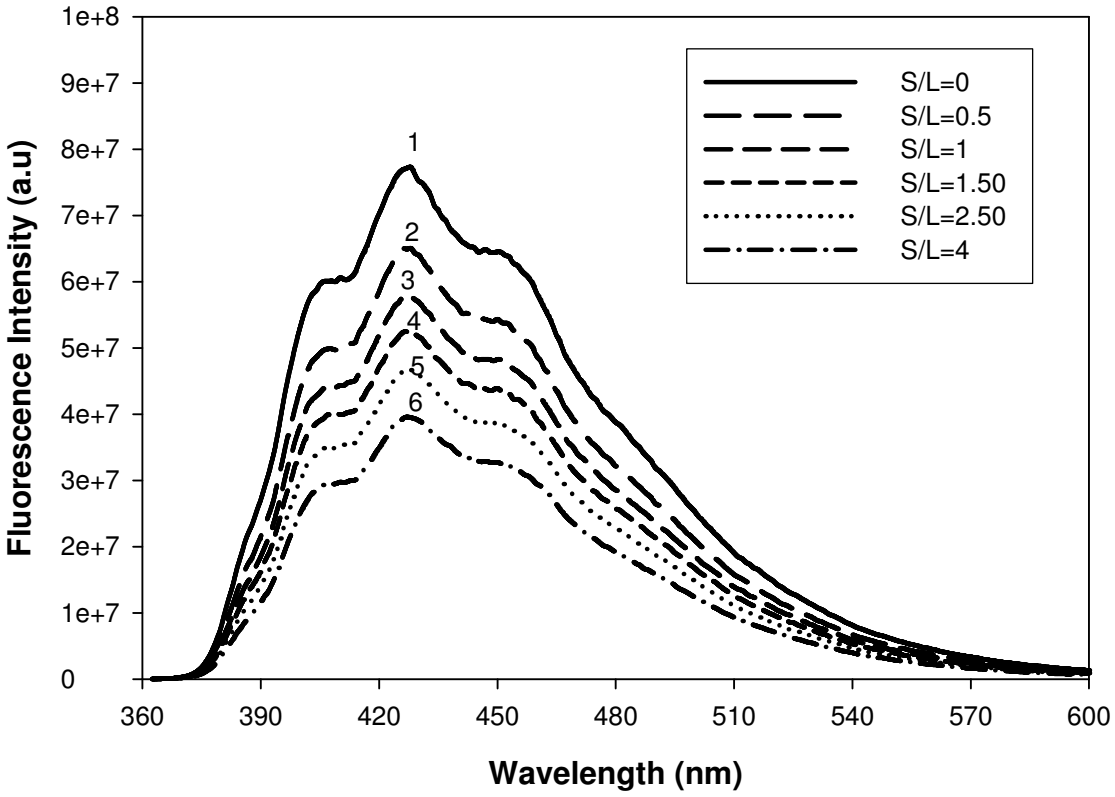

Figure 27: Fluorescence emission spectra: Titration of TMA-DPH labeled DMPC SUVs with C8P at 30°C, obtained with excitation at 355 nm and emission at 430 nm. Excitation and emission bandwidths were each 4 nm, respectively. [L]= DMPC SUVconcentration. $[S]_{tot}$ = Total surfactant concentration.

Spectrum 1: [L] = 0.25 mM, $[S]_{tot}$= 0 mM; 2: [L] = 0.244 mM, $[S]_{tot}$= 0.122 mM; 3: [L] = 0.238 mM, $[S]_{tot}$= 0.238 mM; 4: [L] = 0.233 mM, $[S]_{tot}$= 0.349 mM; 5: [L] = 0.222 mM, $[S]_{tot}$= 0.556 mM; 6: [L] = 0.208 mM, $[S]_{tot}$= 0.833 mM.

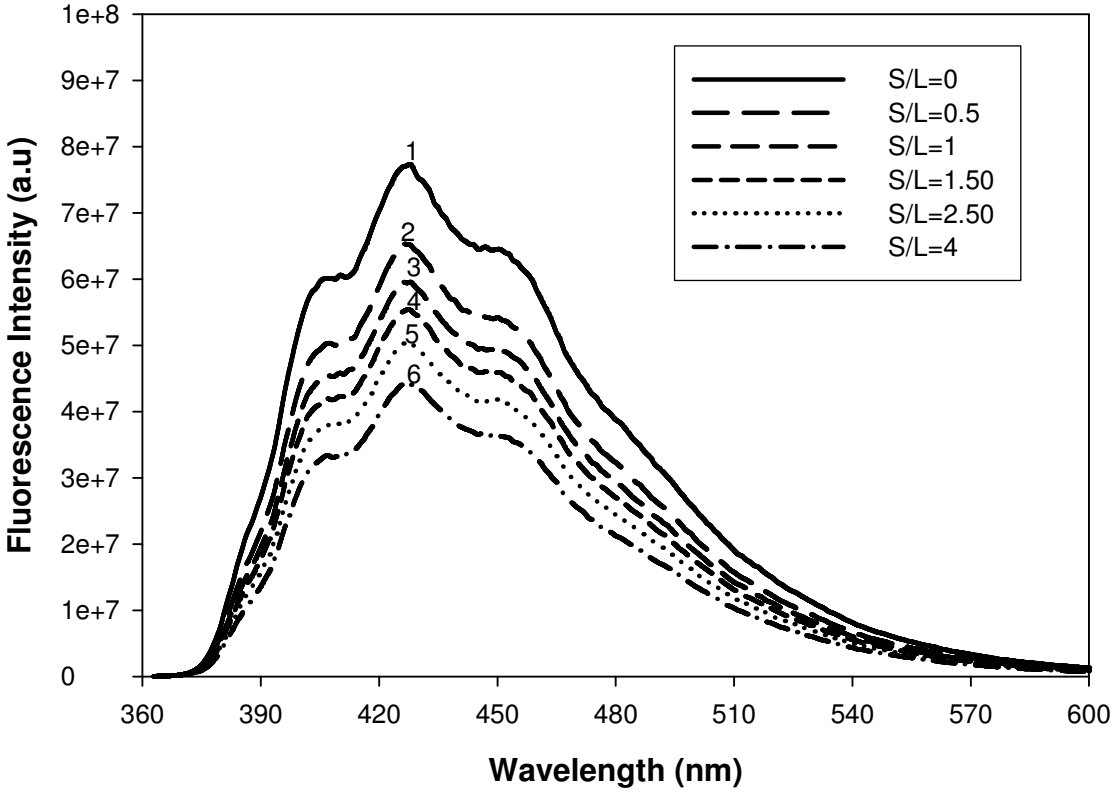

Figure 28: Fluorescence emission spectra: Titration of TMA-DPH labeled DMPC SUVs with C2,6P at 30°C, obtained with excitation at 355 nm and emission at 430 nm. Excitation and emission bandwidths were each 4 nm, respectively. [L]= DMPC SUVconcentration. $[S]_{tot}$ = Total surfactant concentration.

Spectrum 1: [L] = 0.25 mM, $[S]_{tot}$= 0 mM; 2: [L] = 0.24 mM, $[S]_{tot}$= 0.12 mM; 3: [L] = 0.24mM, $[S]_{tot}$= 0.24 mM; 4: [L] = 0.23 mM, $[S]_{tot}$= 0.35 mM; 5: [L] = 0.22 mM, $[S]_{tot}$= 0.56 mM; 6: [L] = 0.21 mM, $[S]_{tot}$= 0.83 mM.

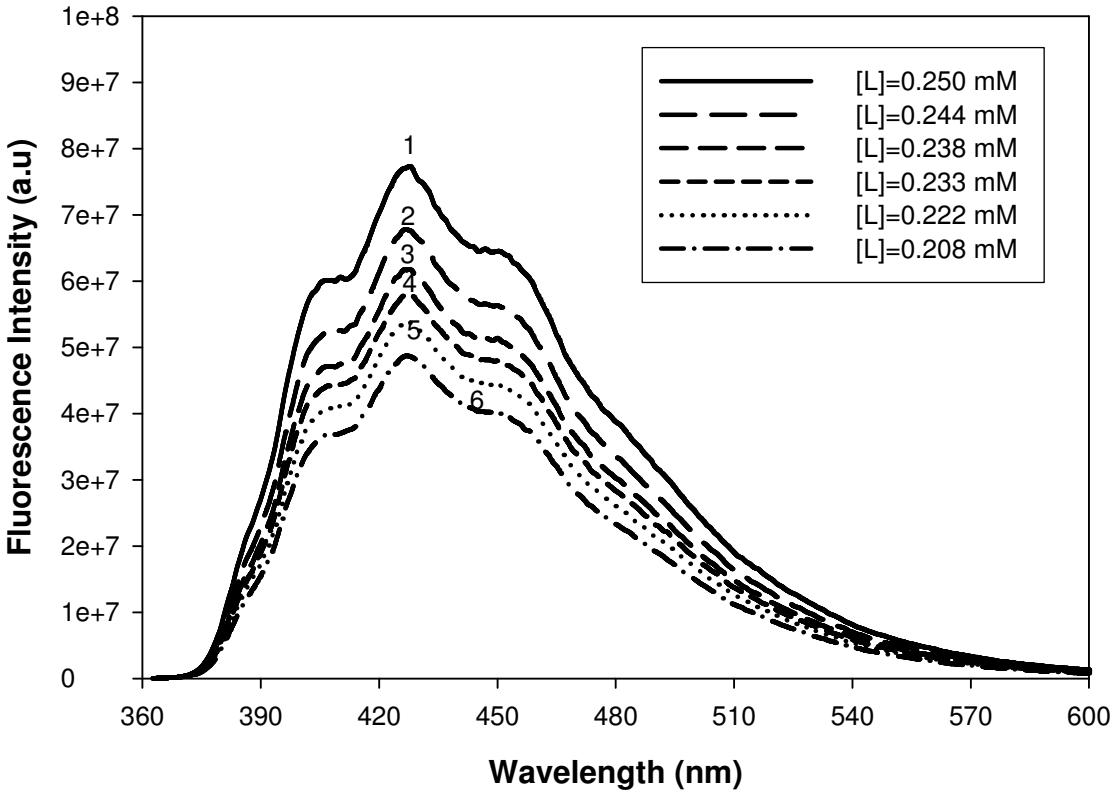

Figure 29: Fluorescence emission spectra: Titration of TMA-DPH labeled DMPC SUVs with buffer at 30°C, obtained with excitation at 355 nm and emission at 430 nm. Excitation and emission bandwidths were each 4 nm, respectively. [L]= DMPC SUVconcentration. $[S]_{tot}$ = Total surfactant concentration.

Spectrum 1: [L] = 0.25 mM, $[S]_{tot}$= 0 mM; 2: [L] = 0.24 mM, $[S]_{tot}$= 0 mM; 3: [L] = 0.24 mM, $[S]_{tot}$= 0 mM; 4: [L] = 0.23 mM, $[S]_{tot}$= 0 mM; 5: [L] = 0.22 mM, $[S]_{tot}$= 0 mM; 6: [L] = 0.21 mM, $[S]_{tot}$= 0 mM.

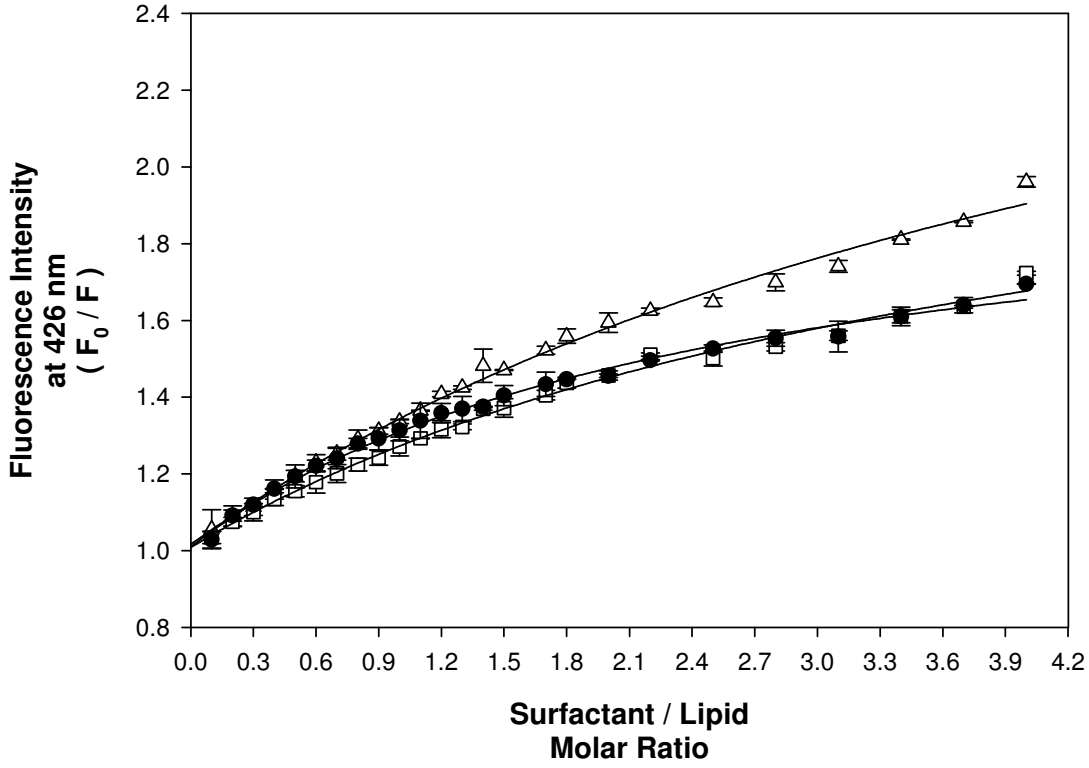

Figure 30: Titration of TMA-DPH labeled DMPC SUVs with surfactants at 30°C, obtained with excitation at 355 nm and emission at 430 nm. Excitation and emission bandwidths were each 4 nm, respectively. The absence of surfactant (control) (●) and presence of C2,6P (□) and C8P (Δ) at λ_{max} = 426 nm. The standard deviations reflect 3 trials for each sample studied. The continuous line is drawn to guide the eye.

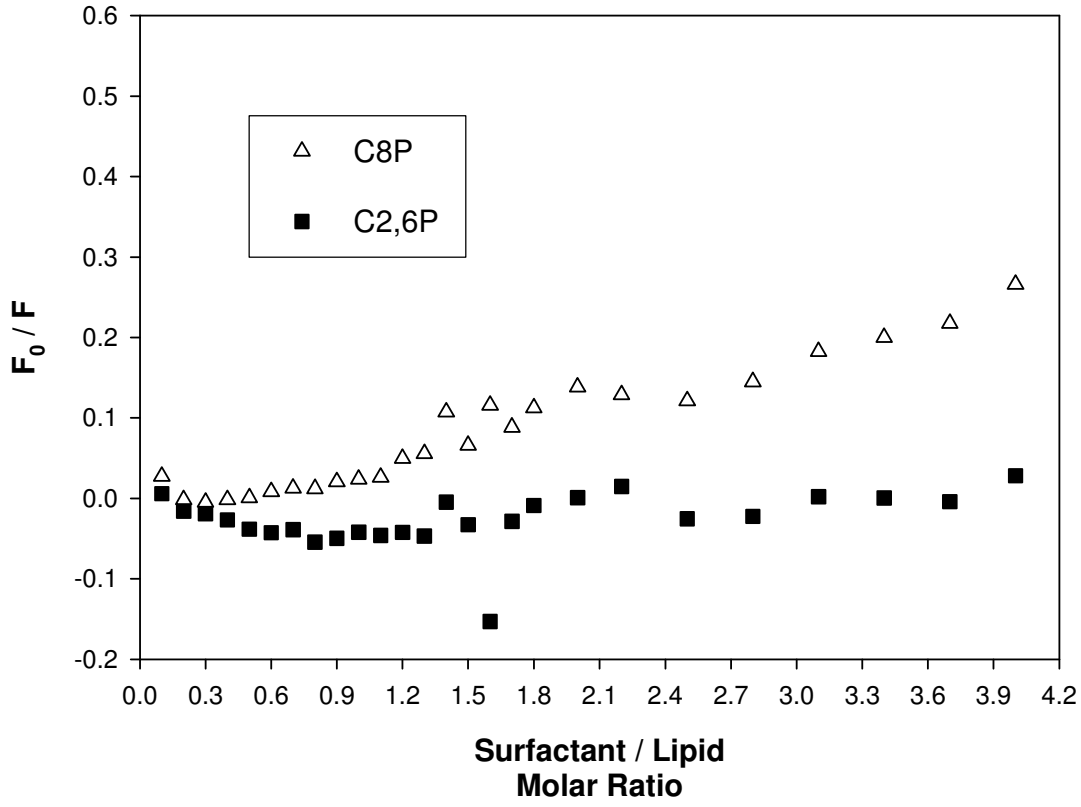

Figure 31: TMA-DPH embedded in DMPC SUVs, correction of Figure 30 for dilution effect by subtraction of control from samples. In presence of C2,6P (■) and C8P (Δ).

3.2.2. Effects of Surfactants on the Main Lipid Phase Transition Temperature of DMPC SUVs

Membrane lipids can exist in a gel or fluid liquid crystalline state phases, depending on the temperature and their main lipid phase phase transition temperature (T_m). Below the transition temperature, the lipid exists in the gel phase. Whereas for temperatures > T_m , the lipid usually assumes a less ordered, liquid crystalline arrangement. The gel-fluid physical state of the bilayer and T_m are potentially sensitive to the addition of membrane perturbant, including surfactants.

In this study, changes in steady-state emission anisotropy of the two fluorescent probes, DPH and TMA-DPH, were used to assess the effect of surfactant on the physical state (fluidity and ordering) of DMPC SUVs. In addition, as discussed above, these two probes can also provide information on the effect of the surfactant at different locations in the bilayer.

In order to obtain phase transition temperatures for DMPC SUVs, retrieved parameters from polarized fluorescence data were used to determine the fluorescence emission anisotropy (using equations 14 and 15) and plotted as a function of temperature. Where appropriate, the parameters were fit (Sigma Plot 8.0) to a sigmoidal two-state (logistic; 4 parameter) expression used to retrieve the lipid phase transition temperature (T_m)

$$< r >=< r >_{min} + \frac{< r >_{\max}}{1 + e^{\frac{-(T - T_m)}{b}}} \qquad (26)$$

Where, $\langle r \rangle_{min}$ and $\langle r \rangle_{max}$ are the minimum and maximum emission anisotropy values, respectively, b is the slope parameter, T is the temperature and the mid-point of the transition and reflects the gel-liquid phase transition temperature (T_m). The quality of the fit was assessed by a correlation function (R^2), where all values greater than 0.99 were judged to be good fit.

The effects of the non-ionic surfactants, C8P and C2,6P, on DMPC SUV transition temperatures (T_m) were obtained using surfactant to lipid molar ratios of ([S]/L]) 0, 1, 3 and 5.

3.2.2.1. DPH Data

Figures 32, 33, and 34 show the temperature dependence of the steady-state emission anisotropy (<r>) of DPH labeled DMPC SUVs with no surfactant, and in the presence of C8P, and C2,6P. T_m values were extracted from the data using equation 26 and the average T_m values arising from 4 separate experiments, are plotted as a function of increasing surfactant to lipid molar ratio (Figure 35). Data are summarized in Table 7.

An inflexion in emission anisotropy values *versus* temperature is observed for DPH labeled DMPC SUVs centered about the phospholipid gel-to-liquid melt temperature (T_m) for the control (no surfactant) experiments (Figure 32). With increasing temperature, the increased rotational motions of DPH accurately reports the gel-fluid lipid melt transition temperature for DMPC. From the average of three measurements using different lipid concentrations, the T_m value (same lipid:probe molar labeling ratio) measured for DMPC SUVs is 23.41±0.33°C. As expected there

are no marked differences in T_m values with varying DMPC SUV concentration. These value are in excellent agreement with previously reported literature values for DMPC SUVs (23°C) [108, 118, 228] and (23.5°C) [98].

It is important to note that DPH and TMA-DPH have partition coefficients of unity ($K_p^{g/f} = 1$) for gel and fluid lipid phases [69]. Thus, shifts in emission anisotropy *versus* temperature profiles as a result of the addition of surfactant, are not expected to arise from preferential partitioning artifacts. Any changes in T_m values due to the presence of surfactant arise from a fluidizing of the bilayer, reflected in the altered rotational motions of the fluorophores.

The effect of surfactants on the phase transition profiles of DMPC SUVs labeled with DPH are shown in Figure 33 and 34 at a constant DMPC SUVs lipid concentration. In general, an effective "shift" of T_m values (C8P>C2,6P) to lower temperatures, and a broadening of the emission anisotropy *versus* temperature phase transition profiles was observed with increasing surfactant concentration for both C8P and C2,6P. The decrease in T_m values is proportional to the amount of incorporated surfactant within the bilayer resulting in a fluidizing effect on the lipid bilayer. Interestingly, (Figure 34), for DPH labeled DMPC SUVS with increasing C2,6P surfactant concentration, an increase in emission anisotropy values was observed at concentrations > [S]/[L]=1. The origins for these trends are unclear but may arise from altered fluorescence lifetimes for DPH with addition of surfactant. Further fluorescence lifetime studies for this system are needed to assess such potential effects.

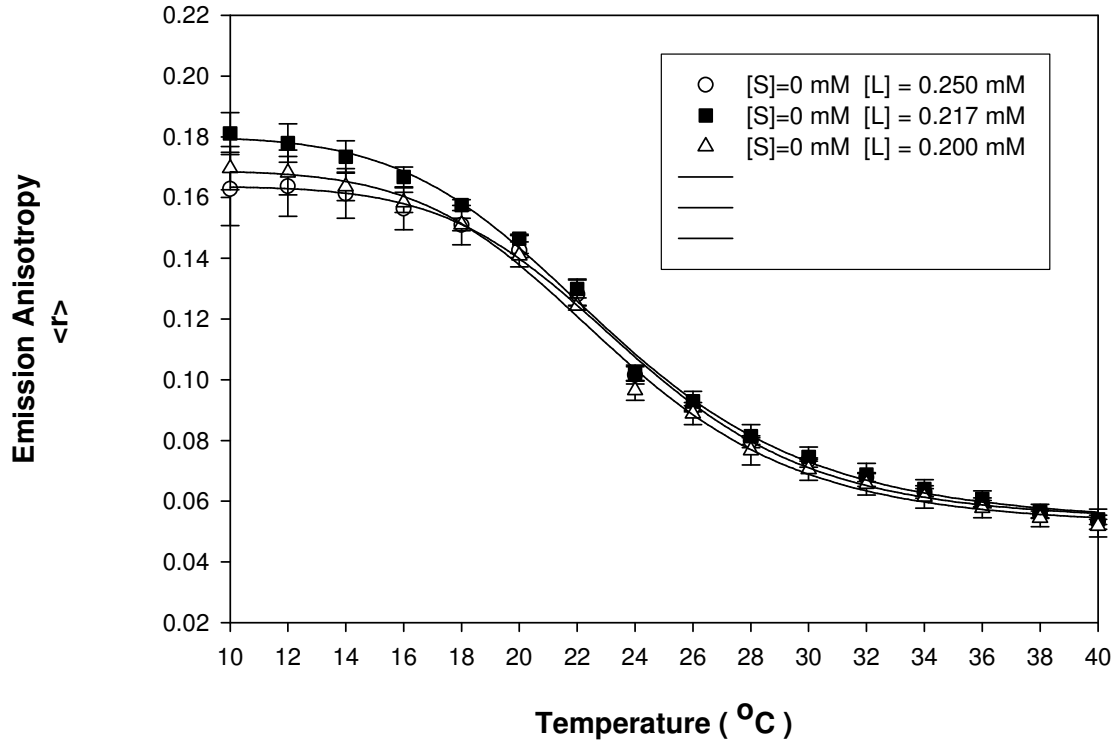

Figure 32: DPH labeled DMPC SUVs phase transition temperatures with no surfactants as a control, obtained with excitation at 355 nm and emission at 430 nm. Excitation and emission bandwidths were both 4 nm. The standard deviations reflect 4 trials for each. The lines represent a sigmoidal fit (Equation 26) to the data with transition midpoints at 23.79±0.35 (○); 23.26±0.34 (■); and 23.18±0.21 (Δ).

(○) [S] =0 mM, [L] = 0.250 mM; (■) [S] =0 mM, [L] =0.217 mM; (Δ) [S] =0 mM, [L] = 0.200 mM.

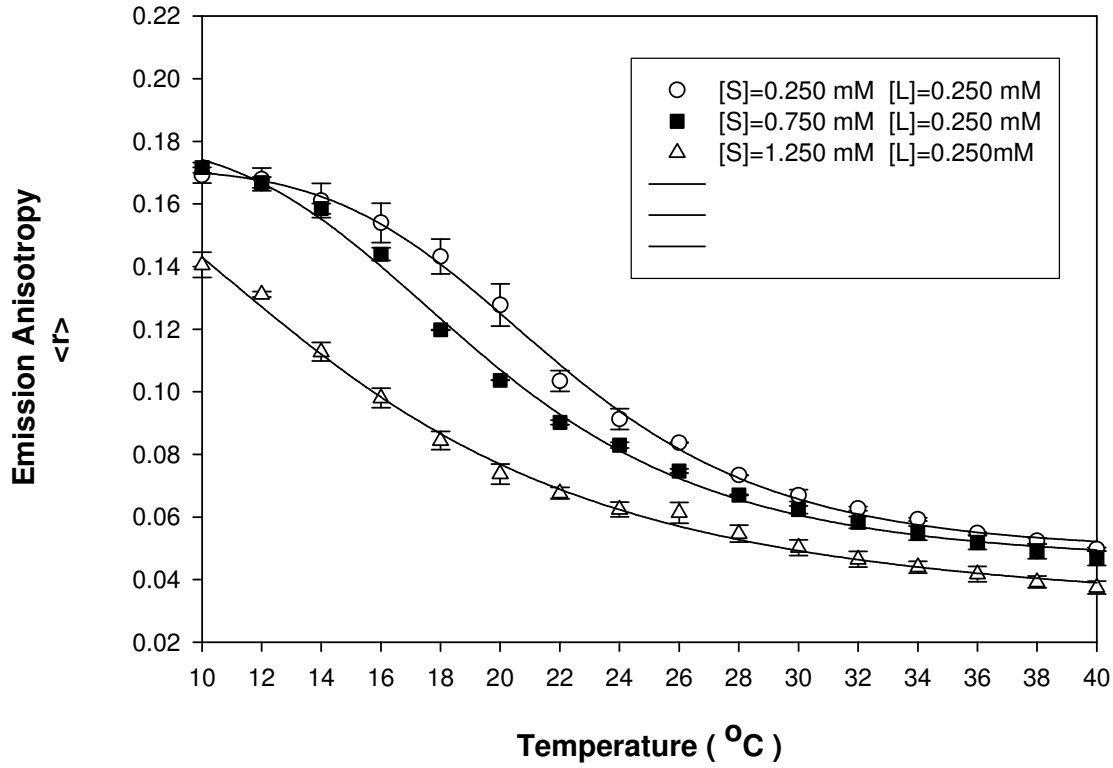

Figure 33: Effect of C8P surfactant on the phase transition temperature of DPH labeled DMPC SUVs, obtained with excitation at 355 nm and emission at 430 nm. Excitation and emission bandwidths were both 4 nm. The standard deviations reflect 4 trials for each. The lines represent a sigmoidal fit (Equation 26) to the data with transition midpoints at 21.72±0.07 (○); 19.29±0.09 (■); and 14.92±0.41 (Δ).

(○) [S] =0.250 mM, [L] = 0.250 mM, [S]/[L] =1; (■) [S] =0.750 mM, [L] =0.250mM, [S]/[L]=3; (Δ) [S] =1.250 mM, [L] = 0.250 mM, [S]/[L]=5.

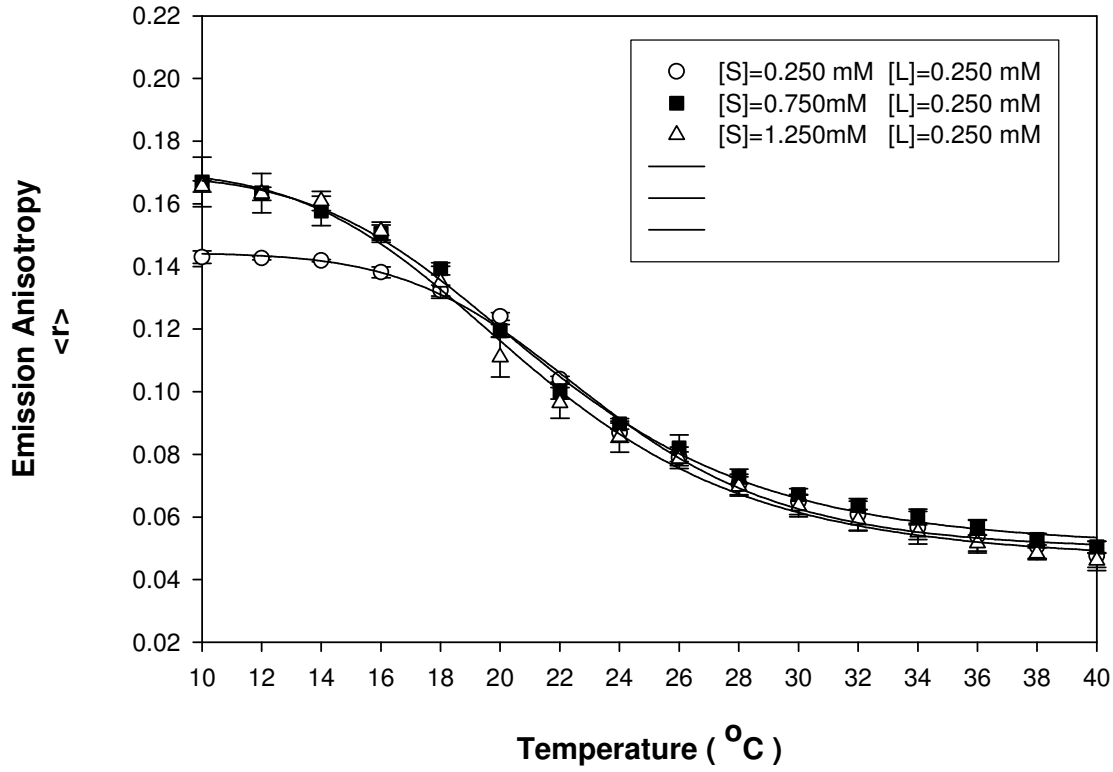

Figure 34: Effect of C2,6P surfactant on the phase transition temperature of DPH labeled DMPC SUVs, obtained with excitation at 355 nm and emission at 430 nm. Excitation and emission bandwidths were both 4 nm. The standard deviations reflect 4 trials for each. The lines represent a sigmoidal fit (Equation 26) to the data with transition midpoints at 23.36±0.21 (○); 21.41±0.04 (■); and 21.06±0.32 (Δ).

(○) [S] =0.250 mM, [L] = 0.250 mM, [S]/[L] =1; (■) [S] =0.750 mM, [L] =0.250mM, [S]/[L]=3; (Δ) [S] =1.250 mM, [L] = 0.250 mM, [S]/[L]=5.

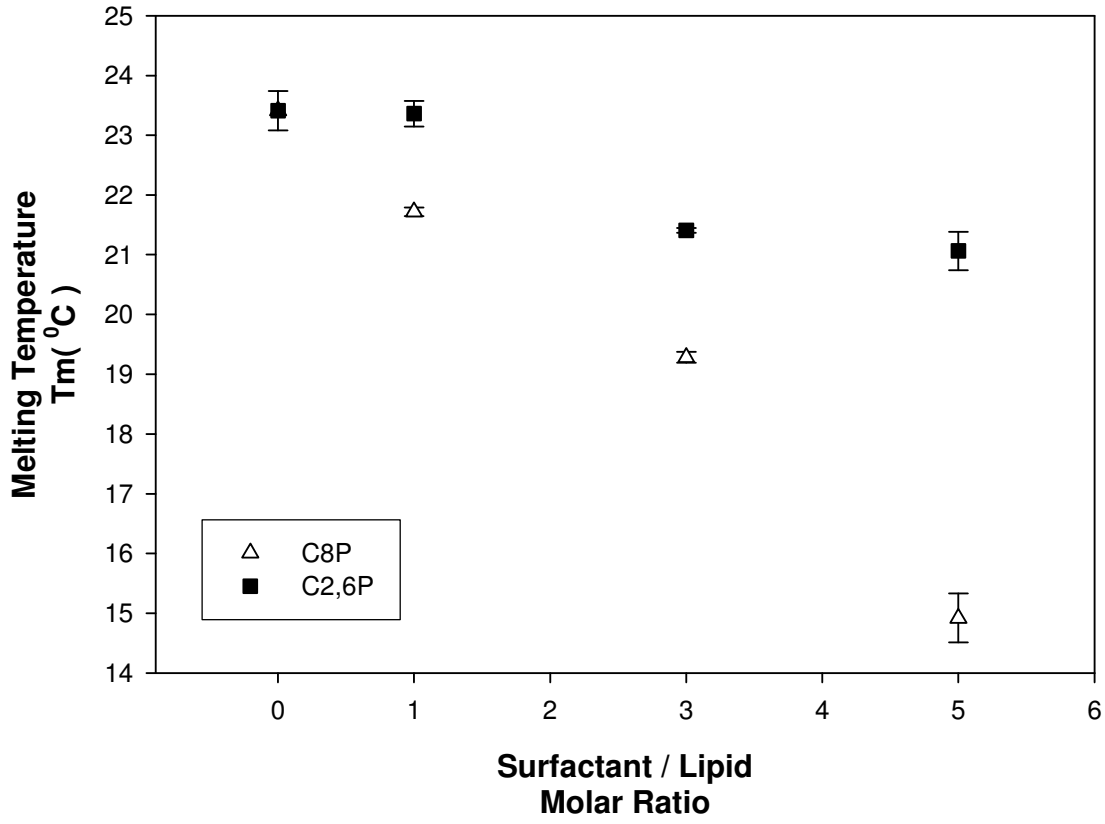

Figure 35: Effect of surfactant on the phase transition temperature (T_m) of DMPC SUVs as reported from the steady-state emission anisotropy of DPH. The standard deviations reflect 4 trials for each. (Δ) C8P; and (■) C2,6P.

Table 7
Effect of Surfactant on the Phase Transition Temperature (T_m) of DMPC SUVs as Reported from the Steady-state Emission Anisotropy of DPH. (The standard deviations reflect 4 trials for each measurement)

Molar Ratio (surfactant to lipid)	***C8P Surfactant T_m (°C)***	***C2,6P Surfactant T_m (°C)***
1	21.72±0.07	23.36±0.21
3	19.29±0.09	21.41±0.04
5	14.92±0.41	21.06±0.32

DMPC SUVs Concentration	***T_m (°C)***
0.250 mM	23.79±0.35
0.217 mM	23.26±0.34
0.200 mM	23.18±0.21
AVERAGE	23.41±0.33

3.2.2.2. TMA-DPH Data

The temperature dependence of the steady-state emission anisotropy (<r>) of TMA- DPH labeled DMPC SUVs with no surfactant, and in the presence of C8P, and C2,6P are shown in Figure 36, Figure 37, and Figure 38, respectively. In general the rotational motions of TMA-DPH, oriented at the headgroup region, appear to be less sensitive to the disordering effect of the surfactant within the gel region of the bilayer (<T_m) as reported by DPH. T_m values were extracted from the data using equation 26. Average T_m values, resulting from four separate experiments are plotted as a function of increasing surfactant to lipid molar ratio (Figure 39). The data are summarized in Table 8.

Compared with DPH/DMPC samples, the corresponding TMA-DPH labeled samples emission anisotropy profiles, in the absence of surfactant, show a somewhat broader transition in emission anisotropy values with increasing temperature. From the average of three lipid SUV concentrations, the T_m value for TMA-DPH/ DMPC SUVs is 23.32±0.37°C. As expected this values does not show any marked differences with varying DMPC SUVs concentration (Figure 36). In addition, the data presented here do not show any marked differences in T_m values for DMPC SUVs labeled with either TMA-DPH (23.32±0.37°C) or DPH (23.41±0.33°C). Indeed, *a priori* there is no reason to believe that T_m should be dependent on the region of the bilayer being probed.

Further, emission anisotropy values for TMA-DPH at temperature greater than T_m remained high, compared with DPH labeled samples. It is well established that because of the cationic charge, TMA-DPH is tethered at the lipid-water interface with

its DPH moiety intercalated between the fatty acyl chains. As a result, the rotational motions of TMA-DPH are influenced by the glycerol backbone region of the bilayer probably as far down as C_8-C_{10} [66] (Figure 13). The emission anisotropy data suggest that at temperatures greater than T_m, the bilayer environment around TMA-DPH is more restricted than for DPH, as evidenced by the observed higher <r> values. This effect has been previously observed by Prendergast *et.al*, [66] and results presented here are in excellent agreement.

With addition of C8P and C2,6P to the bilayer, the emission anisotropy data for TMA-DPH/DMPC SUVs (Figure 37 and Figure 38) showed evidence for some degree of interaction at the head group region of the DMPC bilayer, although as stated above, the effect of the surfactants at the head group regon is not as dramatic as reported by DPH residing in the apolar region of the bilayer. A shift of T_m values (C8P>C2,6P) to lower temperatures and a broadening of the phase transition with increasing surfactant concentration is observed.

Both DPH and TMA-DPH show a decrease in transition temperature of DMPC SUVs with increasing surfactant concentration (C8P>C2,6P). C8P has an appreciable effect compared to C2,6P on the lipid melt transition temperature as detected both by DPH within the bilayer and at the head group region (TMA-DPH).

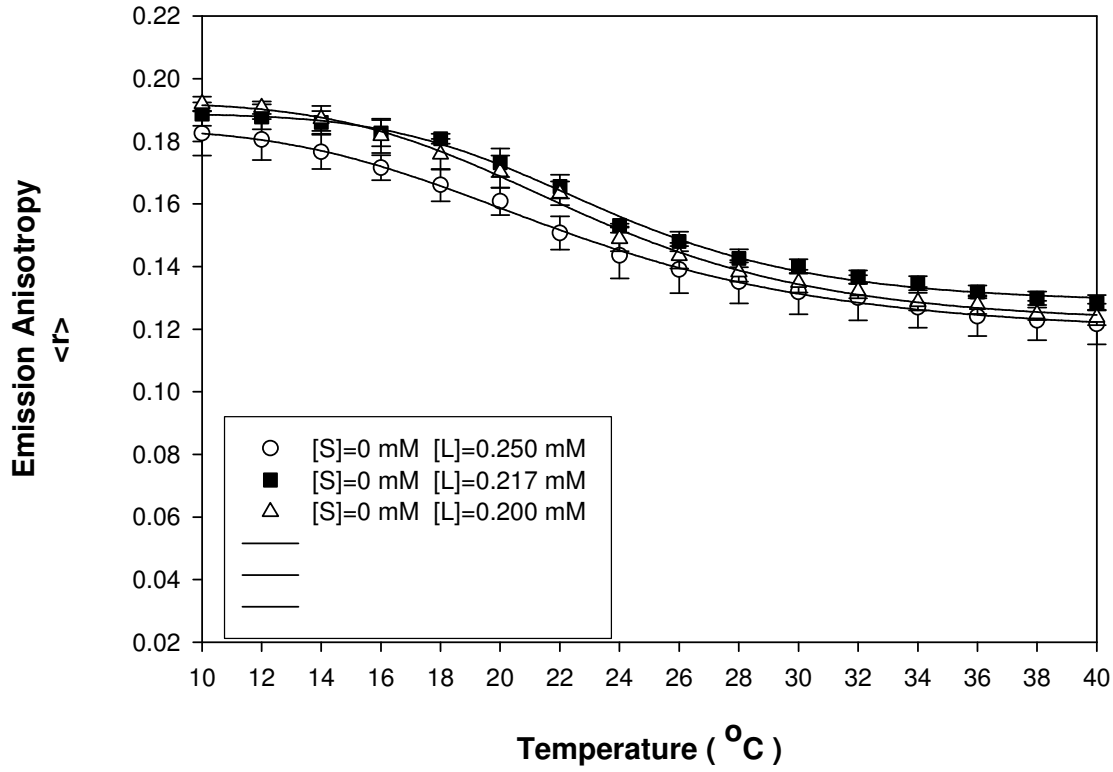

Figure 36: TMA-DPH labeled DMPC SUVs phase transition temperatures with no surfactants as a control, obtained with excitation at 355 nm and emission at 430 nm. Excitation and emission bandwidths were both 4 nm. The standard deviations reflect 4 trials for each. The lines represent a sigmoidal fit (Equation 26) to the data with transition midpoints at 23.60±0.42 (○); 23.46±0.22 (■); and 22.90±0.62 (Δ).

(○) [S] =0 mM, [L] = 0.250 mM; (■) [S] =0 mM, [L] =0.217 mM; (Δ) [S] =0 mM, [L] = 0.200 mM.

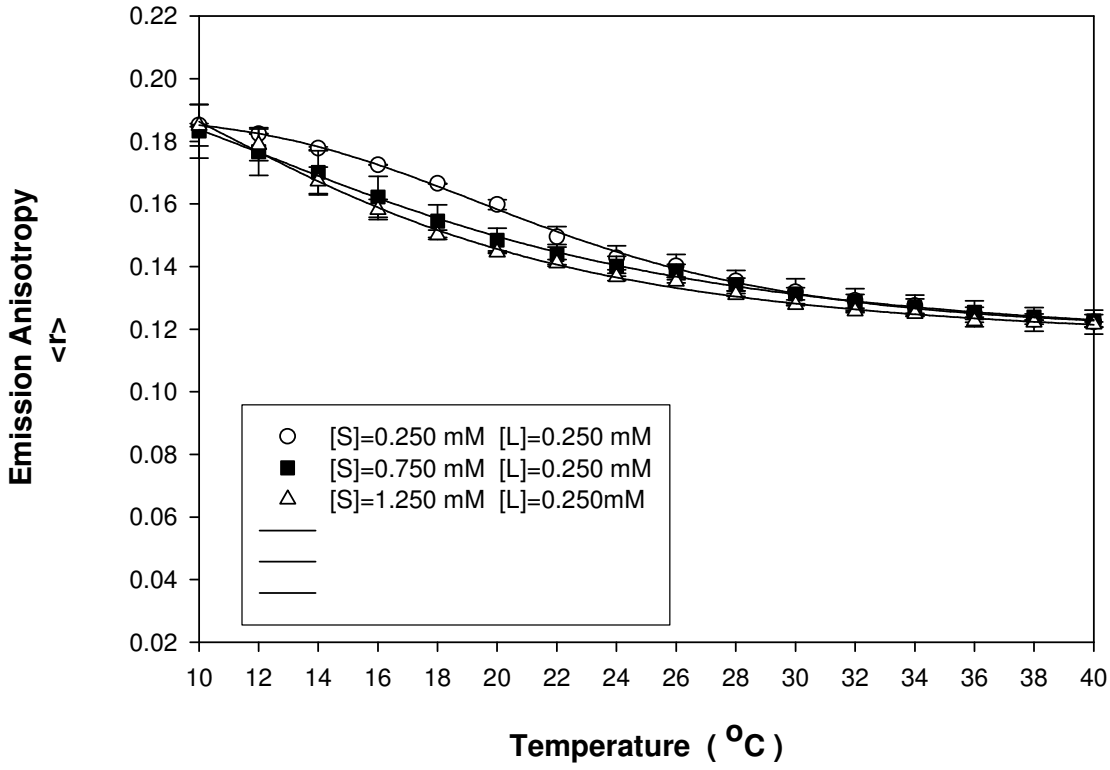

Figure 37: Effect of C8P surfactant on the phase transition temperature of TMA-DPH labeled DMPC SUVs, obtained with excitation at 355 nm and emission at 430 nm. Excitation and emission bandwidths were both 4 nm. The standard deviations reflect 4 trials for each. The lines represent a sigmoidal fit (Equation 26) to the data with transition midpoints at 21.51±0.23 (○); 17.35±0.11 (■); and 15.06±0.35 (Δ).

(○) [S] =0.250 mM, [L] = 0.250 mM, [S]/[L] =1; (■) [S] =0.750 mM, [L] =0.250mM, [S]/[L]=3; (Δ) [S] =1.250 mM, [L] = 0.250 mM, [S]/[L]=5.

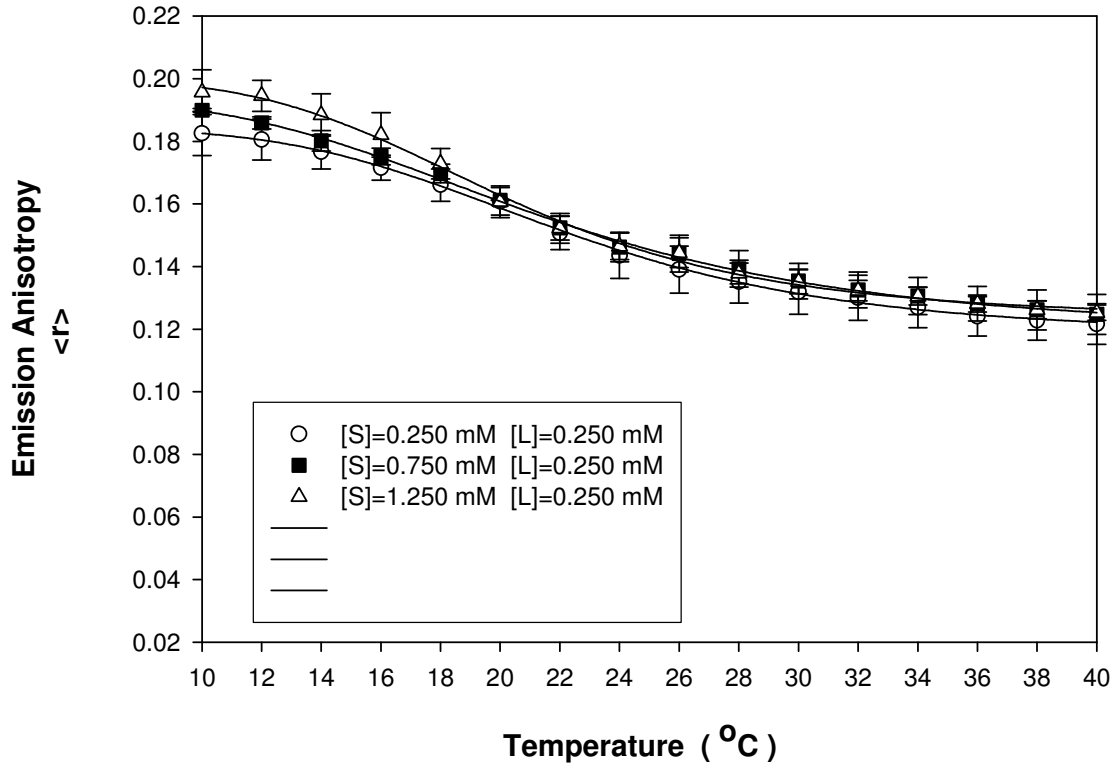

Figure 38: Effect of C2,6P surfactant on the phase transition temperature of TMA-DPH labeled DMPC SUVs, obtained with excitation at 355 nm and emission at 430 nm. Excitation and emission bandwidths were both 4 nm. The standard deviations reflect 4 trials for each. The lines represent a sigmoidal fit (Equation 26) to the data with transition midpoints at 22.28±0.23 (○); 21.30±0.04 (■); and 20.25±0.18 (Δ).

(○) [S] =0.250 mM, [L] = 0.250 mM, [S]/[L] =1; (■) [S] =0.750 mM, [L] =0.250mM, [S]/[L]=3; (Δ) [S] =1.250 mM, [L] = 0.250 mM, [S]/[L]=5.

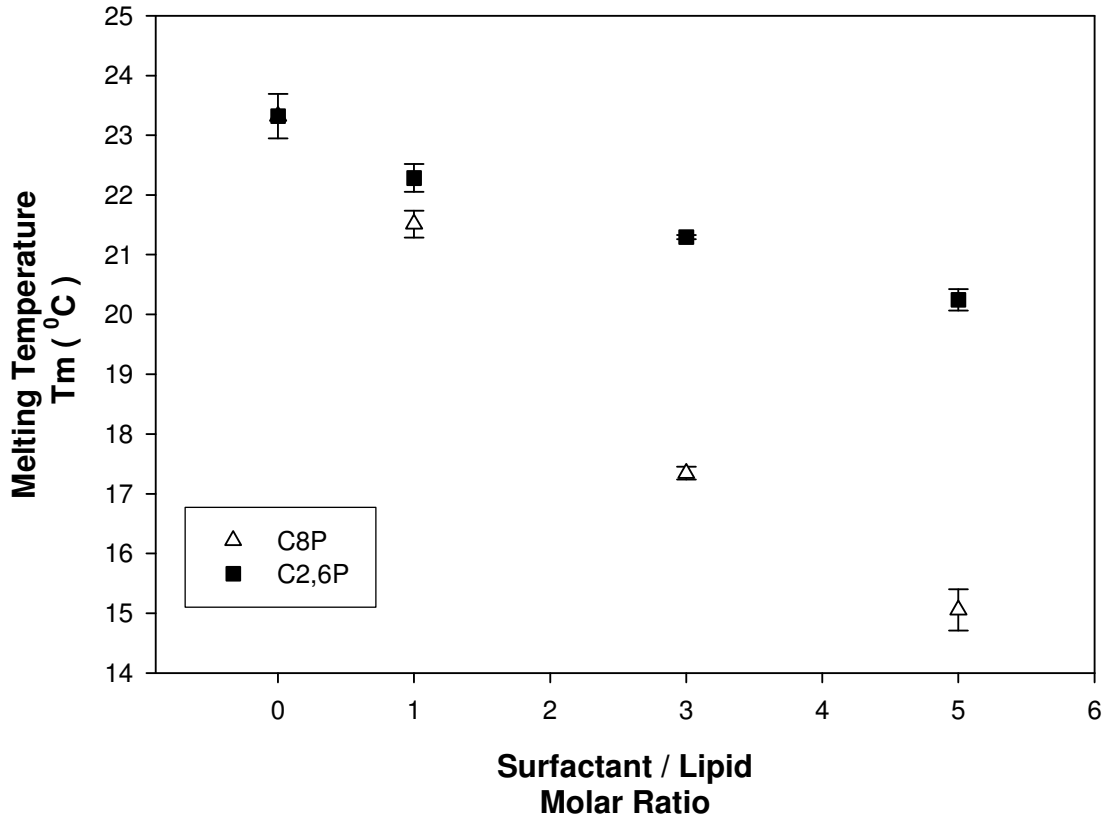

Figure 39: Effect of surfactant on the phase transition temperature (T_m) of DMPC SUVs as reported from the steady-state emission anisotropy of TMA-DPH. The standard deviations reflect 4 trials for each. (Δ) C8P; and (■) C2,6P.

Table 8
Effect of Surfactant on the Phase Transition Temperature (T_m) of DMPC SUVs as Reported from the Steady-state Emission Anisotropy of TMA-DPH. (The standard deviations reflect 4 trials for each measurement)

Molar Ratio (surfactant to lipid)	***C8P Surfactant T_m (°C)***	***C2,6P Surfactant T_m (°C)***
1	21.51±0.23	22.28±0.23
3	17.35±0.11	21.30±0.04
5	15.06±0.35	20.25±0.18

DMPC SUVs Concentration	***T_m (°C)***
0.250 mM	23.60±0.42
0.217 mM	23.46±0.22
0.200 mM	22.90±0.62
AVERAGE	23.32±0.37

3.2.2.3. Lipid Bilayer-Water Partition Coefficient of Surfactants Estimated from the Depression of Phase Transition Temperature

The depression of the phase transition temperature of a phospholipid vesicle membranes induced by the interaction with small molecular ligands has been successfully analyzed using the van't Hoff model for freezing-point depression [229-232]. According to this model, the depression of the phase transition temperature of the lipid bilayer may be attributed to the lowering of the chemical potential of a lipid molecule in the liquid-crystalline state membrane due to mixing with surfactant molecules. Then, the degree of the temperature depression is proportional to the mole fraction of surfactant in the lipid bilayer under conditions of sufficiently low surfactant concentration (*ie.* approaching ideal conditions). When surfactant molecules are partitioned between bulk water and a lipid bilayer, the partition coefficient (K_p) between these phases can be estimated from the relationship of the phase transition temperature with surfactant concentration according to equation:

$$T_m = T_{m,0} - \frac{RT_{m,0}^2}{\Delta H} \frac{K_p}{55.5 + C_L K_p} C_s \qquad (27)$$

where $T_{m,0}$ represents the bilayer phase transition temperature in the absence of surfactants, ΔH is the enthalpy change associated with the phase transition, R is the gas constant, C_L and C_s are the total molar concentrations of lipid and surfactant, respectively, 55.5 is the number of moles of water per liter of water and K_p is the surfactant partition coefficient defined as:

$$K_p = \frac{X_S^l}{X_S} \qquad (28)$$

where X_S^l and X_S are the mole fractions of the surfactants in the liquid-crystalline membrane and water phases, respectively.

According to equation 27 one can estimate the partition coefficient from the slope of the straight line of a T_m *versus* Cs plot with the knowledge of ΔH . Equation 27 was applied to the DMPC SUVs / N-alkyl-2-pyrrolidinone surfactant systems, and the Kp values were estimated from the slopes of Figures 40 (DPH labeled) and Figure 41 (TMA-DPH labeled) using the reported ΔH value for DMPC (22.6 kJ/mol) [233-234], a $T_{m,0}$ value of 296.4 K and C_L value 2.5×10^{-4} M. Obtained results are shown in Table 9. Such a treatment is possible because as discussed above, the gel-fluid partition coefficient, $K_p^{g/f}$, for DPH and TMA-DPH is one. Thus T_m values determined from emission anisotropy *versus* temperature profiles are believed to accurately reflect the phase transition temperature for DMPC SUVs. The averaged K_p values obtained from values determined using the two probes are as follows: $K_p = (1.22\pm0.08)\times10^4$ for C8P and $K_p = (4.09\pm0.78)\times10^3$ for C2,6P. It is interesting to note that the partition coefficient determined for C8P (straight chain), as might be expected, is somewhat larger than that for the branched chain surfactant, (C2,6P) by one order of magnitude.

The interaction of surfactants with the lipid vesicles by observing their effects on the lipid phase transition behavior has been investigated for various types of surfactants with different head groups (anionic, cationic, and nonionic) and different hydrocarbon chain length [229-232]. The membrane/water partition coefficients of

other non-ionic surfactants for lipid vesicles estimated from the depression of phase transition temperature of vesicle membrane are shown in Table 10. Our results are similar to those reported by other groups for other non-ionic surfactants. In most studies, the phase transition temperature of lipid is depressed linearly with the increasing surfactant concentration. As seen from Table 10, depression of the main lipid phase transition temperature resulting from surfactant incorporation depends strongly on the phospholipid species, zwitterionic or anionic, and on the relative length of the surfactant hydrocarbon chain to lipid acyl chain

The larger partition coefficient (K_p) value for C8P over C2,6P suggests greater hydrophobic interactions between C8P and DMPC SUVs due to greater penetration into the acyl chain region of the bilayer. These data support our previous results obtained from fluorescence intensity studies. However, direct measurements of K_p values are required to confirm these results. The model used here represents the ideal case where the surfactant concentration in the lipid membrane is sufficiently low (our results were obtained at relatively high surfactant concentrations). Nevertheless, straight lines with no break were obtained and partitition coefficients from these linear plots were estimated.

Inoue *et.al*, [230] also have established a linear relationship between K_p and *cmc* for partitioning of surfactants into DPPC membranes (Table 10). They showed that when $log\ K_p$ is plotted agains *log cmc*, for ionic and nonionic surfactant series, straight lines with a slope of -1 are obtained. Thus, from their studies, differences in K_p values can be related to cmc values for a surfactant series. While there are no data reported comparing K_p values for straight and branched chain surfactants, it is

tempting to suggest that differences in K_p values observed for C8P and C2,6P may arise from differences in apparent cmc values. Further studies to determine such relationships are required.

Table 9

Partition coefficients (K_p) of C8P and C2,6P surfactants between water and DMPC vesicle membranes obtained from plots of depression of the phase transition temperature -ΔT *versus* the concentration of added surfactant.

Surfactant	K_p ***obtained with DPH***	K_p ***obtained with TMA-DPH***	***Average*** K_p
C8P	1.17×10^4	1.28×10^4	$(1.22\pm0.08)\times10^4$
C2,6P	3.53×10^3	4.64×10^3	$(4.09\pm0.78)\times10^3$

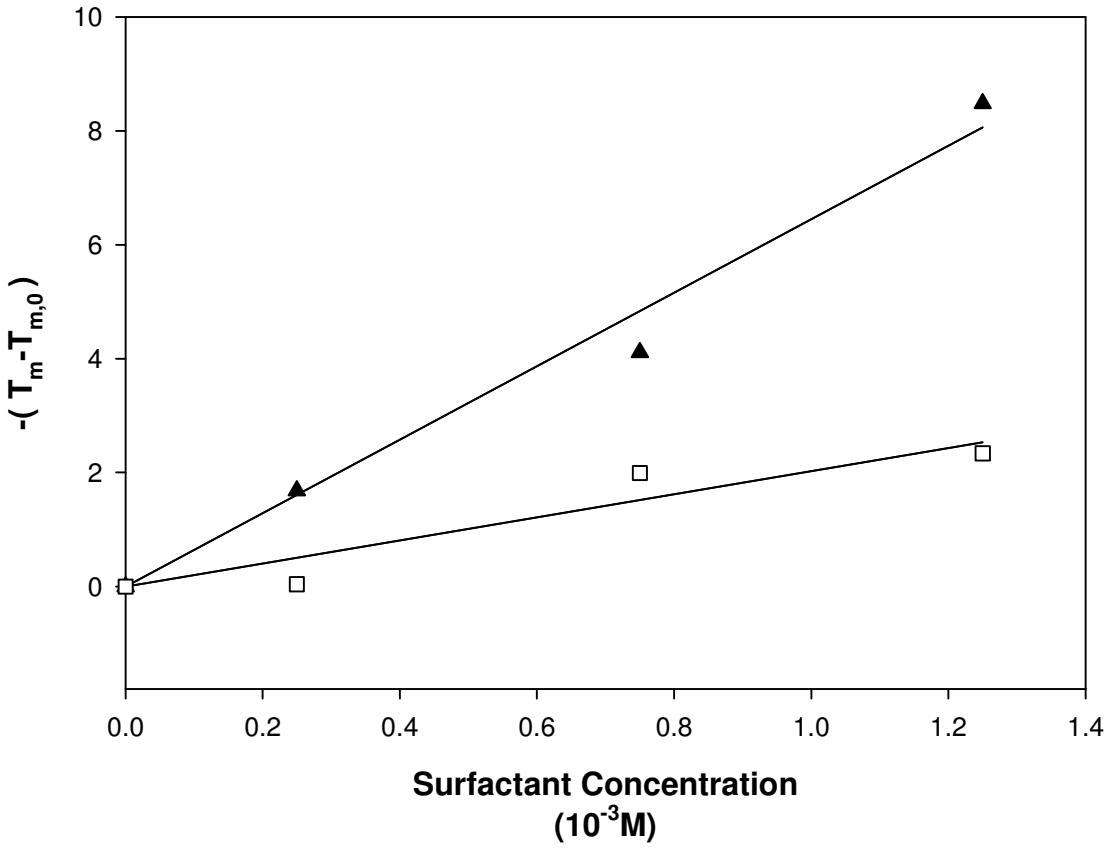

Figure 40: Plot of the depression of the phase transition temperature -ΔT, against the concentration of added surfactant obtained with DPH as the probe. (□) C2,6P; (▲) C8P. Data represent an average of 4 measurements.

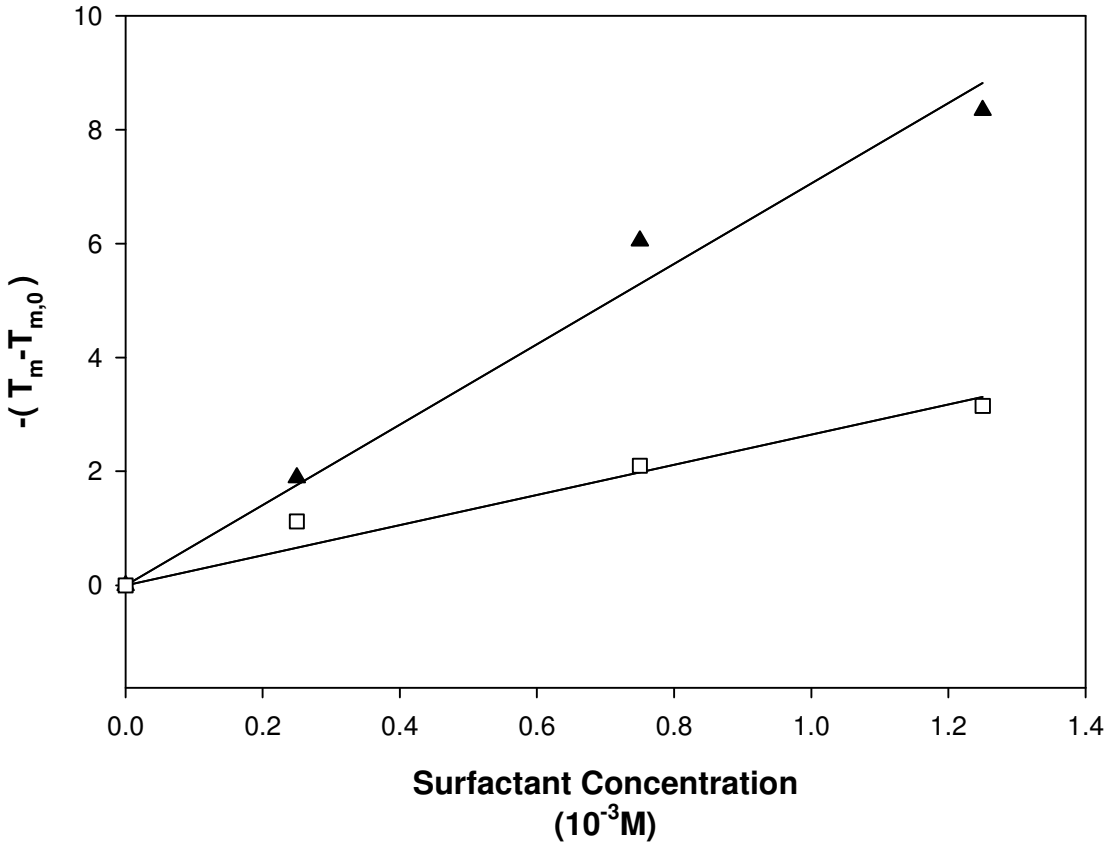

Figure 41: Plot of the depression of the phase transition temperature -ΔT, against the concentration of added surfactant obtained with TMA-DPH as the probe. (□) C2,6P; (▲) C8P. Data represent an average of 4 measurements.

Table 10
The membrane/water partition coefficients of other non-ionic surfactants for lipid vesicles estimated from the depression of phase transition temperature of vesicle membrane. Taken from Ref. 8, 230, and 232.

Surfactant ***Non-ionic***	K_p	***cmc*** ***(M)***	***log*** K_p	***Lipid***
MEGA-8	5.59×10^{2}	6.60×10^{-2}	2.75	DPPC
MEGA-9	1.33×10^{3}	1.81×10^{-2}	3.12	DPPC
MEGA-10	5.74×10^{3}	5.31×10^{-3}	3.76	DPPC
$C_{12}E_5$	3.48×10^{5}	6.4×10^{-5}	5.54	DPPC
$C_{12}E_6$	2.91×10^{5}	8.7×10^{-5}	5.46	DPPC
$C_{12}E_7$	1.92×10^{5}	8.2×10^{-5}	5.28	DPPC
$C_{12}E_8$	1.11×10^{5}	1.0×10^{-4}	5.05	DPPC
MEGA-8	1.12×10^{3}	6.60×10^{-2}	3.05	DLPA
MEGA-9	2.27×10^{3}	1.81×10^{-2}	3.36	DLPA
MEGA-10	7.51×10^{3}	5.31×10^{-3}	3.88	DLPA
C8P*	1.22×10^{4}		4.09	DMPC
C2,6P*	4.09×10^{3}		3.61	DMPC

Rosoff, Morton (Ed.). Vesicles, Surfactant Science Series. 1996, 62, Marcel Dekker, New York [8]

Inoue, T., Miyakawa, K., and Shimozawa, R. Interaction of surfactants with vesicle membrane of dipalmitoylphosphatidylcholine. Effect on gel-to-liquid-crystalline phase transition of lipid bilayer. *Chem. Phys. Lipids*. 1986, 42(4), 261-270 [230].

Inoue, T., Iwanaga, T., Fukushima, K., Shimozawa, R., and Suezaki, Y. Interaction of surfactants with bilayer of negatively charged lipid: effect on gel-to-liquid-crystalline phase transition of dilauroylphosphatidic acid vesicle membrane. *Chem. Phys. Lipids*. 1988, 48(3-4), 189-196 [232].

* Current study

3.3. Isothermal Titration Calorimetry Data

Isothermal titration calorimetry (ITC) can be used to characterize the interactions between a biological macromolecule (lipid) and a small ligand (surfactant). This method lends itself to the simultaneous determination of the binding constant (K_a), the stoichiometry of ligand/macromolecule (n), binding enthalpy (ΔH), entropy of binding (ΔS), and free energy of binding (ΔG). In an ITC experiment, heats of reaction are measured as the temperature changes during repeated injections of a fixed amount of ligand (surfactant) into a solution of the macromolecule (lipid). The integrated heats of reaction are corrected for heats of dilution (titration of ligand into buffer and buffer into macromolecule). The resulting titration curves can then be analyzed using various non-interacting site models.

The thermodynamics of C8P and C2,6P partitioning into DMPC SUVs were explored using isothermal titration calorimetry at 30°C, above the lipid phase transition temperature (23°C). Figure 42 and 43, show the changes in heat of reaction (μcal/sec) with the titration of DMPC SUVs (C_M^0 = 0.25 mM in buffer) with C8P and C2,6P (C_L^0 = 5 mM in buffer) *versus* time, respectively. Using a ligand delivery syringe, 10 μL aliquots of the surfactant solution are injected into the sample cell (volume V_{cell}=1.43 mL). Each injection gives rise to an endothermic heat of reaction, h_i, produced by the partitioning of C8P and C2,6P surfactants into DMPC SUVs. h_i is given by the area of the titration peak. Figures 42 and 43 demonstrate that the heat of reaction decreases with consecutive injections as less lipid is available for binding and saturation is ultimately achieved. Since the observed heats of binding include contributions from the dilution of the ligand (surfactant) and dilution of the

macromolecule (DMPC SUVs), control experiments were performed to correct for the heats of dilution. The same surfactant solutions, C8P and C2,6P, were injected into buffer without lipid, leading to an exothermic heat of reaction, h_c, as shown in Figures 44 and 45, respectively. Figure 46 shows the heat of dilution, h_c, of the macromolecule (DMPC SUVs) as determined from injection of equal volumes of buffer solution into the sample cell containing the macromolecule (DMPC SUVs) alone. The heats of dilution arising from the titration of surfactant with buffer are more significant compared with dilution of the macromolecule. This is because the initial concentration of surfactant in the sample cell is zero; surfactant is added from a high concentration in to the injection syringe until the final concentration in the cell is several times the final macromolecule (DMPC SUVs) concentration. Figure 47 and 48 show the heat released per mole of C8P and C2,6P surfactant solution injected *versus* the molar ratio of surfactant to buffer, respectively. Similarly, Figure 49 shows the heat released per mole of buffer injected *versus* the molar ratio of buffer/DMPC SUVs. Binding plots of surfactant partitioning into DMPC SUVs were generated based on the corrected heats of titrations, δh_i, given by

$$\delta h_i = h_i - h_c \tag{29}$$

using the software provided by MicroCal.

The ITC ORIGIN data fitting software (MicroCal) provides three built-in (homogenous) curve-fitting models for binding: single set of identical sites; two sets of independent sites; and sequential binding sites. Resultant binding plots for C8P and

C2,6P partitioning into DMPC SUVs are shown in Figures 50 and 51, respectively. The data shown in Figures 50 and 51 were fit to a model that represents a single set of identical sites (equation 19 and 20). Use of other binding models did not provide improved fits to the data and were judged inappropriate. While fitting of the enthalpy data to a more complicated mixed model for binding (invoking membrane heterogeneity) might be expected to improve the fits, the results shown here represent the simplest model that adequately fit the binding data (as judged from χ^2 values).

Initial guesses for the binding constant (K_a), the stoichiometry of surfactant / DMPC SUVs (n), and reaction enthalpy (ΔH) parameters are made by the ORIGIN software. The K_a, n, ΔH, and ΔS parameters were then optimized using the standard Marquardt non-linear method routine provided in the ORIGIN software. From the retrieved values, the free energy values for the surfactant partitioning into the lipid bilayers (ΔG) were then calculated using equation (21). The results obtained are shown in Table 11.

Reaction Enthalpies: The δh_i for injection of surfactant monomers into buffer was exothermic. However, the δh_i for injection of surfactant into the lipid solution was endothermic. Overall, the binding of surfactant with lipid DMPC SUVs is endothermic (C8P = +0.8 kcal/mol and C2,6P = +1.4 kcal/mole) suggesting an overall increase in the entropy of the system (Table 11).

The surfactant partitioning process appears to result from a hydrophobic effect in which the reduction of the intermolecular hydrogen bonding capacity of water, caused by the hydrophobic moieties of the surfactant molecules, forces the surfactant molecules to be distributed between the hydrophobic environment in the membranes

and the bulk water. Therefore, removal of the hydrophobic moieties from the polar phase to the bulk hydrocarbon in the lipid membrane increases the overall entropy of the system and facilitates partitioning. Hence, the overall free energy change for surfactant/membrane association is favorable with $\Delta G<0$ and $T.\Delta S>\Delta H$. The higher ΔH value for C2,6P compared with C8P suggests a higher energy barrier must be overcome during partitioning of C2,6P into DMPC SUVs *versus* C8P. This result agrees with our surfactant/lipid fluorescence data.

Interestingly, the enthalpy of reaction for the non-ionic surfactant OG on partitioning into DMPC vesicles has also been found to be endothermic (+3.1 kcal/mol) at 27°C using ITC measurements [77] (Table 12). Our values for C8P and C2,6P (+0.8 kcal/mol and +1.4 kcal/mole, respectively for partitioning into DMPC vesicles at 30°C) suggest a more favorable interaction (or synergism with lipid bilayers) as evidenced by the lower enthalpies of reaction.

Surfactant/SUV Binding Constants: For N-alkyl-2-pyrrolidinones, the binding constants K_a (M^{-1}) were determined to be 1491±188 M^{-1} and 1191±112 M^{-1} for C8P and C2,6P with DMPC SUVs, respectively. These data suggest a preferential interaction of both surfactants for the bilayer with a somewhat greater binding affinity for C8P K_d= [(6.78±0.92)×10^{-4} M] for the membrane bilayer compared with C2,6P K_d= [(8.46±0.83)×10^{-4} M]. These data also suggest a general preference of both surfactants for the lipid bilayer, as evidenced by the low membrane dissociation constants for both surfactants. These surfactant-bilayer data confirm results obtained from fluorescence spectroscopic techniques.

Studies by Heerklotz et al., [81] have established a linear relationship between the association constant, K_a (M^{-1}) and the *cmc* for partitioning of surfactants into POPC membranes at room temperature. Thus, micellization, partitioning into membranes and formation of mixed lipid/surfactant micelles are expected to be intimately connected. From a double logarithmic plot of K_a vs *cmc* Heerklotz *et* al., [81] have shown that a slope of -1 corresponds to $K_a.cmc = 1$. Using this fact, strong and weak surfactants can be distinguished. "Strong" surfactants are defined by $K_a.cmc<1$, and "weak" surfactants by $K_a.cmc > 1$. Further, surfactants with the larger headgroups have lower K_a value due to the additional strain on the lipid packing. This leads to an early disruption of the bilayer with addition of surfactant. In contrast, "weak" surfactants ($K_a.cmc > 1$) with small headgroups induce less membrane packing strain and are incorporated to larger saturation (Re) values. Hence "strong" surfactants initiate membrane disintegration at a surfactant to lipid ratio of Re^{sat} <1, whereas "weak" surfactants require a surfactant to lipid ratio, Re^{sat} >1. By these criteria, alkylmaltosides (C_mEO_n, n=7,8) and the Triton surfactants are characterized as "strong" surfactants, whereas the alkyl glucosides and the shorter chain alkylmaltosides (C_mEO_n , n=3-6) are "weak" surfactants.

We suggest that both C8P and C2,6P are "weak" surfactants because they have relatively small hydrophilic head groups and high cmc values. Since surfactants with $K_a.cmc > 1$ are considered as "weak" surfactants from ITC data, using K_a values (K_a =1491 M^{-1} for C8P and K_a =1191 M^{-1} for C2,6P) and assuming their cmc values are their solubilization limits (C8P (5.2×10^{-3} M) and C2,6P (1.3×10^{-2} M)) we can assume that C8P and C2,6P are "weak" surfactants.

In addition, according to Lichtenbergs's three stage model [108], Re^{sat} (see Section 1.7 above) marks the beginning of stage II on the lipid-surfactant interaction pathway, i.e., conversion of surfactant-saturated bilayers into mixed micelles. Values for Re^{sat} and Re^{sol} can be estimated from the points of inflexion on the binding plots [77, 184]. The mid-transition point reflects the characteristic surfactant to lipid molar ratio, (Re^{sat}), where vesicles become saturated with surfactant. As seen in Figures 50 and 51, only one inflection point was observed for both surfactants. From the mid point of the transition, Re^{sat} values (0.96±0.28) for C8P and (1.18±0.25) for C2,6P were determined. Values for Re^{sat} are the same within experimental error for both C8P and C2,6P. Using these values, it is also possible to classify C8P and C2,6P as intermediate strength surfactants with Re^{sat} values of around one.

Thermodynamic parameters of Triton X-100, Triton X-114, and OG partitioning into POPC vesicles at room temperature obtained with other groups [81] are shown in Table 13. Our results are similar to those reported by other groups for these non-ionic surfactants and compare favorably with OG.

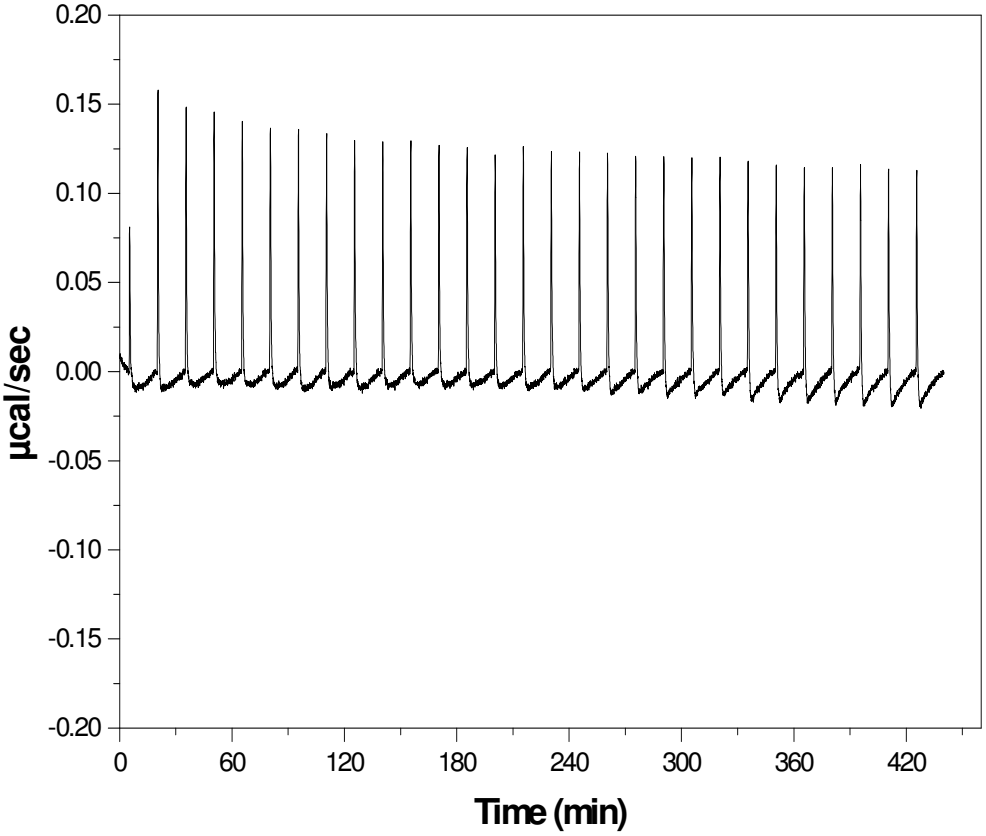

Figure 42: The heat of uptake per unit time (microcalories per second) is plotted *versus* time (min), where each peak corresponds to the injection of an aliquot of C8P surfactant (5 mM) into DMPC SUVs (0.25 mM) at 30° (row data). Reported ITC data represents the mean of four measurements of separately prepared SUVs. One representative figure is shown.

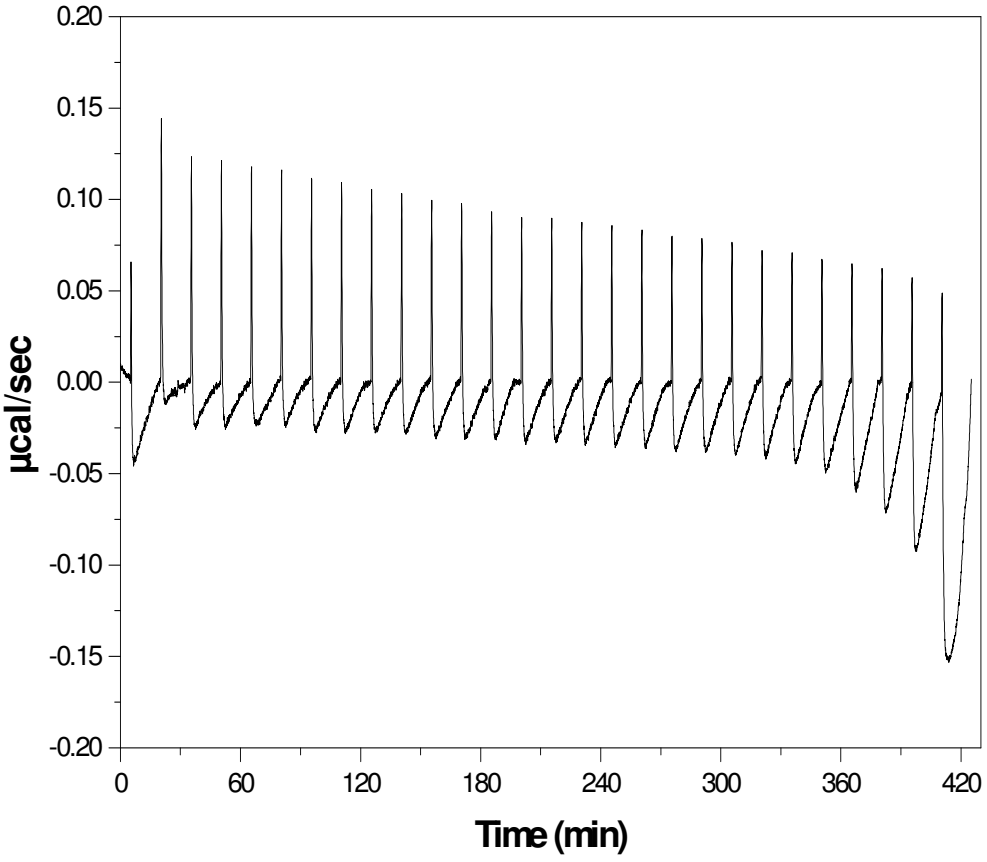

Figure 43: The heat of uptake per unit time (microcalories per second) is plotted *versus* time (min), where each peak corresponds to the injection of an aliquot of C2,6P surfactant (5.0 mM) into DMPC SUVs (0.25 mM) at 30°(row data). Reported ITC data represents the mean of four measurements of separately prepared SUVs. One representative figure is shown.

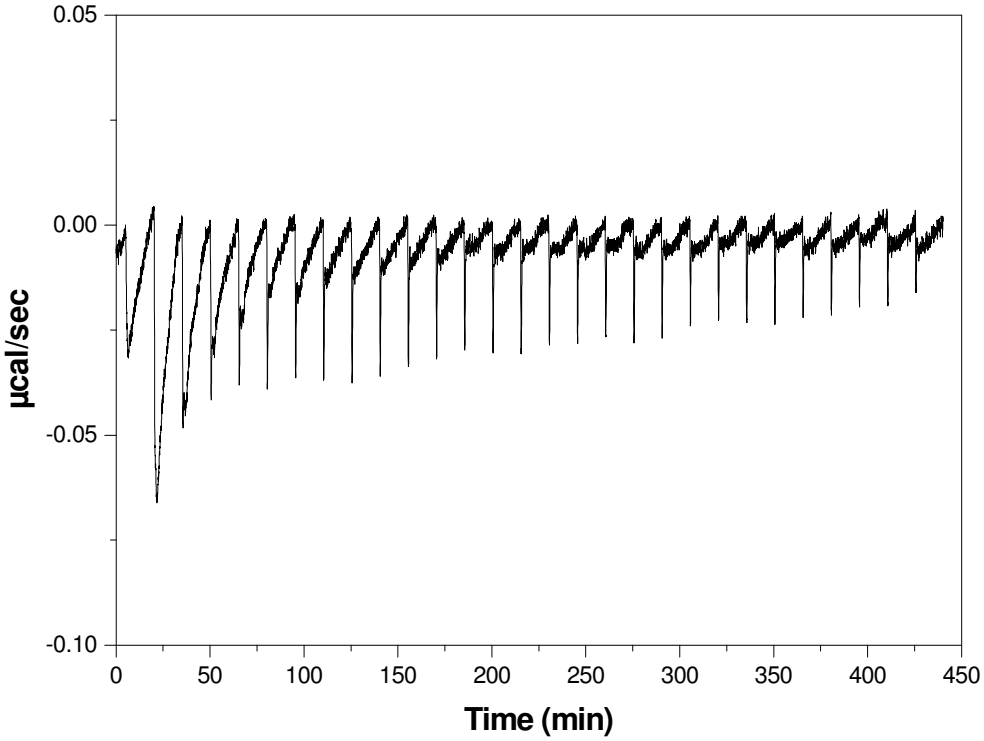

Figure 44: The heat of release per unit time (microcalories per second) is plotted *versus* time (min), where each peak corresponds to the injection of an aliquot of C8P (5.0 mM) into buffer (0.01M Tris.HCl buffer containing 0.1 M NaCl ,pH 8.3) at 30°(row data). Reported ITC data represents the mean of four measurements of separately prepared SUVs. One representative figure is shown.

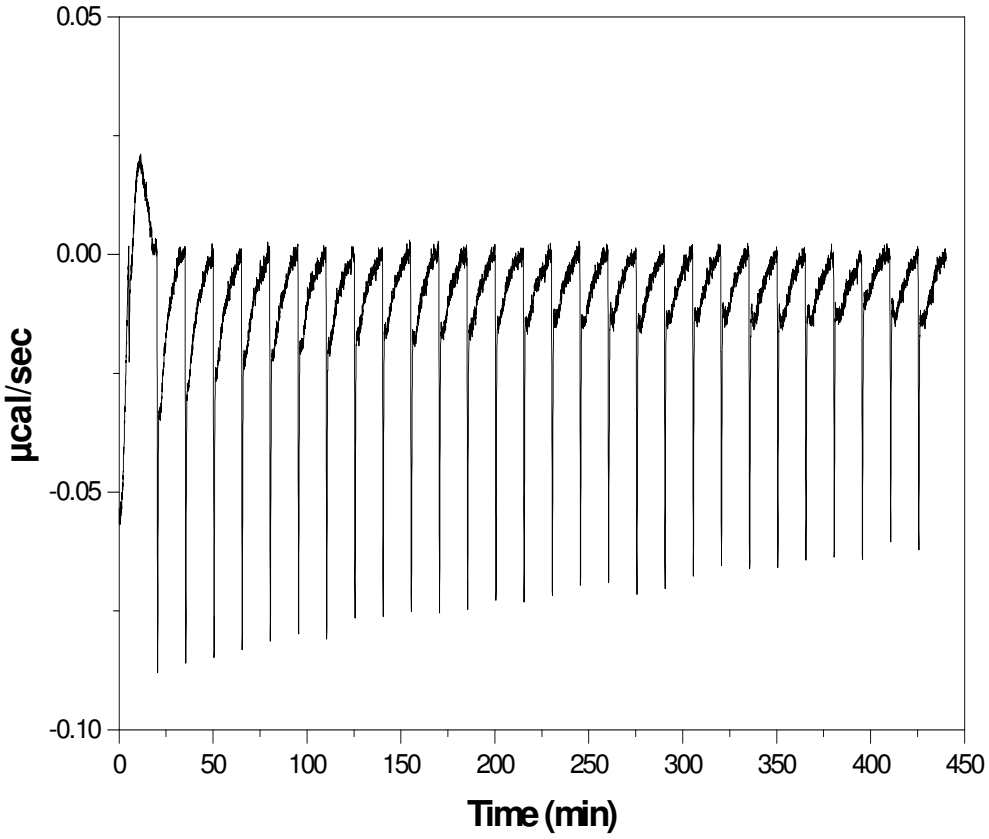

Figure 45: The heat of release per unit time (microcalories per second) is plotted *versus* time (min), where each peak corresponds to the injection of an aliquot of C2,6P (5.0 mM) into buffer (0.01M Tris.HCl buffer containing 0.1 M NaCl ,pH 8.3) at 30°(row data). Reported ITC data represents the mean of four measurements of separately prepared SUVs. One representative figure is shown.

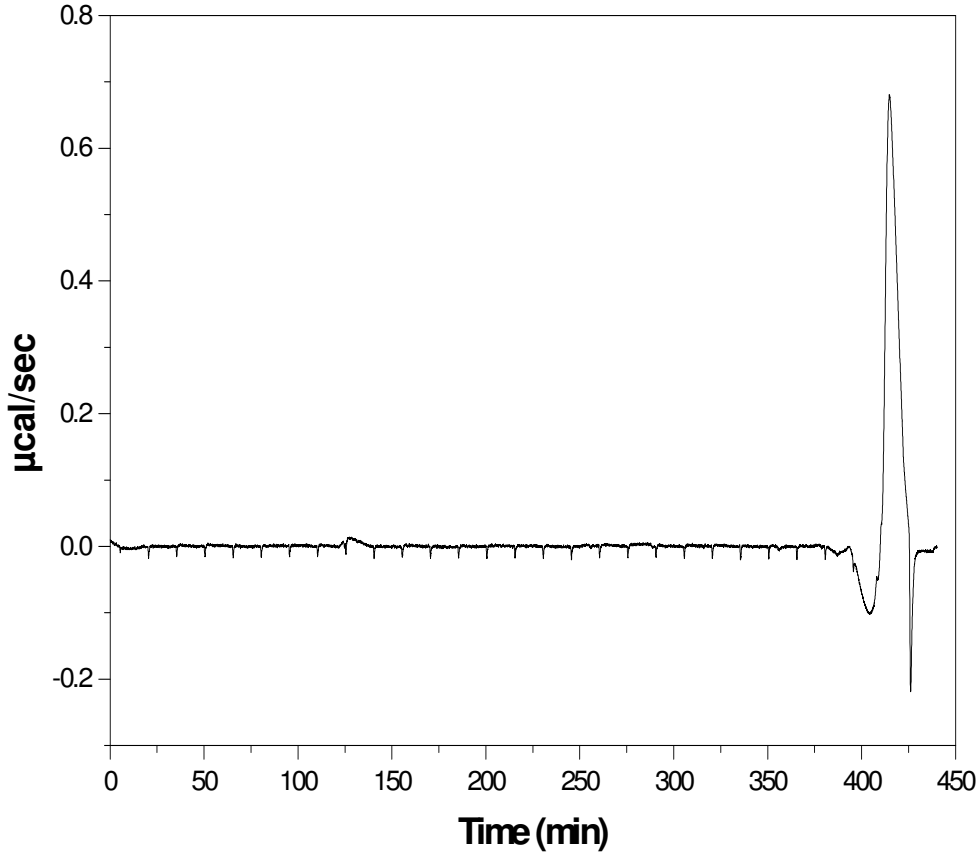

Figure 46: The heat of dilution per unit time (microcalories per second) is plotted *versus* time (min), where each peak corresponds to the injection of an aliquot of buffer (0.01M Tris.HCl buffer containing 0.1 M NaCl ,pH 8.3) into DMPC SUVs (0.25 mM) at 30°(row data). Reported ITC data represents the mean of four measurements of separately prepared SUVs. One representative figure is shown.

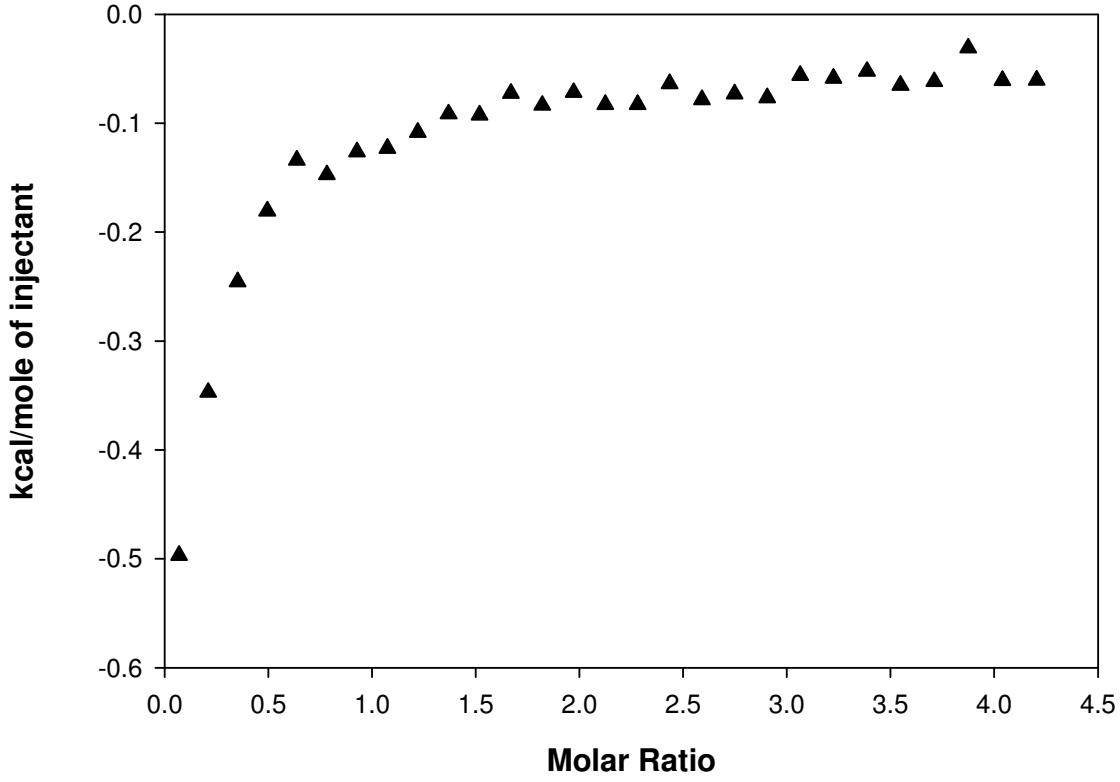

Figure 47: The heat of reaction per injection in kilocalories per mole of C8P surfactant (the area under each peak, Figure 44) *versus* Molar Ratio (C8P/Buffer). Reported ITC data represents the mean of four measurements of separately prepared SUVs. One representative figure is shown.

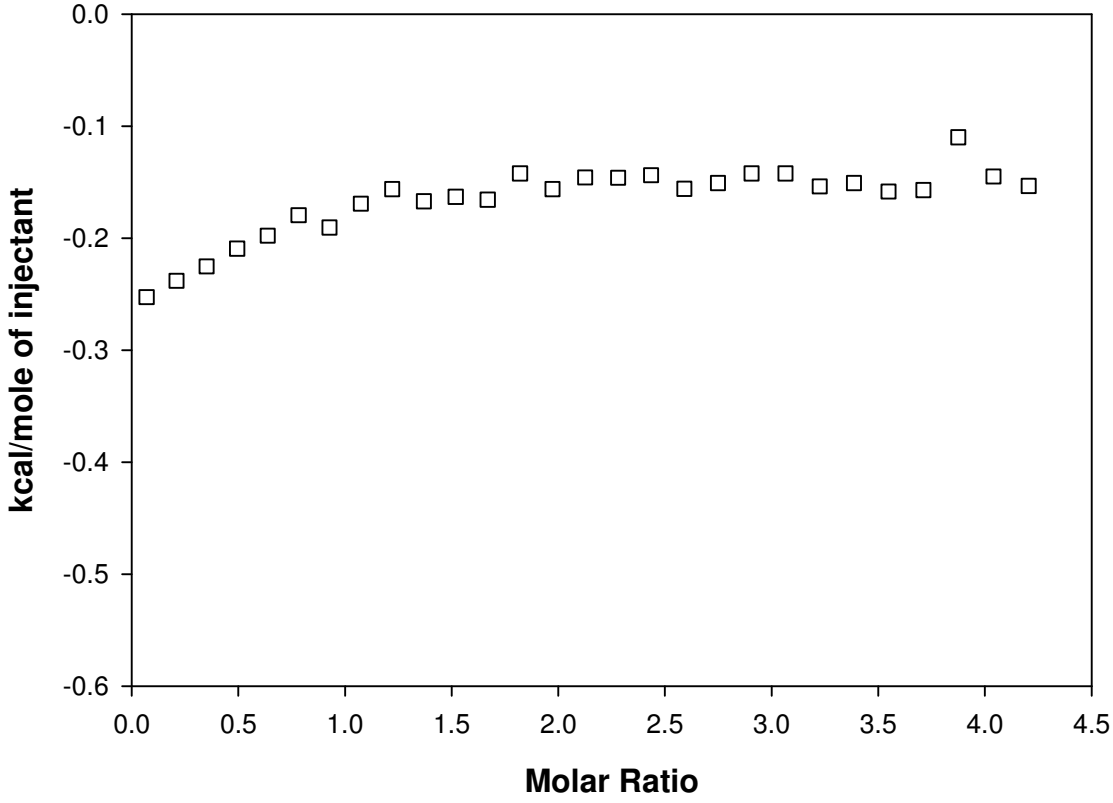

Figure 48: The heat of reaction per injection in kilocalories per mole of C2,6P surfactant (the area under each peak, Figure 45) *versus* Molar Ratio (C2,6P/Buffer). Reported ITC data represents the mean of four measurements of separately prepared SUVs. One representative figure is shown.

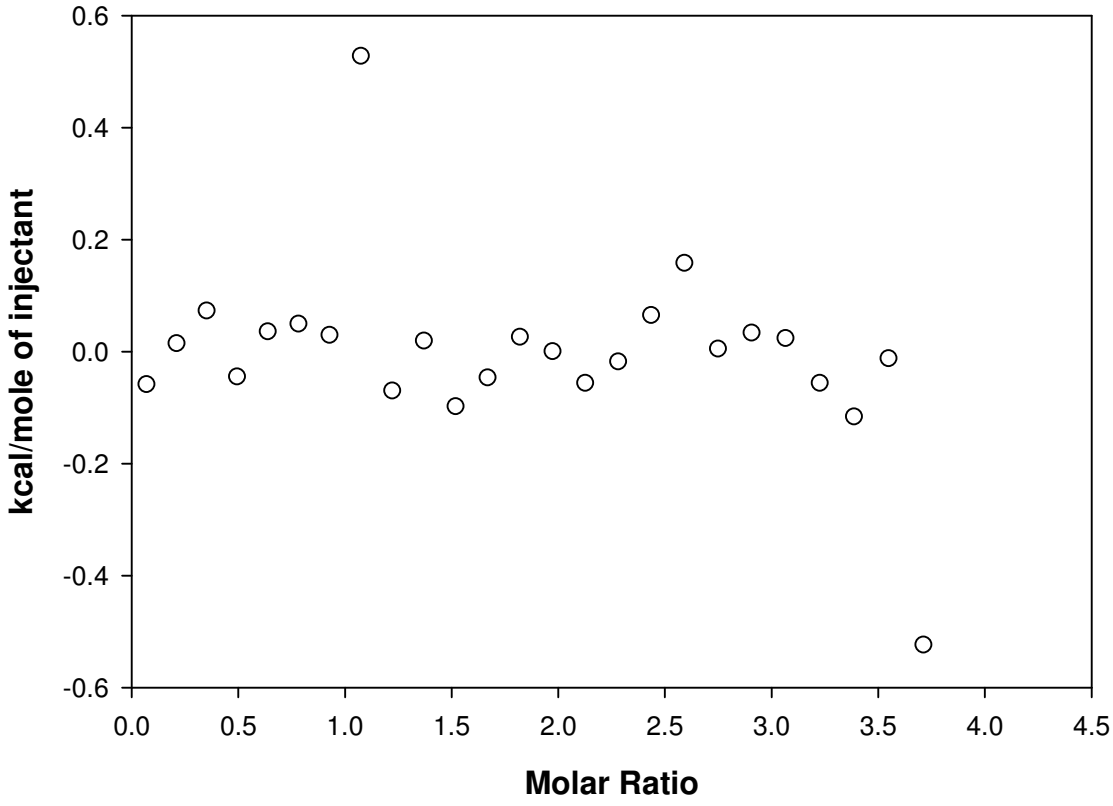

Figure 49: The heat of reaction per injection in kilocalories per mole of buffer (the area under each peak, Figure 46) *versus* Molar Ratio (Buffer/DMPC SUVs). Reported ITC data represents the mean of four measurements of separately prepared SUVs. One representative figure is shown.

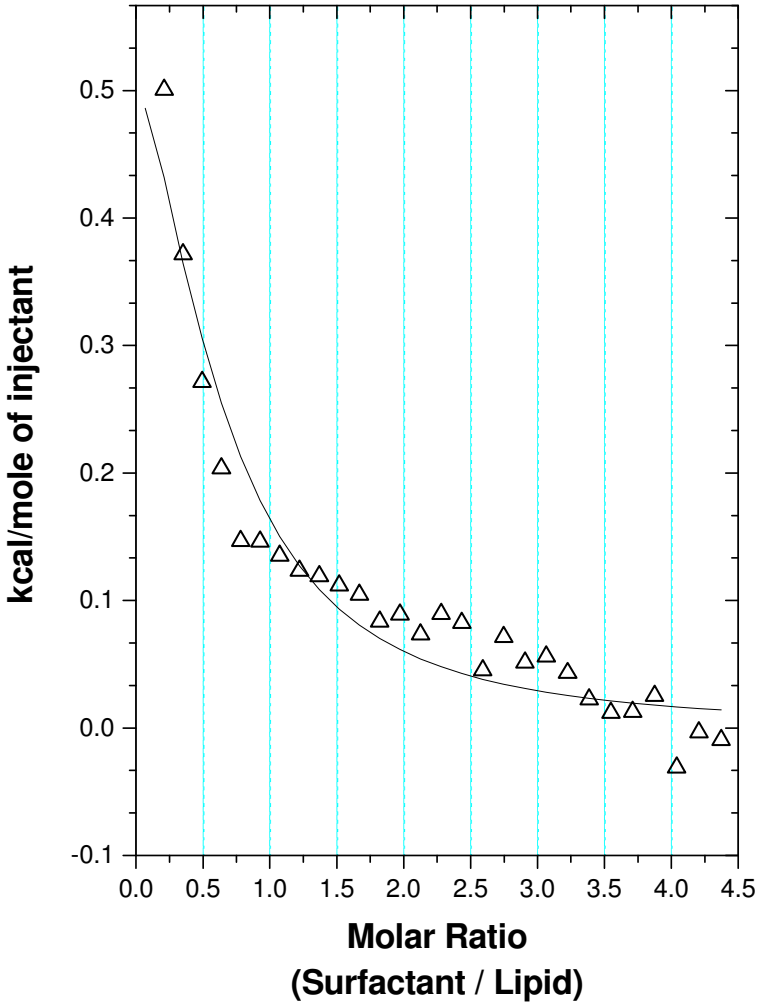

Figure 50: Corrected heat of reaction (δh_i) per injection in kilocalories per mole of C8P surfactant *versus* Molar Ratio (C8P/DMPC SUVs). The line represents the fit to the single set of identical sites model (equation 16 and 17) using the analysis software ORIGIN provided by MicroCal with transition midpoint at 0.96±0.28. Reported ITC data represents the mean of four measurements of separately prepared SUVs. One representative figure is shown.

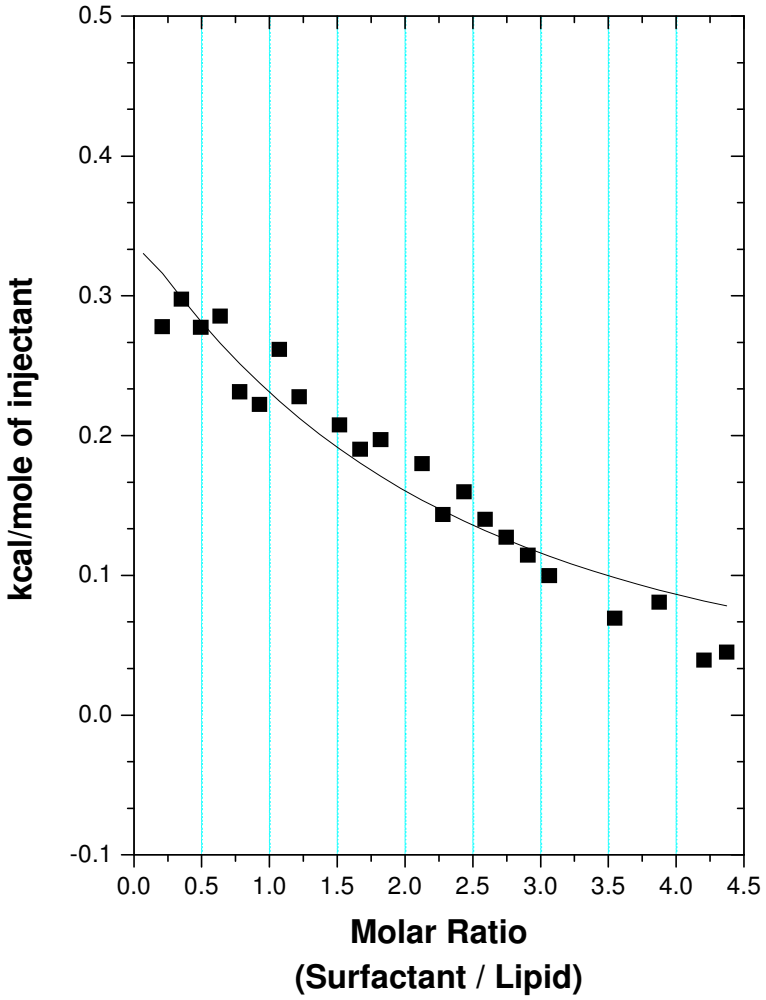

Figure 51: Corrected heat of reaction (δh_i) per injection in kilocalories per mole of C2,6P surfactant *versus* Molar Ratio (C2,6P/DMPC SUVs). The line represents the fit to the single set of identical sites model (equation 16 and 17) using the analysis software ORIGIN provided by MicroCal with transition midpoint at 1.18±0.25. Reported ITC data represents the mean of four measurements of separately prepared SUVs. One representative figure is shown.

Table 11

Thermodynamic Parameters of Partitioning C8P and C2,6P surfactants into DMPC SUVs as Reported from the Isothermal Titration Calorimetry at 30°C. Reported ITC data represents the mean of four measurements of separately prepared SUVs.

Surfactant	Re^{sat} *Molar Ratio*	K_a *(M^{-1})*	K_d *M*
C8P	0.96±0.28	1491±188	$6.78.10^{-4}$±$9.23.\ 10^{-5}$
C2,6P	1.18±0.25	1191±112	$8.46.10^{-4}$±$8.30.\ 10^{-5}$

Surfactant	*ΔH cal/mole*	*ΔS cal/mole/deg*	*ΔG kcal/mole*
C8P	826±117	17.24±0.23	-4.40±0.08
C2,6P	1414±185	18.73±0.63	-4.26±0.06

Table 12
Thermodynamic Parameters of Partitioning OG, C8P and C2,6P surfactants into DMPC vesicles as Reported from the Isothermal Titration Calorimetry .
(OG data taken from ref. 77)

Surfactant	*ΔH (cal/mole)*	*T.ΔS (cal/mole)*	*ΔG (cal/mole)*	*Re^{sat}*	*K_a (M^{-1})*	*Temperature (°C)*
OG	3100	8223	-5123	1.56	100	27
*C8P	826	5224	-4400	0.98	1491	30
*C2,6P	1414	5675	-4260	1.18	1191	30

Keller, M., Kerth, A., and Blume, A. Thermodynamics of interaction of octyl glucoside with phosphatidylcholine vesicles: partitioning and solubilization as studied by high sensitivity titration calorimetry. *Biochim. Biophys. Acta*. 1997, 1326**,** 178-192 [77].

*Data from Table 11.

Table 13
Thermodynamic parameters of partitioning of other non-ionic surfactants into lipid bilayers obtained by ITC

Surfactant	*Lipid*	*Temperature*	*ΔH(cal/mole)*	K_a (M^{-1})	*cmc (mM)*	K_a.*cmc*	Re^{sat}
TX-100	POPC	Room temperature	3585	3000	0.23	0.69	0.8
TX-114	POPC	Room temperature	1912	3500	0.17	0.59	0.9
OG	POPC	Room temperature	1300	120	23	2.3	1.3
C8P*	DMPC	30°C	826.4	1491			0.98
C2,6P*	DMPC	30°C	1414	1191			1.18

Heerklotz, H., and Seelig, J. Correlation of membrane/water partition coefficients of detergents with the critical micelle concentration. *Biophys. J.* 2000, 78, 2435-2440 [81].

* current study

CHAPTER 4: CONCLUSION

The aim of this study is to assess the effects of two non-ionic surfactants, the branched chain N-(2-ethylhexyl)-2-pyrrolidinone (C2,6P) and saturated chain N-octyl-2-pyrrolidinone (C8P), on the physical structure of DMPC SUV bilayers above the lipid phase transition temperature. In order to accomplish this goal, a combination of varying methods, including surface tension, fluorescence spectroscopy and isothermal titration calorimetry (ITC) methods, have been employed to more completely describe the surfactant-lipid interactions. The C8 series of the pyrrolidinone class were selected because of their similarity of the acyl chain length with octyl glucoside, a commonly used surfactant in membrane research due to its high cmc value and attractive solubilization properties.

Fluorescence spectroscopic methods can provide sensitivity to "local" (short-range/microscopic) environmental effects and are thus ideal for investigation of surfactant-lipid interactions. In contrast, surface tension and isothermal titration calorimetry (ITC) provide information on larger scale (long range/macroscopic) lipid packing and ordering.

Surface tension methods have been used to explore the mixed-monolayer and mixed-micelle formation of N-alkyl-2-pyrrolidinones with DMPC monomers, and to study their interfacial and bulk micellar behavior at the air/aqueous solution interface. A greater total surfactant adsorption, Γ_{LA}^{mix},was observed for DMPC-C8P mixtures at the air aqueous interface over the corresponding DMPC-C2,6P mixtures. This can arise because C8P-DMPC mixtures occupy a smaller area per molecule compared with C2,6P-DMPC and attributed to differences in the acyl chain characteristics (C8P

(saturated) *versus* C2,6P (branched)). However, C8P/DMPC and C2,6P/DMPC mixtures showed a similar tendency and efficiency for adsorption ($-\Delta G^{0}_{mix}$ and pC_{20} values, respectively).

The strength of the interactions between DMPC monomers and the surfactants was determined from their β^{σ} and β^{M} parameters. All DMPC/C8P and DMPC/C2,6P systems showed synergism with regards to surface tension reduction efficiency. Negative β^{σ} and β^{M} values indicate that the attractive interactions between the two different surfactants (DMPC and C8P, or DMPC and C2,6P) following mixing, greatly exceeds the attractive self-interactions of the two individual surfactants before mixing. Since large β values usually arise from electrostatic interactions, the values obtained here may result from such (electrostatic) interactions between the phosphocholine group of DMPC and the zwitterionic resonance form of the pyrrolidinones. Surprisingly, in contrast to fluorescence and ITC studies, C2,6P showed enhanced lipid synergism compared with C8P. However, it is important to note that surface tension measurements involve the interactions at the air/aqueous interface, in contrast to the macromolecular interactions measured from fluorescence spectroscopy and ITC methods.

Short-range lipid-surfactant interactions were studied using fluorescence spectroscopic methods. The fluorophores employed, DPH and TMA-DPH, are specific probes of the acyl chain and head group regions of the bilayer, respectively. The two fluorescence probes are ideal for surfactant-lipid investigations. Firstly, they exhibit rotational sensitivity to their environment and when embedded in the bilayer

can provide information about membrane phases and local fluidity (order) on addition of surfactant. Secondly their fluorescence emissions are sensitive to the polarity of the surrounding lipid matrix.

The fluorescence intensities of both DPH and TMA-DPH labeled DMPC SUVs decreased with addition of C8P. The largest quenching effect, attributed to altered lipid packing within the bilayer, was observed for DPH labeled vesicles, suggesting that the binding of C8P to the DMPC SUVs affects predominantly the acyl chain region of the bilayer. In contrast, only small intensity quenching effects were observed with addition of C2,6P to DMPC SUVs (labeled with DPH or TMA-DPH). These data suggest little penetration of this surfactant into the bilayer or alternatively, reduced bilayer binding/association of this surfactant.

That C2,6P does not penetrate the bilayer to any large extent is further supported by fluorescence emission anisotropy measurements. These studies provide insights into the effects of surfactants on bilayer lipid ordering. From our data, we have shown that both surfactants affect the membrane lipid order within the gel phase lipid, together with apparent "shifts" in the DMPC phospholipid 'melt' transition temperature (T_m) values, which decrease in a linear fashion to lower temperatures with increasing surfactant concentrations. Since both DPH and TMA-DPH exhibit equal partitioning into gel or fluid regions of the bilayer, the lowered T_m values suggest a fluidization effect of the surfactants on interacting with the bilayer. As described above from intensity data, our emission anisotropy studies suggest that C8P affects the lipid packing within the bilayer to a greater extent than C2,6P. This effect is further supported from determination of lipid bilayer-water partition coefficients

for the surfactants from the van't Hoff model from depression of the lipid phase transition temperature. The partition coefficient (K_p) for C8P [$(1.22\pm0.08)\times10^4$], suggests a more favorable association with the acyl chain region of the bilayer compared with C2,6P [$(4.09\pm0.78)\times10^3$].

Since the effects of the two surfactants on the bilayer may arise from differences in binding affinities, isothermal titration calorimetry was used to derive thermodynamics quantities for C8P and C2,6P partitioning into DMPC SUVs. ITC data reveals that C8P has a somewhat higher binding affinity (K_a) (1491 M^{-1}) compared with C2,6P (1191 M^{-1}) and this finding confirms our results obtained with fluorescence intensity and fluorescence emission anisotropy measurements, suggesting that C8P has preferential association with the lipid membrane.

The values for the two partition constants, K_a (obtained with ITC at 30°C) and K_p (estimated from the depression of phase transition temperature using fluorescence emission anisotropy), for the surfactant/lipid systems are different. This is not surprising given that K_a 'counts' the bound surfactant only in relation to lipid at constant temperature, whereas K_p 'counts' the surfactant in relation to both lipid and bound surfactant. At low surfactant concentrations, based on the assumption of ideal mixing of surfactant and lipid in the membrane, the two models differ only by the constant factor C_w according to relationship: $K_p = K_a C_w$ where C_w=55.5 M (the number of moles of water per liter of water) [82]. If K_p values are converted to K_a using this relationship then K_a = 220.7±14 M^{-1} for C8P and 73.6±14.1 M^{-1} for C2,6P. These calculated K_a values differ from those obtained by direct methods

(ITC) because systems studied so far differ markedly from ideal mixing. This is particularly true for bilayer systems where heterogeneity of lipid packing may exists. Thus the estimated K_p value fails to adequately describe the partitioning process completely . Nevertheless, both fluorescence spectroscopy and ITC studies show that C8P has higher binding affinity comparing to C2,6P.

From the Re^{sat} values, C8P and C2,6P are classified as intermediate strength surfactants, with values (0.96±0.28 and 1.18±0.25 for C8P and C2,6P, respectively) lying in the range: Re^{sat} <1 and Re^{sat} >1. Furthermore, our thermodynamic studies show that partitioning of these surfactants within the bilayer is an endothermic process with + ΔH values that compare favorably with similar surfactants such as the non-ionic surfactants, OG and the Tritons.

In summary, from our data, we propose that C8P affects the lipid packing of the bilayer membranes to a greater extent than C2,6P. The branched chain C2,6P appears to predominantly affect the head group region of the bilayer (Figure 52). Our studies suggest that the short-chain N-pyrrolidinones, C2,6P and in particular C8P have favorable bilayer interactions, with smaller enthalpies of binding, larger partition coefficients and affinity for lipid bilayers compared with the commonly used OG. We conclude that C8P has great potential for biological applications, particularly membrane solubilization and membrane formation from micellar mixtures. In contrast, C2,6P may have potential for solubilization of extrinsic surface associated membrane proteins.

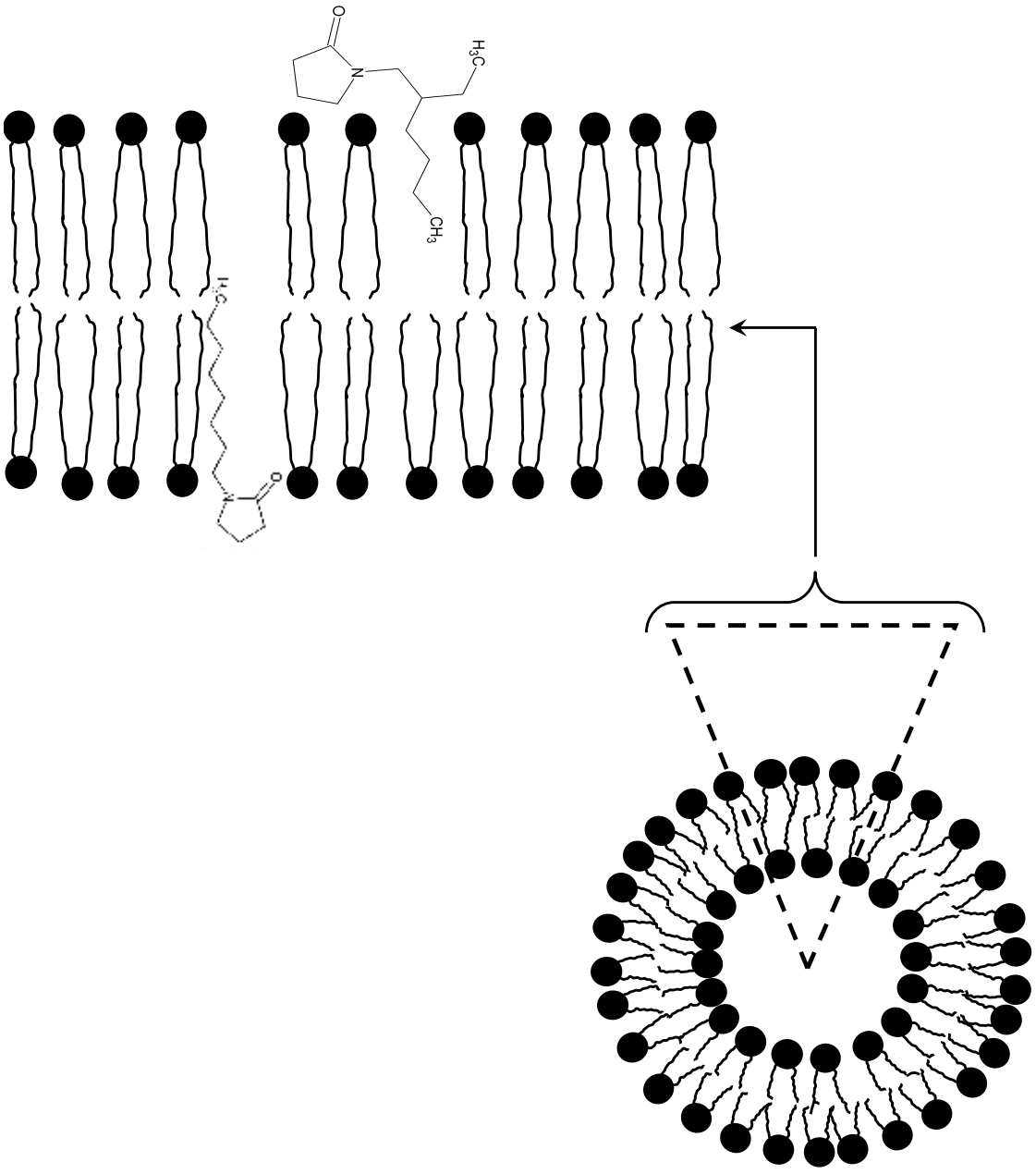

Figure 52: Proposed model of the interactions of C8P and C2,6P surfactants with DMPC SUVs.

CHAPTER 5: BIBLIOGRAPHY

1. Rosen, M. J., Zhu, Z. H., Gu, B., and Murphy, D.S. Relationship of structure to properties of surfactants. 14. Some N-Alkyl-2-pyrrolidinones at various interfaces. *Langmuir*. 1988, 4(6), 1273-1277.

.

2. Zhu, Z. H., Yang, D., and Rosen, M. J. Some synergistic properties of N-alkyl-2-pyrrolidinones, a new class of surfactants. *J. Amer.Oil Chem.Soc*. 1989, 66, 998-1001.

3. Rosen, M. J., Gu, B., Murphy, D. S., and Zhu, Z. H. Synergism in binary mixtures of surfactants. *J. Colloid Interface Sci*. 1989, 129, 468-475.

4. Rosen, M. J., Zhu, Y., and Morrall, S. W. Effect of hard river water on the surface properties of surfactants. *J.Chem.Eng.Data*. 1996, 41(5), 1160-1167.

5. Rosen, M. J., and Wu, Y. Superspreading of Trisiloxane surfactant mixtures on hydrophobic surfaces. 1. Interfacial adsorption of aqueous Trisiloxane surfactant-N-Alkyl Pyrrolidinone mixtures on polyethylene. *Langmuir*. 2001, 17, 7296-7305.

6. Zhou, Q., Wu, Y., and Rosen, M. J. Surfactant-surfactant molecular interactions in mixed monolayers at a highly hydrophobic solid/aqueous solution interface and their relationship to enhanced spreading on the solid substrate. *Langmuir*. 2003, 19, 7955-7962.

7. Forest, C.L. Effects of non-ionic detergents on *Chlamydomonas* mating. Possible modes of action. Department of Biology, Brooklyn College of CUNY, Brooklyn, NY, 11210.

8. Rosoff, Morton (Ed.). Vesicles, Surfactant Science Series. 1996, 62, Marcel Dekker, New York.

9. Helenius, A., McCaslin, D. R., Fries, E., and Tanford, C. Properties of Detergents. *Methods in Enzymology*. 1979, 56, 734-749.

10. Jones, M. N., and Chapman, D. Micelles, monolayers and biomembranes. Wiley-Liss, Inc., New York, 1995.

11. Rosen, M. J., and Gu, B. Synergism in binary mixtures of surfactants. 6. Interfacial tension reduction efficiency at the liquid/hydrophobic solid interface. *Colloids Surf.* 1987, 23, 119-135.

12. Aratona, M., Ohta, A., Minamizawa., Ikeda, N., Iyota, H., and Takiue, T. The excess thermodynamic quantities of adsorption of a binary nonionic surfactant mixture. *J. Colloid Interface Sci*. 1999, 217, 128-136.

13. Rosen, M. J., and Hua, X. Y. Surface concentrations and molecular interactions in binary mixtures of surfactants. *J. Colloid Interface Sci*. 1981, 86(1), 164-172.

14. Sarmoria, C., Puvvada, S., and Blankschtein, D. Prediction of critical micelle concentrations of nonideal binary surfactant mixtures. *Langmuir*. 1992, 8, 2690-2697.

15. Rosen, M. J., and Sulthana, S. B. The interaction of alkylglycosides with other surfactants. *J. Colloid Interface Sci*. 2001, 239, 528-534.

16. Zhang, R., Zhang, L., and Somasundaran, P. Study of mixtures of n-dodecyl-β-D-maltoside with anionic, cationic, and nonionic surfactant in aqueous solutions using surface tension and fluorescence techniques. *J. Colloid Interface Sci*. 2004, 278, 453-460.

17. Hierrezuelo, J. M., Aguiar, J., and Ruiz, C. Stability, interaction, size, and microenvironmental properties of mixed micelles of decanoyl-n-methylglucamide and sodium dodecyl sulfate. *Langmuir*. 2004, 20, 10419-10426.

18. Zhao, B., Zhu, L., Li, W., and Chen, B. Solubilization and biodegradation of phenanthrene in mixed anionic-nonionic surfactant solutions. *Chemosphere*. 2005, 58, 33-40.

19. Gerber, S., Garamus, V. M., Milkereit, G., and Vill, V. Mixed micelles formed by SDS and a bolaamphiphile with carbohydrate headgroups. *Langmuir*. 2005, 21, 6707-6711.

20. Treiner, C., and Makayssi, A. Structural micellar transition for dilute solutions of long chain binary cationic surfactant systems: a conductance investigation. *Langmuir.* 1992, 8, 794-800.

21. Moulik, S. P., Haque, Md. E., Jana, P. K., and Das, A. R. Micellar properties of cationic surfactants in pure and mixed states. *J. Phys. Chem*. 1996, 100, 701-708.

22. Cummins, P. G., Penfold, J., and Staples, E. A study of the structure of mixed cationic/nonionic micelles by small-angle neutron scattering spectrometry. *Langmuir*. 1992, 8, 31-35.

23. Bakshi, M. S., Sachar, S., Singh, K., and Shaheen, A. Mixed micelle behavior of pluronic L64 and Triton X-100 with conventional and dimeric cationic surfactants. *J. Colloid Interface Sci*. 2005, 286, 369-377.

24. Kumar, A., Alami, E., Holmberg, K., Seredyuk, V., and Menger, F. M. Branched zwitterionic gemini surfactants micellization and interaction with ionic surfactants. *Coll. Surf. A Physicochem. Eng. Aspects*. 2003, 228, 197-207.

25. Prosser, A. J., and Franses, E. I. New thermodynamic/electrostatic models of adsorption and tension equilibria of aqueous ionic surfactant mixtures: application to sodium dodecyl sulfate/sodium dodecyl sulfonate systems. *J. Colloid Interface Sci*. 2003, 263, 606-615.

26. Bakshi, M. S., and Singh, K. Synergistic interactions in the mixed micelles of cationic gemini with zwitterionic surfactants: fluorescence and krafft temperature studies. *J. Colloid Interface Sci*. 2005, 287, 288-297.

27. Jackson, M. L., Schmidt, C. F., Lichtenberg, D., Litman, B. J., and Albert, A. D. Solubilization of phosphatidylcholine bilayers by octyl glucoside. *Biochemistry*.1982, 21, 4576-4582.

28. Alonso, A., Sáez, R., and Goñi, F. M. *FEBS Lett*. The interaction of detergents with phospholipids vesicles: a spectrofluorimetric study. 1982, 137, 141-145.

29. Ollivon, M., Eidelman, O., Blumenthal, R., and Walter, A. Micelle-Vesicle transition of egg phosphatidylcholine and octyl glucoside. *Biochemistry*. 1988, 27, 1695-1703.

30. Eidelman, O., Blumenthal, R., and Walter, N. Composition of octyl glucoside-phosphatidylcholine mixed micelles. *Biochemistry*. 1988, 27, 2839-2846.

31. Miguel, M. G., Eidelman, O., Ollivon, M., and Walter, A. Temperature dependence of the vesicle-micelle transition of egg phosphatidylcholine and octyl glucoside. *Biochemistry*. 1989, 28, 8921-8928.

32. Kragh-Hansen, U., le Maire, M., Nöel, J. P., Gulik-Krzywicki, T., and Moller, J. V. Transitional steps in the solubilization of protein-containing membranes and liposomes by nonionic detergent. *Biochemistry*. 1993, 32(6), 1648-1656.

33. Soltys, C. E., and Roberts, M. F. Fluorescence studies of phosphatidylcholine micelle mixing: Relevance to phospholipase kinetics. *Biochemistry*. 1994, 33, 11608-11617.

34. Heerklotz, H., Binder, H., Lantzsch, G., and Klose, G. Membrane/water partition of oligo (ethyleneoxide) dodecyl ethers and its relevance for solubilization. *Biochim. Biophys. Acta*. 1994, 1196, 114-122.

35. Parasassi, T., Giusti, A. M., Raimondi, M., and Gratton, E. Abrupt modifications of phospholipid bilayer properties at critical cholesterol concentrations. *Biophys. J*. 1995, 68, 1895-1902.

36. Das, T. K. Rotational dynamics of lipid/detergent mixtures: A mechanism for membrane protein reconstitution into lipid vesicles. *J. Phys. Chem*. 1996, 100(51), 20143-20147.

37. Das, T. K. Rotational dynamics of lipid-detergent mixtures probed by a cyanine dye: A mechanism for vesicle formation. *J. Chem. Soc., Faraday Trans*. 1996, 92(21), 4279-4283.

38. Koga, K., Murakami, M., and Kawashima, S. Contribution of hydrophobicity of nonionic detergents to membrane lipid fluidity and disopyramide uptake by rat intestinal brush-border membrane vesicles. *Biol. Pharm. Bull*. 1997, 20(6), 674-679.

39. Yegutkin, G. G. Effect of increasing concentrations of nonionic detergent Triton X-100 on solubilization and structure of rat liver and adipose plasma membranes. *Membr .Cell. Biol.* 1997, 10, 515-520.

40. Paternostre, M., Viard, M., Meyer, O., Ghanam, M., Ollivon, M., and Blumenthal, R. Solubilization and reconstitution of vesicular stomatitis virus envelope using octylglucoside. *Biophys. J.* 1997, 72, 1683-1694.

41. Rawat, S. S., and Chattopadhyay, A. Structural transition in the micellar assembly: A fluorescence study. *J. Fluoresc*. 1999, 9(3), 233-244.

42. Kokkona, M., Kallinteri, P., Fatouros, D., and Antimisiaris, S. G. Stability of SUV liposomes in the presence of cholate salts and pancreatic lipases: effect of lipid composition. *European journal of pharmaceutical sciences*. 2000, 9, 245-252.

43. Cócera, M., López, O., Estelrich, J., Parra, J. L., and de la Maza, A. Use of a fluorescence spectroscopy technique to study the adsorption of sodium dodecylsulfonate on liposomes. *Chem. Phys. Lipids*. 2001, 110, 19-26.

44. Kragh-Hansen, U., Hellec, F., de Foresta, B., le Maire., M., and Møller, J. Detergents as probes of hydrophobic binding cavities in serum albumin and other water-soluble proteins. *Biophys. J.* 2001, 80, 2898-2911.

45. Viard, M., Gallay, J., Vincent, M., and Paternostre, M. Origin of laurdan sensitivity to the vesicle-to-micelle transition of phospholipids-octylglucoside system: A time-resolved fluorescence study. *Biophys. J*. 2001, 80, 347-359.

46. Gelamo, E. L., Silva, C. H.T. P., Imasato, H., and Tabak, M. Interaction of bovine (BSA) and human (HSA) serum albumins with ionic surfactants: spectroscopy and modeling. *Biochim. Biophys. Acta*. 2002, 1594, 84-99.

47. Westerlund, F., Wilhelmsson, L. M., Nordén, B., and Lincoln, P. Micelle-sequestered dissociation of cationic DNA-intercalated drugs: unexpected surfactant-induced rate enhancement. *J. Am. Chem. Soc*. 2003, 125, 3773-3779.

48. Allen, S. J., Curran, A. R., Templer, R. H., Meijberg, W., and Booth, P. J. Folding kinetics of an α helical membrane protein in phospholipid bilayer vesicles. *J. Mol. Biol*. 2004, 342, 1279-1291.

49. Andrieux, K., Forte, L., Lesieur, S., Paternostre, M., Ollivon, M., and Grabielle-Madelmont, C. Insertion and partition of sodium taurocholate into egg phosphatidylcholine vesicles. *Pharmaceutical Research*. 2004, 21(8), 1505-1516.

50. Bombelli, C., Caracciolo, G., Profio, P. D., Diociaiuti, M., Luciani, P., Mancini, G., Mazzuca, C., Marra, M., Molinari, A., Monti, D., Toccacieli, L., and Venanzi, M. Inclusion of a photosensitizer in liposomes formed by DMPC/Gemini surfactant: correlation between physicochemical and biological features of the complexes. *J. Med. Chem*. 2005, 48, 4882-4891.

51. Ranganathan, R., Vautier-Giongo, C., Bakshi, M. S., Bales, B. L., and Hajdu, J. Phospholipid containing mixed micelles characterization of diheptanoyl phosphatidylchline (DHPC) and sodium dodecyl sulfate and DHPC and dodecyl trimethylammonium bromide. *Chem. Phys. Lipids*. 2005, 135, 93-104.

52. Simões, S. I., Tapadas. J. M., Marques, C. M., Cruz, M. E. M., Martins, M. B. F., and Cevc, G. Permeabilisation and solubilisation of soybean phosphatidylcholine bilayer vesicles, as membrane models, by polysorbate, Tween 80. *European Journal of Pharmaceutical Sciences*. 2005, 26, 307-317.

53. Bakshi, M. S., Singh, J., Singh, K., and Kaur, G. Effect of hydrophobic tail on the mixed micelles of diheptanoylphosphatidycholine with cationic and zwitterionic surfactants: a fluorescence study. *J. Photochem. Photobiol. A: Chem*. 2005, 169, 63-70.

54. Bakshi, M. S., Singh, J., and Kaur, G. Fluorescence study of solubilizaion of L-α-dilauroylphosphatidylethanolamine in the mixed micelles with monomeric and dimeric cationic surfactants. *J. Photochem. Photobiol. A: Chem*. 2005, 173, 202-210.

55. Vautier-Giongo, C., Bakshi, M. S., Singh, J., Ranganathan, R., Hajdu, J., and Bales, B. B. Effects of interactions on the formation of mixed micelles of 1,2-diheptanoyl-sn-glycero-3-phosphocholine with sodium dodecyl sulfate and dodecyltrimethylammonium bromide. *J. Colloid. Interface. Sci*. 2005, 282, 149-155.

56. Shinitzky, M., and Barenholz, Y. Dynamics of the hydrocarbon layer in liposomes of lecithin and sphingomyelin containing dicetylphosphate. *J. Biol.Chem*. 1974, 249(8), 2652-2657.

57. Shinitzky, M., and Inbar, M. Difference in microviscosity induced by different cholesterol levels in the surface membrane lipid layer of normal lymphocytes and malignant lymphoma cells. *J. Mol. Biol*. 1974, 85, 603-615.

58. Lentz, B.R., Barenholz, Y., and Thompson, T.E. Fluorescence depolarization studies of phase transitions and fluidity in phospholipid bilayers. 1. Single component phosphatidylcholine liposomes. *Biochemistry*. 1976, 15(20), 4521-4528.

59. Lentz, B. R., Barenholz, Y., and Thompson, T. E. Fluorescence depolarization studies of phase transitions and fluidity in phospholipid bilayers. 2. Two-component phosphatidylcholine liposomes. *Biochemistry*. 1976, 15(20), 4529-4537.

60. Chen, L.A., Dale, R.E., Roth, S., and Brands, L. Nanosecond time-dependent fluorescence depolarization of diphenylhexatriene in dimyristoyllecithin vesicles and the determination of "Microviscosity". *J. Biol.Chem*. 1977, 252(7), 2163-2169.

61. Dale, R. E., Chen, L. A., and Brand, L. Rotational relaxation of the "microviscosity" probe diphenylhexatriene in paraffin oil and egg lecithin vesicles. *J. Biol.Chem*. 1977, 252(21), 7500-7510.

62. Kawato, S., Kinosita, K., Jr., and Ikegami, A. Dynamic structure of lipid bilayers studied by nanosecond fluorescence techniques. *Biochemistry*. 1977, 16(11), 2319-2324.

63. Lakowicz, J. R., Prendergast, F. G., and Hogen, D. Fluorescence anisotropy measurements under oxygen quenching conditions as a method to quantify the depolarizing rotations of fluorophores. Application to diphenylhexatriene in isotropic solvents and in lipid bilayers. *Biochemistry*. 1979, 18(3), 520-527.

64. Lakowicz, J. R., Prendergast, F. G., and Hogen, D. *Biochemistry*. Differential polarized phase fluorometric investigations of diphenylhexatriene in lipid bilayers. Quantitation of hindered depolarizing rotations. 1979, 18(3), 508-519.

65. Shinitzky, M., and Inbar, M. Microviscosity parameters and protein mobility in biological membranes. *Biochim. Biophys. Acta*. 1976, 433, 133-149.

66. Prendergast, F. G., Haugland, R. P., and Callahan, P. J. 1-[4-(Trimethylamino) phenyl]-6-phenylhexa-1, 3, 5-triene: Synthesis, fluorescence properties, and use as a fluorescence probe of lipid bilayers. *Biochemistry*. 1981, 20, 7333-7338.

67. Wang, S., Beechem, J. M., Gratton, E., and Glaser, M. Orientational distribution of 1,6-Diphenyl-1,3,5-hexatriene in phospholipids vesicles as determined by global analysis of frequency domain fluorimetry data. *Biochemistry*. 1991, 30, 5565-5572.

68. Kitagawa, S., Matsubayashi, M., Kotani, K., Usui, K., and Kametani, F. Asymmetry of membrane fluidity in the lipid bilayer of blood platelets: Fluorescence study with diphenylhexatriene and analogs. *J. Membrane Biol*. 1991, 119, 221-227.

69. Davenport, L. Fluorescence probes for studying membrane heterogeneity. *Methods in Enzymology*. 1997, 278, 487-512.

70. Slavik, J. *Fluorescent Probes in Cellular and Molecular Biology*, CRC Press, Inc., 1994.

71. Cranney, M., Cundall, R. B., Jones, G. R., Richards, J. T., and Thomas, E. W. Fluorescence lifetime and quenching studies on some interesting diphenylhexatriene membrane probes. *Biochim. Biophys. Acta.* 1983, 735, 418-425.

72. Huang, Z., and Haugland, R. P. Partition coefficients of fluorescent probes with phospholipid membranes. *Biochim.Biophys.Res.Commun*. 1991, 181(1), 166-171.

73. Cundall, R. B., Johnson, I., Jones, M. W., Thomas, E. W., and Munro, I. H. Photophysical properties of DPH derivatives. *Chem. Phys. Letters*. 1979, 64(1), 39-42.

74. Wenk, M. R., Alt, T., Seelig, A., and Seelig, J. Octyl-β-D-glucopyranoside partitioning into lipid bilayers: thermodynamics of binding and structural changes of the bilayer. *Biophys. J.* 1997, 72, 1719-1731.

75. Wenk, M. R., and Seelig, J. Interaction of octyl-β-thioglucopyranoside with lipid membranes. *Biophys. J.* 1997**,** 73, 2565-2574.

76. Heerklotz, H., Lantzsch, G., Binder, H., Klose, G., and Blume, A. Lipid/detergent interaction thermodynamics as a function of molecular shape. *J. Phys. Chem. B*. 1997, 101, 639-645.

77. Keller, M., Kerth, A., and Blume, A. Thermodynamics of interaction of octyl glucoside with phosphatidylcholine vesicles: partitioning and solubilization as studied by high sensitivity titration calorimetry. *Biochim. Biophys. Acta*. 1997, 1326**,** 178-192.

78. Opatowski, E., Kozlov, M. M., and Lichtenberg, D. Partitioning of octyl glucoside between octyl glucoside/phosphatidylcholine mixed aggregates and aqueous media as studied by isothermal titration calorimetry. *Biophys. J.* 1997, 73, 1448-1457.

79. Opatowski, E., Lichtenberg, D., and Kozlov, M. M. The heat of transfer of lipid and surfactant from vesicles into micelles in mixtures of phospholipids and surfactant. *Biophys. J.* 1997, 73, 1458-1467.

80. Heerklotz, H., Binder, H., and Epand, R. M. A "Release" protocol for isothermal titration calorimetry. *Biophys. J*. 1999, 76, 2606-2613.

81. Heerklotz, H., and Seelig, J. Correlation of membrane/water partition coefficients of detergents with the critical micelle concentration. *Biophys. J*. 2000, 78, 2435-2440.

82. Heerklotz, H., and Seelig, J. Titration calorimetry of surfactant-membrane partitioning and membrane solubilization. *Biochim. Biophys. Acta.* 2000, 1508, 69-85**.**

83. Funari, S. S., Nuscher, B., Rapp, G., and Beyer, K. Detergent-phospholipid mixed micelles with a crystalline phospholipid core. *PNAS.* 2001, 98(16), 8938-8943.

84. Heerklotz, H., and Seelig, J. Detergent-like action of the antibiotic peptide surfactin on lipid membranes. *Biophys. J.* 2001, 81, 1547-1554.

85. Majhi, P. R., and Blume, A. Temperature-induced micelle-vesicle transitions in DMPC-SDS and DMPC-DTAB mixtures studied by caloimetry and dynamic light scattering. *J. Phys. Chem. B*. 2002, 106, 10753-10763.

86. Ollila, F., and Slotte, J. P. Partitioning of Triton X-100, Deoxycholate and $C_{10}EO_8$ into bilayers composed of native and hydrogenated egg yolk sphingomyelin. *Biochim. Biophys. Acta.* 2002, 1564, 281-288.

87. Hildebrand, A., Garidel, P., Neubert, R., and Blume, A. Bile salt induced solubilization of synthetic phosphatidylcholine vesicles studied by isothermal titration calorimetry. *Langmuir* 2002, 18(7), 2836-2847.

88. Tan, A., Zieglar, A., Steinbauer, B., and Seeling, J. Thermodynamics of sodium dodecyl sulfate partitioning into lipid membranes. *Biophys. J.* 2002, 83, 1547-1556.

89. Carneiro, F. A., Bianconi, M. L., Weissmüller, G., Stauffer, F., and Da Poian, A. T. Membrane recognition by vesicular stomatitis virus involves enthalpy-driven protein-lipid interaction. *J. Virol*. 2002, (76)8, 3756-3764.

90. Pozharski, E., and MacDonald, R. C. Lipoplex thermodynamics: Determination of DNA-Cationic lipoid interaction energies. *Biophys. J*. 2003, 85, 3969-3978.

91. Heerklotz, H., Szadkowska, H., Anderson, T., and Seelig, J. The sensitivity of lipid domains to small perturbations demonstrated by the effect of Triton. *J. Mol. Biol.* 2003, 329, 793-799.

92. Mel'nikov, S. M., Seijen ten Hoorn, J. W. M.., and Eijkelenboom, A .P. A. M. Effect of phytosterols and phytostanols on the solubilization of cholesterol by dietary mixed micelles: an in vitro study. *Chem. Phys. Lipids*. 2004, 127, 121-141.

93. Blandamer, M. J., Cullis, P. M., and Engberts, J. B. F. N. Titration calorimetry. *J.Chem.Soc., Fraday Trans*. 1998, 94(16), 2261-2267.

94. Holdgate, G. A. Making cool drugs hot: isothermal titration calorimetry as a tool to study binding energetics. *BioTechniques*. 2001, (30), 164-184.

95. Ward, W. H. J., and Holdgate, G. A. Isothermal titration calorimetry in drug discovery. *Progress in Medicinal Chemistry*. Elsevier Science B. V. (Vol. 38), 309-376.

96. Jelesarov, I., and Bosshard, H. R. Isothermal titration calorimetry and differential scanning calorimetry as complementary tools to investigate the energetics of biomolecular recognition. *J. Mol. Recognit*. 1999, 12, 3-18.

97. Pierce, M. M., Raman, C. S., and Nall, B. T. Isothermal titration calorimetry of protein-protein interactions. *Methods*. 1999, (19), 213-221.

98. Lasic, D. D. Liposomes, from Physics to Applications. Elsevier, Amsterdam, the Netherlands, 1993.

99. Rosen, M.J. *Surfactants and Interfacial Phenomena*, 3rd. Edition, John Wiley & Sons, Inc. 2004. a) pp.3-28 b) pp.211-212 c) pp. 321-324 d) pp.62-64 e) p.382 f) pp.398-401 g) pp. 386-396.

100. Neugebauer, J. *A Guide to the Properties and Uses of Detergents in Biology and Biochemistry*, Hoechst Celanese Corporation, 1987.

101. Lasic, D. D. Tibtech. *Novel Applications of Liposomes*. 1998, 16, 307-321.

102. Ruiz, M. B., Prado, A., Goñi, F. M., and Alanso, A. An assessment of the biochemical applications of the non-ionic surfactant Hecameg. *Biochim. Biophys. Acta*. 1994, 1193, 301-306.

103. de la Maza., and Parra, J. L. Vesicle-micelle structural transitions of phospholipid bilayers and sodium dodecyl sulfate. *Langmuir*. 1995, 11, 2435-2441.

104. Schürholz, T. Critical dependence of the solubilization of lipid vesicles by the detergent CHAPS on the lipid composition. Functional reconstitution of the nicotinic acetylcholine receptor into preformed vesicles above the critical micellization concentration. *Biophys. Chem*. 1996, 58, 87-96.

105. Kwon, S. Y., and Kim, M. W. Structure and growth control of a nonionic surfactant micelle by adding a phospholipid. *Langmuir*. 2001, 17, 8016-8023.

106. Bakshi, M. S., Singh, J., and Kaur, G. Mixed micelles of monomeric and dimeric cationic surfactants with phospholipids: effect of hydrophobic interactions. *Chem. Phys. Lipids*. 2005, 138(1-2), 81-92.

107. Neugebauer, J. M. Detergents: An Overview. *Methods in Enzymology*. 1990, 182, 239-253.

108. Lichtenberg, D., Robson, J. R., and Dennis, A. E. *Biochim. Biophys. Acta*. 1983, 737, 285-304.

109. Helenius, A., and Simons, K. Solubilization of membranes by detergents. *Biochim. Biophys. Acta*. 1975, 415, 29-79.

110. Tanford, C., and Reynolds, J. A. Characterization of membrane proteins in detergent solution. *Biochim. Biophys. Acta*. 1976, 457, 133-170.

111. Medina, O. P., Zhu, Y., and Kairemo, K. Targeted liposomal drug delivery in cancer. *Current Pharmaceutical Design*. 2004, 10(24), 2981-2989.

112. Baldeschwieler, J. D., and Schmidt, P. G. Liposomal drugs: from setbacks to success. *Chemtech*, 1997, 27(10), 34-42.

113. Barenholz, Y. Liposome applications: problems and prospects. *Current Opinion in Colloid and Interface Science*. 2001, 6(1), 66.

114. Adler-Moore, J. P., Chiang, S. M., Satorius, A., Guerra, D., McAndrews, B., McManus, E. J., and Proffitt, R. T. Treatment of murine candidosis and Cryptococcosis with a unilamellar liposomal amphotericin B formulation (AmBisome). *Journal of Antimicrobial Chemotherapy*. 1991, 28, 63-71.

115. de Lima, M. C. P., Neves, S., Filipe, A., Duzgunes, N., and Simoes, S. Cationic liposomes for gene delivery: from biophysics to biological applications. *Current Medicinal Chemistry*. 2003, 10(4), 1221-1231.

116. Lopez-Berestein, G., Fainstein, V., Hopfer, R., Mehta, K., Sullivan, M. P., Keating, M., Rosenblum, M. G., Mehta, R., Luna, M., and Hersch, E. M. Liposomal amphotericin B for the treatment of systemic fungal infections in patients with cancer: a preliminary study. *Journal of Infectious Diseases*. 1985, 151(4), 704-710.

117. Lasic, D. D. Recent developments in medical applications of liposomes: sterically stabilized liposomes in cancer therapy and gene delivery in vivo. *Journal of Controlled Release*. 1997, 48, 203-222.

118. Collier, J. H., and Messersmith, P. B. Phospholipid strategies in biomineralization and biomaterials research. *Annu. Rev. Mater. Res*. 2001, 31:237-63.

119. Larsson, K. Lipids. Molecular organization, physical functions and technical applications, volume 5 of The Oily Press Lipid Library. The Oily Press, 1994.

120. Christie, W. High-performance of liquid chromatography and lipids. Pergamon Books, 1987.

121. Tanford, C. The Hydrophobic Effect, 2nd Ed, Wiley, New York, 1980.

122. Israelachvili, J. N., Mitchell, J., and Ninham, B. W. Theory of self-assembly hydrocarbon amphiphiles into micelles and bilayers. *J. Chem. Soc. Farad. Trans. II*. 1976, 72:1525-1568.

123. Bangham, A. D., and Horne, R. W. Negative staining of phospholipids and their structural modification by surface-active agents as observed in the electron microscope. *J. Mol. Biol*. 1964, 8, 660-668.

124. Walde, P., and Ichikawa, S. Enzymes inside lipid vesicles: preparation, reactivity and applications. *Biomol. Eng*. 2001, 18, 143-177.

125. Needham, D., and Evans, E. Structure and mechanical properties of giant lipid (DMPC) vesicle bilayers from 20°C below to 10°C above the liquid crystal-crystalline phase transition at 24°C. *Biochemistry*. 1988, 27, 8261-8269.

126. Fuhrhop, J-H., and Mathieu, J. Routes to functional vesicle membranes without proteins. *Angew. Chem. Int. Ed. Engl*. 1984, 23, 100-113.

127. Hinze, W. L., and Armstrong, D. W. (Eds.). Ordered Media in Chemical Separation (ACS Symposium Series, No.342). 1987. American Chemical Society, Washington, D.C.

128. Chapman, D., Williams, R. M., and Ladbrooke, B. D. Physical studies of phospholipids. VI. Thermotropic and lyotropic mesomorphism of some 1, 2 diacylphosphatidylcholines (lecithins). *Chem. Phys. Lipids*. 1967, 1, 445.

129. Mason, J. T. Ackers, G. K., and Johnson, M. L. (Eds.). Investigation of phase transitions in bilayer membranes. *Methods in Enzymology*, 1998, 295, 468-494.

130. Koynova, R., and Caffrey, M. Phases and phase transitions of the phosphatidylcholines. *Biochim. Biophys. Acta*. 1998, (1376), 91-145.

131. McMullen, T. P., and McElhaney, R. N. New aspects of the interaction of cholesterol with dipalmitoylphosphatidylcholine bilayers as revealed by high-sensitivity differential scanning calorimetry. *Biochim. Biophys. Acta*. 1995, 1234 (1), 90-98.

132. Garidel, P., Johann, C., and Blume, A. Nonideal mixing and phase separation in phosphatidylcholine-phosphatidic acid mixtures as a function of acyl chain length and pH. *Biophys. J*. 1997, 72, 2196-2210.

133. Redfern, D. A., and Gericke, A. Domain formation in phosphatidylinositol monophosphate/phosphatidylcholine mixed vesicles. *Biophys. J*. 2004, 86, 2980-2992.

134. Redfern, D. A., and Gericke, A. pH dependent domain formation in phosphatidylinositol polyphosphate/phosphatidylcholine mixed vesicles. *J. Lipid. Res*. 2005, 46(3), 504-515.

135. Koynova, R., MacDonald, and R. C. Mixtures of cationic lipid o-ethylphosphatidylcholine with membrane lipids and DNA: phase diagrams. *Biophys. J*. 2003, 85(4), 2449-2465.

136. Hung, W. C., Chen, F. Y., and Huang, H. W. Order-disorder transition in bilayers of diphytanoyl phosphatidylcholine. *Biochim. Biophys. Acta*. 2000, 1467, 198-206.

137. Trouard, T. P., Nevzorov, A. A., Alam, T. M., Job, C., Zajicek, J., and Brown, M. F. Influence of cholesterol on dynamics of dimyristoylphosphatidylcholine bilayers as studied by deuterium NMR relaxation. *J. Chem .Phys*. 1999, 110(17), 8802-8818.

138. Veiga, M. P., Arrondo, J. L. R., Goni, F. M., and Alonso, A. Ceramides in phospholipid membranes: Effects on bilayer stability and transition to nonlamellar phases. *Biophys. J*. 1999, 76(1), 342-350.

139. Vrhovnik, K., Kristl, J., Sentjurc, M., and Smid-Korbar, J. Influence of liposome bilayer fluidity on the transport of encapsulated substance into the skin as evaluated by EPR. *Pharm. Res*. 1998, 15(4), 525-30.

140. Morse, R., Ma, L. D., Magin, R. L., and Dunn, F. Ultrasound interaction with large unilamellar vesicles at the phospholipids phase transition: perturbation by phospholipids side chain substitution with deuterium. *Chem. Phys. Lipids*. 1999, 103, 1-10.

141. Momo, F., Fabris, S., Bindoli, A., Scutari, G., and Stevanato, R. EPR and DSC study of the effects of propofol and nitrosopropofol on DMPC multilamellar liposomes. *Current Topics in Biophysics*. 2002, 26(1), 75-81.

142. Suurkuusk, J., Lentz, B. R., Barenholz, Y., Biltonen, R. L., and Thompson, T .E. A calorimetric and fluorescent probe study of the gel-liquid crystalline phase transition in small, single-lamellar dipalmitoylphosphatidylcholine vesicles. *Biochemistry*, 1976, 15(7), 1393-1401.

143. Moya-Quiles, M. R., Muñoz-Delgado, E., and Vidal, C. J. Effects of the pyrethroid insecticide permethrin on membrane fluidity. *Chem. Phys. Lipids*. 1996, 79, 21-28.

144. Cheng, H. Y., Randall, C. S., Holl, W. W., Constantinides, P. P., Yue, T. L., and Feuerstein, G.Z. Carvedilol-liposome interaction: evidence for strong association with the hydrophobic region of the lipid bilayers. *Biochim. Biophys. Acta*. 1996, 1284, 20-28.

145. Krill, S. L., Lau, K. Y., Plachy, W. Z., and Rehfeld, S. J. Penetration of dimyristoylphosphatidylcholine monolayers and bilayers by model β-blocker agents of varying lipophilicity. *J. Pharm. Sci*. 1998, 87(6), 751-756.

146. Kuikka, M., Ramstedt, B., Ohvo-Rekilä, H., Tuuf, J., and Slotte, J. P. Membrane properties of D-erythro-n-acyl sphingomyelins and their corresponding dihydro species. *Biophys. J.* 2001, (80), 2327-2337.

147. Engelke, M., Bojarski, P., Blob, R., and Diehl, H. Tamoxifen perturbs lipid bilayer order and permeability: comparison of DSC, fluorescence anisotropy, Laurdan generalized polarization and carboxyfluorescein leakage studies. *Biophys. Chem*. 2001, 90, 157-173.

148. Castile, J. D., Taylor, K. M. G., and Buckton, G. The influence of incubation temperature and surfactant concentration on the interaction between dimyristoylphosphatidylcholine liposomes and poloxamer surfactants. *International Journal of Pharmaceutics*. 2001, 221, 197-209.

149. Katzer, M., and Stillwell, W. Partitioning of ABA into bilayers of di-saturated phosphatidylcholines as measured by DSC. *Biophys. J*. 2003, 84, 314-325.

150. Andrich, M. P., and Vanderkooi, J. M. Temperature dependence of 1,6-diphenyl-1,3,5-hexatriene fluorescence in phospholipid artificial membranes. *Biochemistry*. 1976, (15)6, 1257-1261.

151. Heyn, M. P., Cherry, R. J., and Dencher, N. A. Lipid-protein interactions in bacteriorhodopsin-dimyristoylphosphatidylcholine vesicles. *Biochemistry*. 1981, 20, 840-849.

152. Santaella, C., and Vierling, P. Molecular order and mobility within liposomal membrane made from highly fluorinated phospholipids. *Chem. Phys. Lipids*. 1995, 77, 173-177.

153. Kogure, K., Nakamura, C., Okuda, O., Hayashi, K., and Ueno, M. Effect of dicetylphosphate or stearic acid on spontaneous transfer of protein from influenza virus-infected cells to dimyristoylphosphatidylcholine liposomes. *Biochim. Biophys. Acta*. 1997, 1329, 174-182.

154. Massey, J. B. Interaction of ceramides with phosphatidylcholine, sphingomyelin and sphingomyelin/cholesterol bilayers. *Biochim. Biophys. Acta*. 2001, 1510, 167-184.

155. Lemp, E., Zanocco, A.L., and Günther, G. Structural changes in DODAC unilamellar liposomes by addition of sucrose esters monitored by using fluorescent techniques. *Colloids and Surfaces A: Physicochem. Eng. Aspects*. 2003, 229, 63-73.

156. Cajal, Y., Busquets, M. A., Carvajal, H., Girona, V., and Alsina, M. A. Effects of a fungal lipase on membrane organization evaluated by fluorescence polarization. *Journal of Molecular Catalysis B: Enzymatic*. 2003, 22, 315-328.

157. Melchior, D. L., and Steim, J. M. Thermotropic transitions in biomembranes. *Annu. Rev. Biophys. Bioeng*. 1976, 5, 205-238.

158. Kabalnov, A. S. Method for enhancing chroma and edge definition of dye-base ink by under printing using vesicle technique. Patent number: *JP2001123099*, 2001.

159. Weiner, N., Lieb, L., Niemiec, S., Ramachandran, C., Hu, Z., and Egbaria, K. Liposomes – a novel topical delivery system for pharmaceutical and cosmetic applications. *Journal of Drug Targeting*. 1994, 2(5), 405-410.

160. Martinez-Gomis, J., Fernandez-Solanas, A., Vinas, M., Gonzalez, P., Planas, M.E., and Sanchez, S. Effects of topical application of free and liposome-encapsulated lactoferrin and lactoperoxidase on oral microbiota and dental caries in rats. *Archives of Oral Biology*. 1999, 44(11), 901-906.

161. Jacques, A., and Schramm, C. J. Fabric softeners. In: Lai, K. (ed.) Liquid Detergents. Surfactant Science Series. 1996, 67, Marcel Dekker, New York.

162. Lichtenberg, D., Opatowski, E., and Kozlov, M. M. Phase boundaries in mixtures of membrane-forming amphiphiles and micelle-forming amphiphiles. *Biochim. Biophys. Acta*. 2000, 1508, 1-19.

163. Lichtenberg, D. Characterization of the solubilization of lipid bilayers by surfactants. *Biochim. Biophys. Acta.* 1985, 821, 470-478.

164. le Maire, M., Champeil, P., and Møller, J. V. Interaction of membrane proteins and lipids with solubilizing detergents. *Biochim. Biophys. Acta.* 2000, 1508, 86-111.

165. Goñi, F. M., Urbaneja, M-A., Arrondo, J. L. R., Alonso, A., Durrani, A. A., and Chapman, D. The interaction of phosphatidylcholine bilayers with Triton X-100. *Eur. J. Biochem*. 1986, 160, 659-665.

166. Paternostre, M-T., Roux, M., and Rigaud, J-L. Mechanisms of membrane protein insertion into liposomes during reconstitution procedures involving the use of detergents. 1. Solubilization of large unilamellar liposomes (prepared by reverse-phase evaporation) by Triton X-100, octyl glucoside, and sodium cholate. *Biochemistry*. 1988, 27, 2668-2677.

167. Foresta, B., Maire, M., Orlowski, S., Champeil, P., Lund, S., Møller, J. V., Michelangeli, F., and Lee, A. G. Membrane solubilization by detergent: use of brominated phospholipids to evaluate the detergent-induced changes in ca^{2+}-ATPase/Lipid interaction. *Biochemistry*. 1989, 28, 2558-2567.

168. Levy, D., Gulik, A., Seigneuret, M., and Rigaud, J-L. Phospholipid vesicle solubilization and reconstitution by detergents. Symmetrical analysis of the two processes using octaethylene glycol mono-n-dodecyl ether. *Biochemistry*. 1990, 29, 9480-9488.

169. Sanchez, J. M., and Perillo, M. A. Membrane topology modulates β-galactosidase activity against soluble substrates. *Biophys. Chem*. 2002, 99, 281-295.

170. Thurmond, R. L., Otten, D., Brown, M. F., and Beyer, K. Structure and Packing of phosphatidylcholines in lamellar and hexagonal liquid-crystalline mixtures with a nonionic detergent: A wide-line deuterium and phosphorus-31 NMR study. *J. Phys. Chem*. 1994, 98, 972-983.

171. Klose, G., Mädler, B., Schäfer, H, and Schneider, K-P. Structural characterization of POPC and $C_{12}E_4$ in their mixed membranes at reduced hydration by solid state ^2H NMR. *J. Phys. Chem. B*. 1999, 103, 3022-3029.

172. Klose, G., and Levine, Y. K. Membranes of palmitoyloleoylphosphatidylcholine and $C_{12}E_4$-A lattice model simulation. *Langmuir*. 2000, 16, 671-676.

173. Karlovská, J., Lohner, K., Degovics, G., Lacko, I., Devínsky, F., and Balgavý, P. Effects of non-ionic surfactants N-alkyl-N,N-dimethylamine-N-oxides on the structure of a phospholipids bilayer: small-angle X-ray diffraction study. *Chem. Phys. Lipids*. 2004, 129, 31-41.

174. Almong, S., Litman, B. J., Wimley, W., Cohen, J., Watchtel, E. J., Barenholz, Y., and Ben-Shaul, A., and Lichtenberg. States of phase transformation in mixtures of phosphatidylcholine and octyl glucoside. *Biochemistry*. 1990, 29, 4582-459.

175. de la Maza., and Parra, J. L. Solubilizing effects caused by alkyl pyridinium surfactants in phosphatidylcholine liposomes. *Chem. Phys. Lipids*. 1995, 77, 79-87.

176. Ko, J-S., Oh, S-W., Kim, K-W., Nakashima, N., Nagadome, S., and Sugihara, G. Blending effects on adsorption and micellization of different membrane protein solubilizers: A thermodynamic study on three mixed systems of CHAPS with MEGA-8, -9, and -10 in pH 7.2 phosphate buffer solution. *Colloids and Surfaces B: Biointerfaces*. 2005, 45, 90-103.

177. Seddon, A. M., Curnow, P., and Booth, P. J. Membrane proteins, lipids and detergents: not just a soap opera. *Biochim. Biophys. Acta.* 2004, 1666, 105-117.

178. Baatz, J.E., Elledge, B., and Whitsett, J.A. Sufactant protein SP-B induces ordering at the surface of model membrane bilayers. *Biochemistry*. 1990, 29, 6714-6720.

179. de la Maza, A., and Parra Juez, J. L. Disintegration of liposomes by anionic surfactants and formation of mixed micelles. *Langmuir*. 1993, 9, 870-873.

180. Sun, C., Kashiwagi, H., and Ueno, M. Physical properties of phosphatidylcholine vesicles containing small amount of sodium cholate and consideration on the initial stage of vesicle solubilization. *Chem. Pharm. Bull*. 2002, 50(9), 1145-1150.

181. Deo, N., and Somasundaran. Electron spin resonance study of phosphatidyl choline vesicls using 5-doxyl stearic acid. Colloids and Surfaces B: *Biointerfaces*. 2002, 25, 225-232.

182. Gandhavadi, M., Allende, D., Vidal, A., Simon, S. A., and McIntosh, T. J. Structure, composition, and peptide binding properties of detergent soluble bilayers and detergent resistant rafts. *Biophys. J*. 2002, 82, 1469-1482.

183. Heerklotz, H., Lantzsch, G., Binder, H., Klose, G., and Blume, A. Application of isothermal titration calorimetry for detecting lipid membrane solubilization. *Chem. Phys. Lett*. 1995, 235, 517-520.

184. Heerklotz, H., Lantzsch, G., Binder, H., Klose, G., and Blume, A. Thermodynamic characterization of dilute aqueous lipid/detergent mixtures of POPC and $C_{12}EO_8$ by means of isothermal titration calorimetry. *J. Phys. Chem*. 1996, 100, 6764-6774.

185. Pinazo, A., Seguer, J., Infante, M. R., Park, S. Y., and Franses, E. I. Surface properties of aqueous systems of new nonionic double-chain surfactants and their mixtures with dilauroylphosphatidylcholine. *Coll. Surf. A Physicochem. Eng. Aspects*. 1997, 126, 49-58.

186. Petkoval, V., Nedyalkov, M., and Benattar, J. –J. Freestanding black films of phospholipids and phospholipid with proteins. *Coll. Surf. A Physicochem. Eng. Aspects*. 2001, 190, 9-16.

187. Possmayer, F., Nag, K., Rodriguez, K., Qanbar, R., and Schürch. Surface activity in vitro: role of surfactant proteins. *Comparative Biochemistry and Physiology Part A.* 2001, 129, 209-220.

188. Sehgal, P., Doe, H., and Bakshi, M. S. Interfacial and micellar properties of binary mixtures of surfactant and phospholipids in an aqueous medium. *Colloid. Polym. Sci.* 2003, 281, 275-282.

189. Vesterkvist, P. S. M., and Meriluoto, J. A. O. Interaction between microcystins of different hydrophobicities and lipid monolayers. *Toxicon.* 2003, 41, 349-355.

190. Yaseen, M., Wang, Y., Su, T. J., and Lu, J. R. Surface adsorption of zwitterionic surfactants: n-alkyl phosphocholines characterized by surface tensiometry and neutron reflection. *J. Colloid. Interface. Sci*. 2005, 288, 361-370.

191. Wilhelmy, L. Ueber die Abhängigkeit der capillaritäts-constanten des alcohols von substanz und Gestalt des benetzten festen körpers. *Ann. Phys*. 1863, 119, 177-217.

192. Chang, C-H., and Franses, E.I. Adsorption dynamics of surfactants at the air/water interface: a critical review of mathematical models, data, and mechanisms. *Coll. Surf. A Physicochem. Eng. Aspects*. 1995, 100, 1-45.

193. Rosen, M. J. Synergism in mixtures containing zwitterionic surfactants. *Langmuir*. 1991, 7, 885-888.

194. Hua, X. Y., and Rosen, M. J. Conditions for synergism in surface tension reduction effectiveness in binary mixtures of surfactants. *J. Colloid Interface Sci*. 1988, 125(2), 730-732.

195. Rosen, M. J., and Zhu, Z. H. Synergism in binary mixtures of surfactants. *J. Colloid Interface Sci*. 1989, 133(2), 473-478.

196. Li, F., Rosen, M. J., and Sulthana, S. B. Surface properties of cationic gemini surfactants and their interaction with alkylglucoside or –maltoside surfactants. *Langmuir*. 2001, 17, 1037-1042.

197. Lakowicz, R.J. *Principles of Fluorescence Spectroscopy*, 2nd Edition, Kluwer Academic/ Plenum Publishers, New York, 1999.

198. Chen, R. F., and Bowman, R. L. Fluorescence polarization: measurement with ultraviolet-polarizing filters in a spectrophotofluorometer. *Science*. 1965, 147, 729-732.

199. Chazotte, B. Comparisons of the relative effects of polyhydroxyl compounds on local versus long-range motions in the mitochondrial inner membrane. Fluorescence recovery after photobleaching, fluorescence lifetime, and fluorescence anisotropy studies. *Biochim. Biophys. Acta.* 1994, 1194(2), 315-328.

200. Newman, G. C., and Huang, C. H. Structural studies on phosphatidylcholine-cholesterol mixed vesicles. *Biochemistry*. 1975, 14, 15, 3363-3370.

201. Illinger, D., Duportail, G., Mély, Y., Poirel-Morale's, N., Gérard. D., and Kuhry, J.G. A comparison of the fluorescence properties of TMA-DPH as a probe for plasma membrane and for endocytic membrane. *Biochim. Biophys. Acta.* 1995, 1239, 58-66.

202. Zolese, G., Gratton, E., and Curatola, G. Phosphatidic acid affects structural organization of phosphatidylcholine liposomes. A study of 1,6-diphenyl-1,3,5-hexatriene (DPH) and 1-(4-trimethylammonium-phenyl)-6-phenyl-1,3,5-hexatriene

(TMA-DPH) fluorescence decay using distributional analysis. *Chem. Phys. Lipids*. 1990, 55, 29-39.

203. Shinitzky, M., Dianoux, A.C., Gitler, C., and Weber, G. Microviscosity and order in the hydrocarbon region of micelles and membranes determined with fluorescent probes. I. Synthetic micelles. *Biochemistry*. 1971, 10(11), 2106-2113.

204. Kantar, A., Giorgi, P. L., Curatola, G., and Fiorini R. Alterations in erythrocyte membrane fluidity in children with trisomy 21: a fluorescence study. *Biol. Cell*. 1992, 75(2), 135-138.

205. Scott, R. B., Collins, J. M., and Hunt, P. A. Alzheimer's disease and Down syndrome: leukocyte membrane fluidity alterations. *Mech. Ageing. Dev*. 1994, 75(1), 1-10.

206. Przybylska, M., Bryszewska, M., and Kdziora , J. Thermosensitivity of red blood cells from Down's syndrome individuals. *Bioelectrochemistry*. 2000, 52(2), 239-249.

207. Przybylska, M., Koceva-Chyła, A., Rózga. B., and Jóźwiak, Z. Cytotoxicity of daunorubicin in trisomic (+21) human fibroblasts: relation to drug uptake and cell membrane fluidity. *Cell Biology Internatonal*. 2001, (25), 2, 157-170.

208. Przybylska, M., Bryszewska, M., and Chapman, IV. Thermal properties and fluidity of human erythrocyte membranes in diabetes mellitus. *Int. J. Radiat. Boil*. 1993, 63(3), 419-424.

209. Jones, S. C., Thomas, T. H., and Marshall, S. M. Abnormal regulation of cell membrane fluidity in diabetic nephropathy. *Diabetologia*. 1998, 41(3), 337-342.

210. Waczulikova I., Sikurova, L., Carsky, J., Strbova, L., and Krahulec, B. Decreased fluidity of isolated erythrocyte membranes in type 1 and type 2 diabetes. The effect of resorcylidene aminoguanidine. *Gen. Physiol. Biophys*. 2000, 19(4), 381-392.

211. Bhor, V. M., and Sivakami, S. Regional variations in intestinal brush border membrane fluidity and function during diabetes and role of oxidative strsss and non-enzymatic glycation. *Mol. Cell. Biochem*. 2003, 252(1-2), 125-132.

212. Caimi, G., and Presti, R. L. Techniques to evaluate erythrocyte deformability in diabetes mellitus. *Acta. Diabetol*. 2004, 41(3), 99-103.

213. Janz, S., Krumbiegel, M., and Gawrisch, K. The fluidity of DOPC bilayers and membrane fractions prepared from murine plasmacytoma cells is unchanged after incorporation of pristine (2,6,10,14-tetramethylpentadecane) as assessed by fluorescence polarization analysis. *Cancer. Biochem. Biophys*. 1992, 13(2), 85-92.

214. Nathan, I., Ben-Valid, I., Henzel, R., Masalha, H., Baram, S. N., Dvilansky, A., and Parola, A. H. Alterations in membrane lipid dynamics of leukemic cells undergoing growth arrest and differentiation: dependency on the inducing agent. *Experimental Cell Research*. 1998, 239, 442-446.

215. Tsuda, H., Maeda, H., and Kishimoto, S. Fluorescence polarization with FDA in leukaemic cells: a clear difference between myelogenous and lymphocytic origins. *Br. J. cancer*. 1981, 43(6), 793-803.

216. Przybylska, M., and Jóźwiak, Z. Relevance of drug uptake, cellular distribution and cell membrane fluidity to the enhanced sensitivity of Down's syndrome fibroblasts to anticancer antibiotic-mitoxantrone. *Biochim. Biophys. Acta.* 2003, 1611, 161-170.

217. Mast, R. C., and Haynes, L. V. Use of fluorescent probes perylene and magnesium 8-anilinonaphthalene-1-sulfonate to determine the critical micelle concentration of surfactants in aqueous solution. *J. Colloid Interface Sci*. 1975, 53, 35-41.

218. Fernandez, M.S. Formation of micelles and membrane action of the local anesthetic tetracaine hydrochloride. *Biochim. Biophys. Acta*. 1980, 597, 83-91.

219. De Vendittis, E., Palumbo, G., Parlato, G., and Bocchini, V. A fluorimetric method for the estimation of the critical micelle concentration of surfactants. *Anal. Biochem*. 1981, 115(2), 278-286.

220. Chattopadhyay, A., and London, E. Fluorimetric determination of critical micelle concentration avoiding interference from detergent charge. *Anal. Biochem*. 1984, 139, 408-412.

221. Chattopadhyay, A., and Harikumar, K.G. Dependence of critical micelle concentration of a zwitterionic detergent on ionic strength: implications in receptor solubilization. *FEBS Letters*. 1996, 391, 199-202.

222. Koga, K., Ohyashiki, T., Murakami, M., and Kawashima, S. Modification of ceftibuten transport by the addition of non-ionic surfactants. *European Journal of Pharmaceutics and Biopharmaceutics*. 2000, 49, 17-25.

223. Indyk, L., and Fisher, H. F. Theoretical aspects of isothermal titration calorimetry. *Methods Enzymology*. 1998, 295, 350-364.

224. Keller, S., Heerklotz, H., and Blume, A. Monitoring membrane translocation by isothermal titration calorimetry. *J. Amer. Chem. Soc*. 2006, (128), 1279-1286.

225. McClare, C.W.F. Accurate and convenient organic phosphorus assay. *Anal. Biochem*. 1971, 39, 527-530.

226. Birdsall, B., King, R. W., Wheeler, M. R., Lewis, Jr. C. A., Godde, S. R., Bunlap, R. B., and Roberts, G. C. K. Correction for light absorption in fluorescence studies of protein-ligand interactions. *Anal. Biochem*. 1983, 132, 353-361.

227. Koenig, B. W., Strey, H. H., and Gawrisch, K. Membrane lateral compressibility measured by NMR and X-ray diffraction of acyl chain polyunsaturation. *Biophys. J.* 1997, 73, 1954-1966.

228. Gaub, H., Büschl, Ringsdorf, H., and Sackmann, E. Phase transitions, lateral phase separation and microstructure of model membranes composed of a polymerizable two-chain lipid and dimyristoylphosphatidylcholine. *Chem. Phys. Lipids*. 1985, 37, 19-43.

229. Banerjee, S., and Chatterjee, S. N. Effect of sodium cholate on the phase transition temperature of dipalmitoyl phosphatidylcholine. *Z Naturforsch [C]*. 1983, (3-4), 302-306.

230. Inoue, T., Miyakawa, K., and Shimozawa, R. Interaction of surfactants with vesicle membrane of dipalmitoylphosphatidylcholine. Effect on gel-to-liquid-crystalline phase transition of lipid bilayer. *Chem. Phys. Lipids*. 1986, 42(4), 261-270.

231. Inoue, T., Iwanaga, T., Fukushima, K., and Shimozawa, R. Effect of sodium octanoate and sodium perfluorooctanoate on gel-to-liquid-crystalline phase transition of dipalmitoylphosphatidylcholine vesicle membrane. *Chem. Phys. Lipids*. 1988, 46(1), 25-30.

232. Inoue, T., Iwanaga, T., Fukushima, K., Shimozawa, R., and Suezaki, Y. Interaction of surfactants with bilayer of negatively charged lipid: effect on gel-to-liquid-crystalline phase transition of dilauroylphosphatidic acid vesicle membrane. *Chem. Phys. Lipids*. 1988, 48(3-4), 189-196.

233. Kamaya, H., Kaneshina, S., and Ueda, I. Partition equilibrium of inhalation anesthetics and alcohols between water and membranes of phospholipids with varying acyl chain-length. *Biochim. Biophys. Acta.* 1981, 646, 135-142.

234. Xie, A.F., Yamada, R., Gewirth, A. A., and Granick, S. Materials science of the gel to fluid phase transition in a supported phospholipids bilayer. *Phys. Rev. Lett*. 2002, 89(24), 246103-(1-4).